Supporting Information

Orthogonal Stimuli Trigger Self-Assembly and Phase Transfer of $Fe^{II}_4L_4$ Cages and Cargoes

Anna J. McConnell,[‡,†,§] Cally J. E. Haynes,[‡,†] Angela B. Grommet,[†] Catherine M. Aitchison,[†] Julia Guilleme,[†] Sigitas Mikutis[†] and Jonathan R. Nitschke*[,†]

[†] Department of Chemistry, University of Cambridge, Lensfield Road, Cambridge CB2 1EW, U.K.

[§] Otto Diels Institute of Organic Chemistry, Kiel University, Otto-Hahn-Platz 4, Kiel D-24098, Germany.

Table of Contents

1 Materials and Methods

Reagents and solvents were purchased from commercial suppliers and used without further purification, unless otherwise specified. For experiments in 98:2 CD_3CN/D_2O, the CD_3CN had been dried over calcium hydride and distilled *in vacuo.*

Centrifugation of cage samples was carried out using a Grant-Bio LMC-3000 low speed benchtop centrifuge.

1.1 NMR Spectroscopy

All NMR spectra were recorded on a Bruker 400 MHz Avance III HD Smart Probe (routine ^{1}H, ^{13}C and 2D NMR experiments) and Bruker 500 MHz DCH Cryoprobe (^{13}C NMR experiments) NMR spectrometers. Chemical shifts are expressed in parts per million (ppm) and reported relative to the resonance of the residual methyl proton and carbon of CD_3CN (δ_H = 1.94 ppm, δ_C = 1.32 ppm). All measurements were carried out at 298 K unless reported otherwise. The following abbreviations are used to describe signal multiplicity for ^{1}H and ^{13}C NMR spectra: b: broad, s: singlet, d: doublet, t: triplet, dd: doublet of doublets; ddd: doublet of doublet of doublets; dt: doublet of triplets; m: multiplet.

1.2 Mass Spectrometry

Low resolution electrospray ionisation mass spectrometry (ESI-MS) was carried out on a Micromass Quattro LC (cone voltage 4-14 eV, desolvation temp. 313 K, ionisation temp. 313 K) infused from a Harvard syringe pump at a rate of 10 µL per minute.

High resolution electrospray ionisation mass spectrometry (HRMS-ESI) was performed on a Waters LCT Premier Mass Spectrometer featuring a Z spray source with electrospray ionisation and modular LockSpray interface.

1.3 UV/Visible Spectroscopy

UV/visible spectra were recorded on a Perkin Elmer Lambda 750 UV-Vis-NIR spectrophotometer fitted with a PTP-1 Peltier temperature controller accessory. Spectra were obtained in double beam mode recording the spectra using the front beam with air in the rear beam. A background spectrum of CH_3CN was recorded using the analyte beam prior to each experiment and a baseline correction was applied using the Perkin Elmer WinLab software suite. Solutions of protecting group **C** or photo-responsive masked subcomponent **A** (20 µM in CH_3CN) were analysed using quartz cuvettes with optical path lengths of 10 mm.

1.4 Irradiations

Irradiations were carried out in a Rayonet RMR-600 Photochemical Reactor using 16 RPR-3000A lamps, unless specified otherwise, from the S.N.E. Ultraviolet Co. that were approximately 10 cm from the sample. NMR experiments were carried out in J Young NMR tubes and the solutions were degassed by 3 freeze/pump/thaw cycles in order for the photoactivated self-assemblies to be carried out under a N_2 atmosphere. UV/visible spectroscopic experiments were carried out in a quartz cuvette without degassing. The temperature in the photochemical reactor was monitored over the course of the irradiations and was not found to exceed 50 °C.

2 Synthesis of Subcomponents

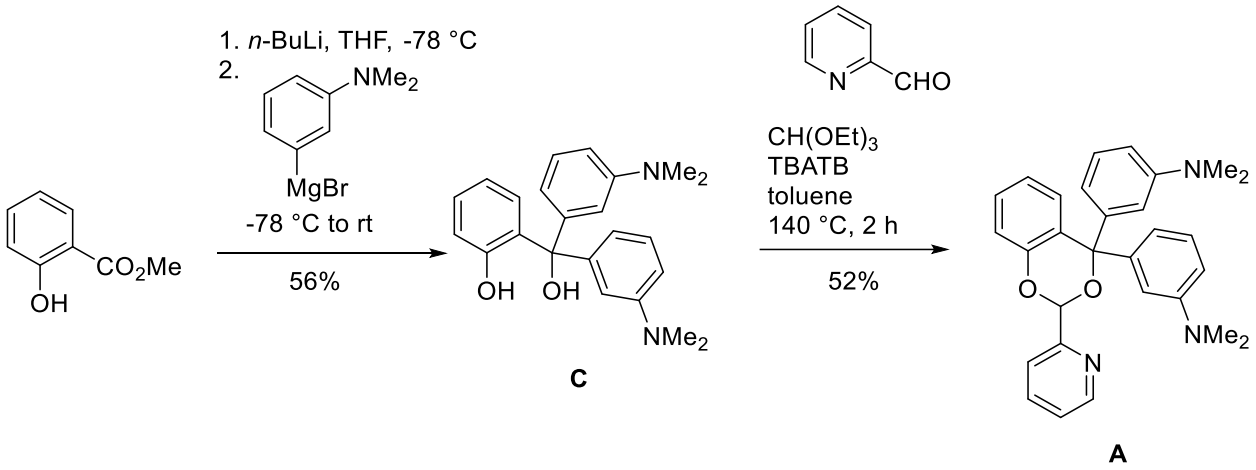

Scheme S1. Synthesis of photolabile protecting group **C** and photo-responsive masked subcomponent **A**.

2.1 Photolabile Protecting Group C

Grignard reagent preparation: Mg turnings (0.19 g, 7.9 mmol) were dried at 130 °C *in vacuo* for 2 h in a 3 neck round-bottom flask. Upon cooling to room temperature, 12 mL THF and a catalytic amount of I_2 were added to the flask. A solution of 3-bromo-*N,N*-dimethylaniline (1.1 mL, 7.7 mmol) in dry THF (8 mL) was added dropwise to the Mg suspension and the mixture was heated at 50 °C for 1 h until the Mg turnings dissolved.

A solution of methyl salicylate (0.5 mL, 3.9 mmol) in dry THF (25 mL) was cooled to -78 °C and *n*-BuLi (1.6 M, 2.4 mL) was added dropwise. The mixture was stirred for 5 min and then added dropwise to the Grignard reagent prepared above. The reaction mixture was allowed to warm to room temperature, stirred overnight then quenched with saturated NH_4Cl (10 mL). Following extraction with DCM (3 x 20 mL), the combined organic layers were dried over $MgSO_4$, filtered and the solvent was removed *in vacuo*. Purification by silica gel chromatography (3:1 hexane/EtOAc) and purification of impure fractions by recrystallization from DCM/hexane gave protecting group **C** as a white solid (0.78 g, 56 %).

^{1}H NMR (CD_3CN, 400 MHz, 298 K) δ (ppm): 8.52 (1H, s, H_k), 7.19 – 7.11 (3H, m, H_b, H_f), 6.79 (1H, dd, J = 8.1 Hz, 1.2 Hz, H_a), 6.74 – 6.67 (5H, m, H_c, H_g, H_i), 6.55 (1H, dd, J = 7.8 Hz, 1.7 Hz, H_d), 6.41 (2H, partially resolved ddd, J = 7.7 Hz, 1.6 Hz, 0.9 Hz, H_e), 5.26 (1H, s, H_j), 2.83 (12H, s, H_h).

^{13}C NMR (CD_3CN, 101 MHz, 298 K) δ (ppm): 157.2 (C_1), 151.5 (C_{12}), 147.4 (C_8), 132.5 (C_6), 130.7 (C_5), 130.0 (C_3), 129.2 (C_{10}), 119.5 (C_4), 117.6 (C_2), 117.3 (C_9), 113.0 ($C_{11/13}$), 112.6 ($C_{11/13}$), 85.0 (C_7), 40.7 (C_{14}).

ESI-MS *m/z*: 182.10 $[M + 2H]^{2+}$, 363.2063 $[M + H]^+$ (calcd for $C_{23}H_{27}N_2O_2$: 363.2073).

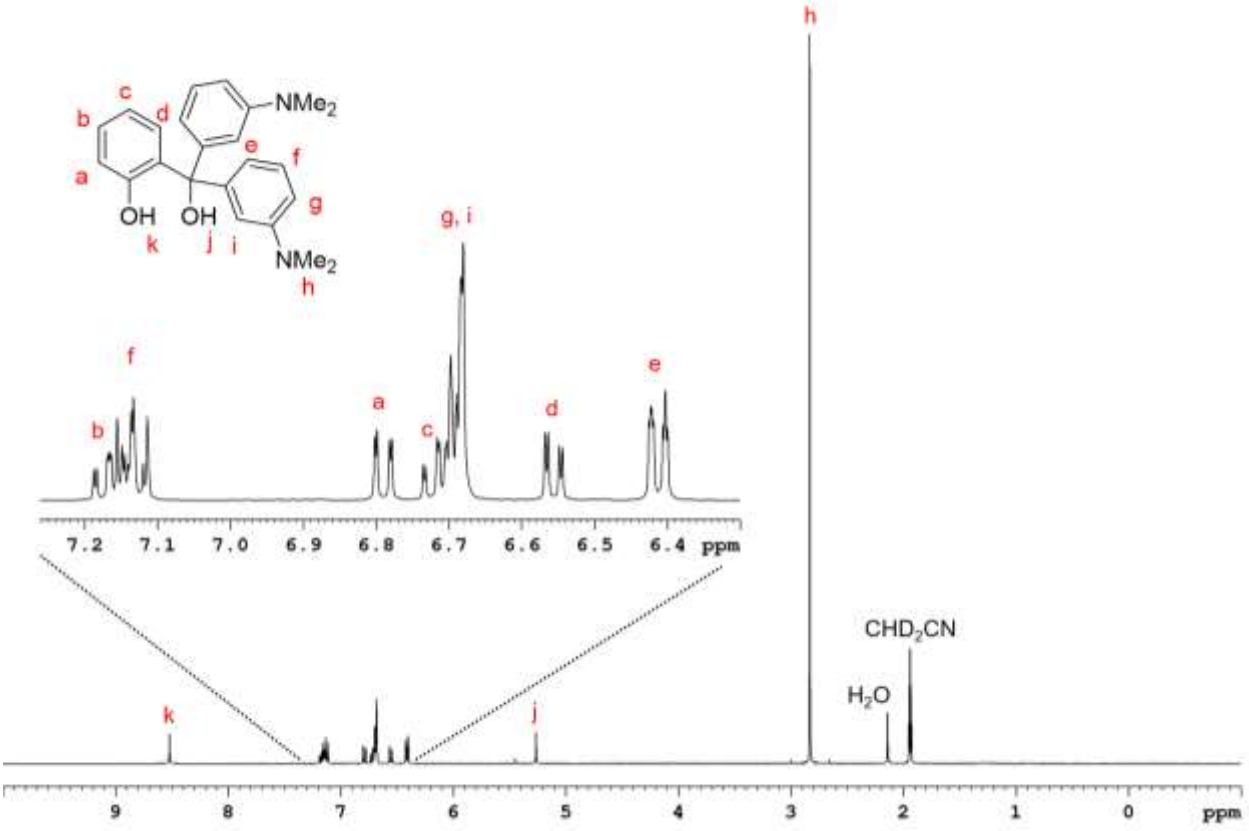

Figure S1. ^{1}H NMR spectrum (400 MHz, 298 K, CD_3CN) of protecting group **C**.

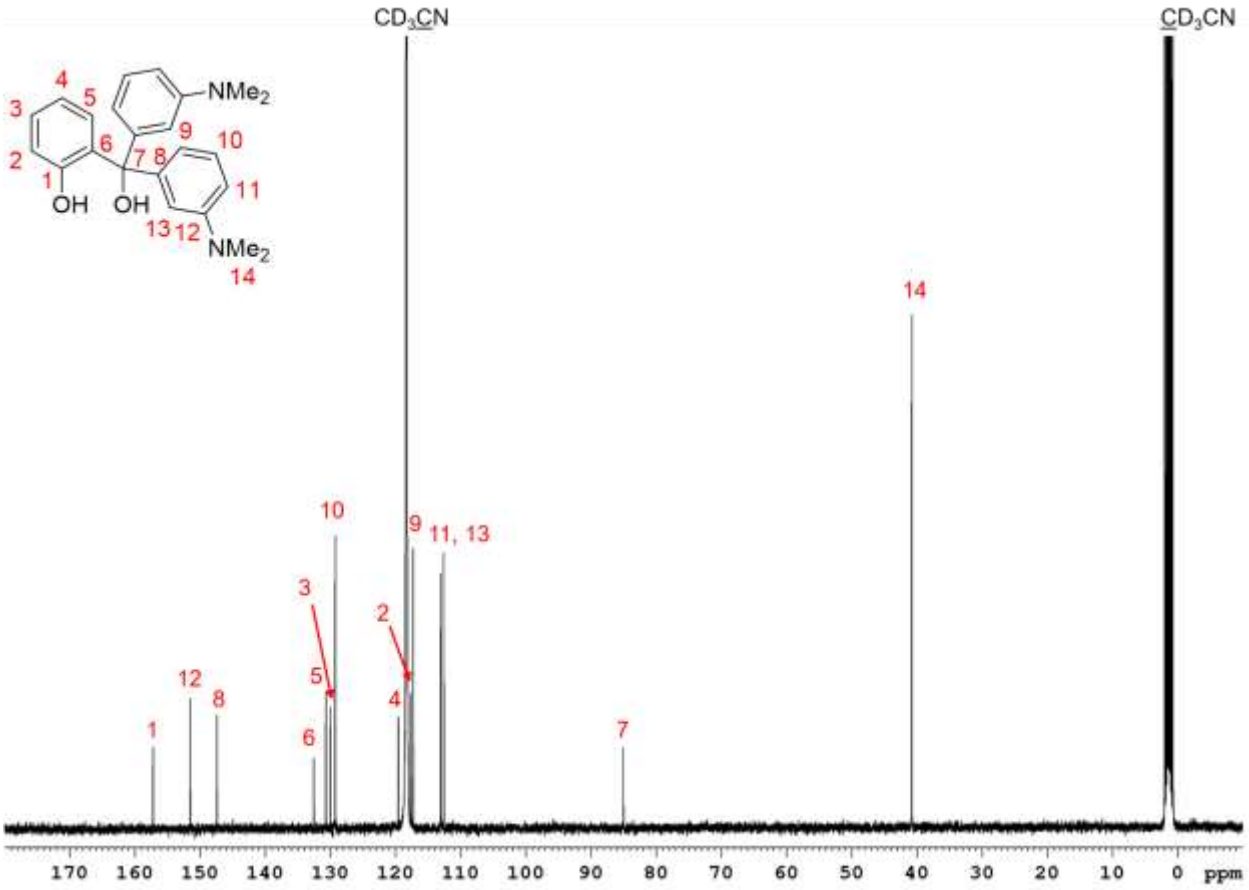

Figure S2. ^{13}C NMR spectrum (101 MHz, 298 K, CD_3CN) of protecting group **C**.

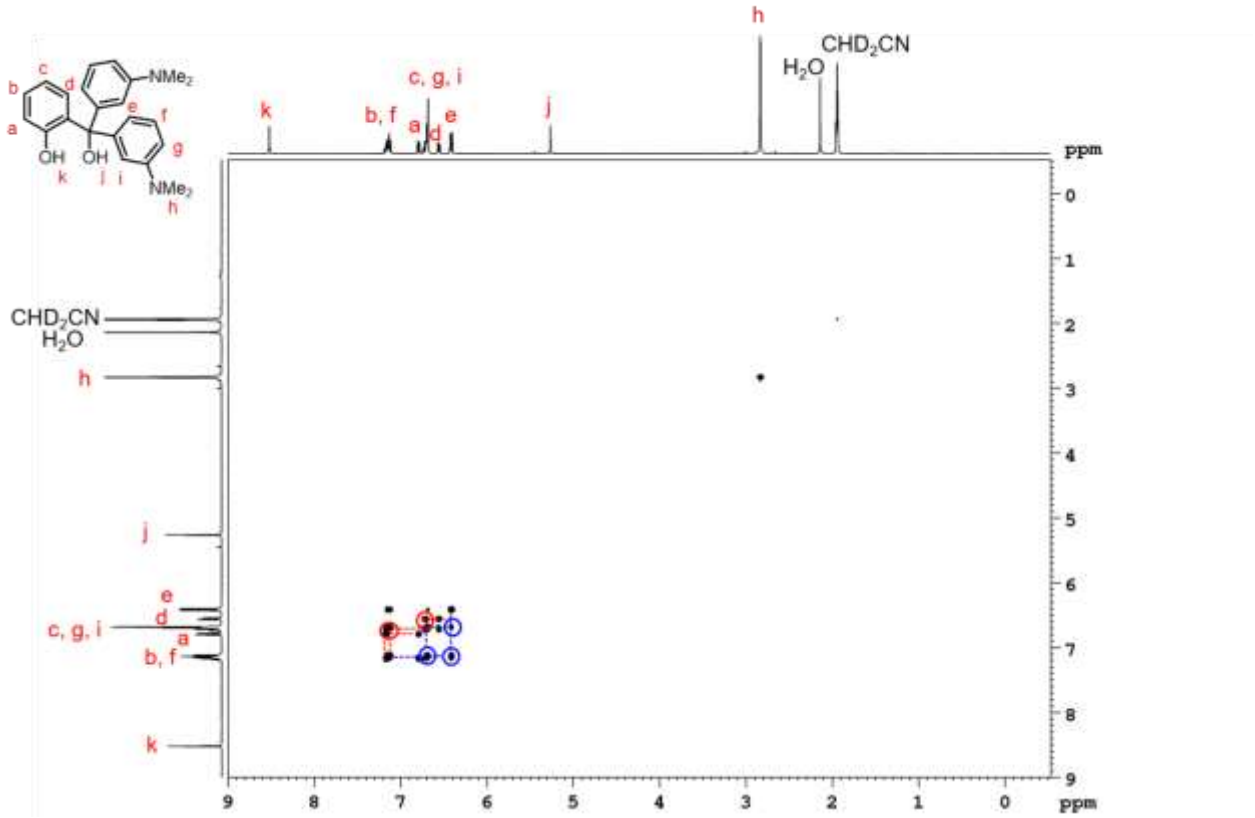

Figure S3. ^{1}H-^{1}H COSY NMR spectrum (400 MHz, 298 K, CD_3CN) of protecting group **C**. Red circles show correlations between protons *a-d* and blue circles show correlations between protons *e-g*.

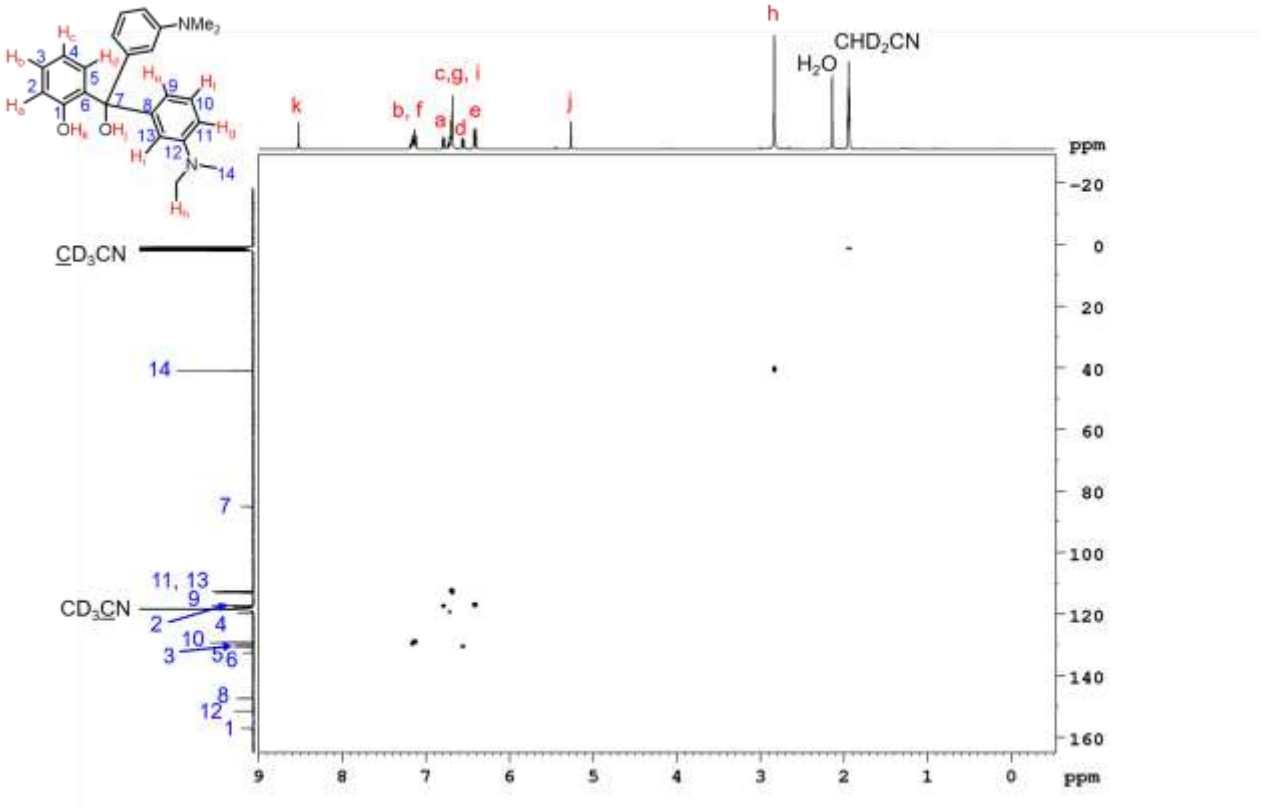

Figure S4. ^{1}H-^{13}C HSQC NMR spectrum (400 MHz/101 MHz, 298 K, CD_3CN) of protecting group **C**.

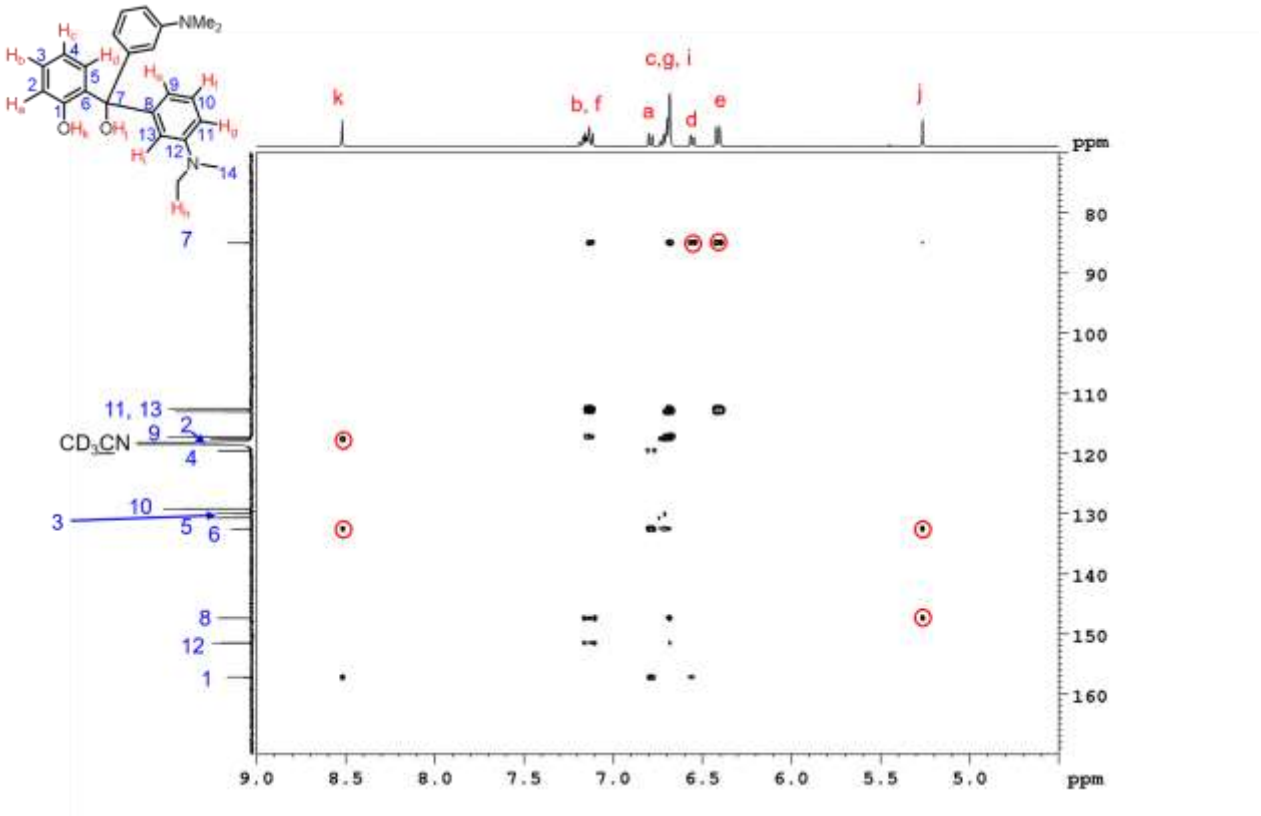

Figure S5. Partial ^{1}H-^{13}C HMBC NMR spectrum (400 MHz/101 MHz, 298 K, CD_3CN) of protecting group **C** with red circles highlighting key correlations for proton and carbon assignments.

2.2 Masked Subcomponent A

Masked subcomponent **A** was synthesised adapting Patel's method for the acetalization of carbonyl compounds using tetrabutylammonium tribromide as an efficient generator of HBr.[1]

Tetrabutylammonium tribromide (1.33 mg, 2 mol%) was added to a solution of 2-pyridinecarboxaldehyde (19.7 µL, 0.21 mmol), triethyl orthoformate (25 µL, 0.15 mmol) and protecting group **C** (50 mg, 0.14 mmol) in toluene. The corresponding solution was heated at 140 °C until the disappearance of **C** was observed (the reaction was monitored by TLC). Subsequently, the reaction mixture was poured into a saturated solution of $NaHCO_3$ and the product was extracted with EtOAc (2 x 10 mL). The combined organic layers were washed with brine and dried over anhydrous $MgSO_4$. The solvent was removed under reduced pressure and the crude was purified by column chromatography on silica gel using DCM/EtOAc (6:1) as eluent. Masked subcomponent **A** was isolated after recrystallization from DCM/hexane as a white solid (32 mg, 52% yield).

^{1}H NMR (CD_3CN, 400 MHz, 298 K) δ (ppm): 8.55 (1H, ddd, J = 4.9 Hz, 1.6 Hz, 1.0 Hz, H_n), 7.93 – 7.85 (2H, m, H_l, H_k), 7.41 (1H, ddd, J = 7.4 Hz, 4.9 Hz, 1.5 Hz, H_m), 7.26 – 7.20 (2H, m, H_b, $H_{f'}$), 7.11 (1H, t, J = 7.9 Hz, H_f), 7.04 (1H, dd, J = 7.7 Hz, 1.6 Hz, H_d), 6.97 (1H, dd, J = 8.2 Hz, 1.1 Hz, H_a), 6.92 (1H, td, J = 7.7 Hz, 1.1 Hz, H_c), 6.79 – 6.73 (3H, m, $H_{g'}$, H_i, $H_{i'}$), 6.67 – 6.62 (2H, m, $H_{e'}$, H_g), 6.59 (1H, dt, J = 7.9 Hz, 1.0 Hz, H_e), 5.97 (1H, s, H_j), 2.83 (6H, s, $H_{h'}$), 2.81 (6H, s, H_h).

^{13}C NMR (CD_3CN, 125 MHz, 298 K) δ (ppm): 157.1 (C_{16}), 153.1 (C_1), 151.6 ($C_{12'}$), 151.4 (C_{12}), 150.0 (C_{20}), 147.5 (C_8), 145.5 ($C_{8'}$), 138.3 (C_{18}), 130.7 (C_5), 129.6 (C_3), 129.5 ($C_{10'}$), 129.4 (C_{10}), 127.1 (C_6), 125.6 (C_{19}), 122.1 (C_{17}), 121.5 (C_4), 118.3 ($C_{9'}$), 118.0 (C_2), 117.3 (C_9), 114.0 ($C_{13'}$), 113.2 ($C_{11'}$, C_{13}), 112.7 (C_{11}), 96.6 (C_{15}), 86.6 (C_7), 40.7 (C_{14}), 40.6 ($C_{14'}$).

ESI-MS *m/z*: 226.61 $[M + 2H]^{2+}$, 345.19 [protecting group **C** fragment – OH]$^{+}$, 452.2333 $[M + H]^{+}$ (calcd for $C_{29}H_{30}N_3O_2$: 452.2338).

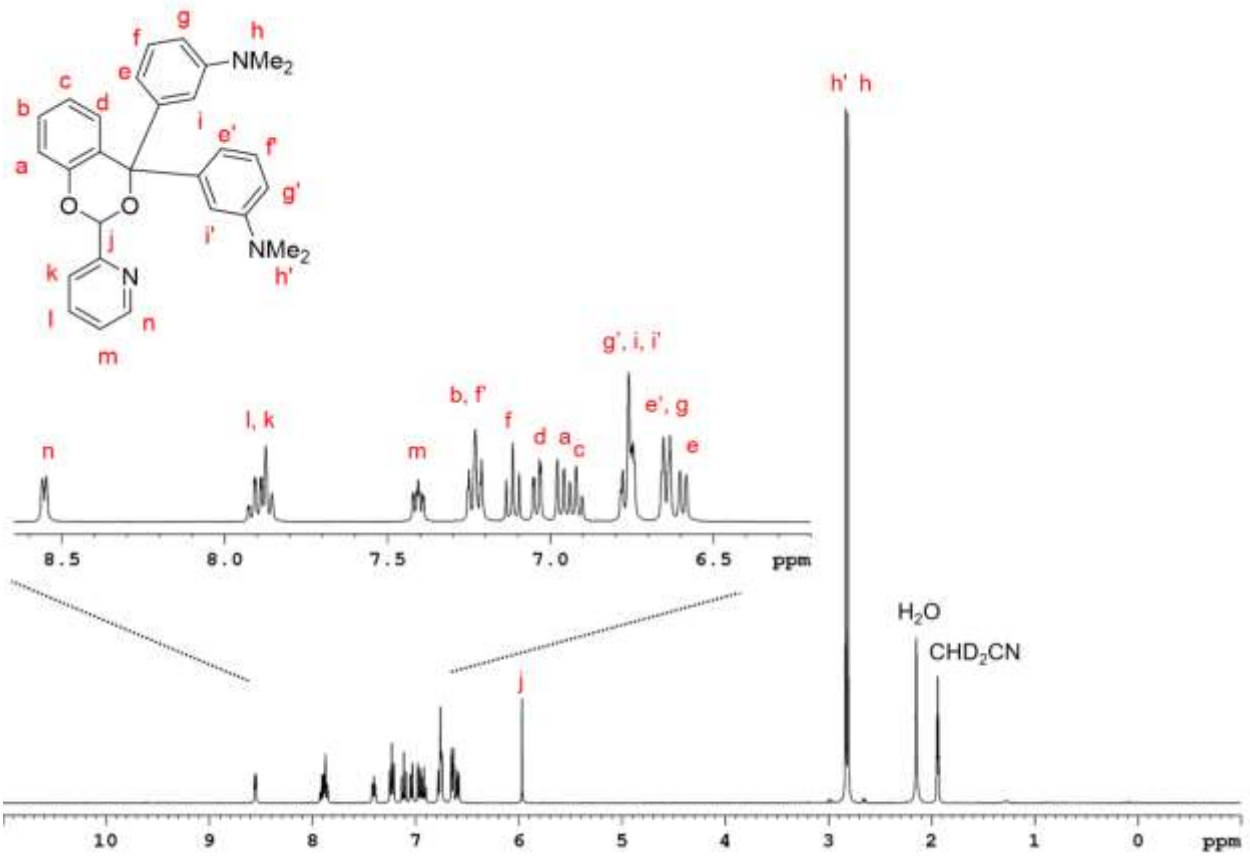

Figure S6. ^{1}H NMR spectrum (400 MHz, 298 K, CD_3CN) of masked subcomponent **A**.

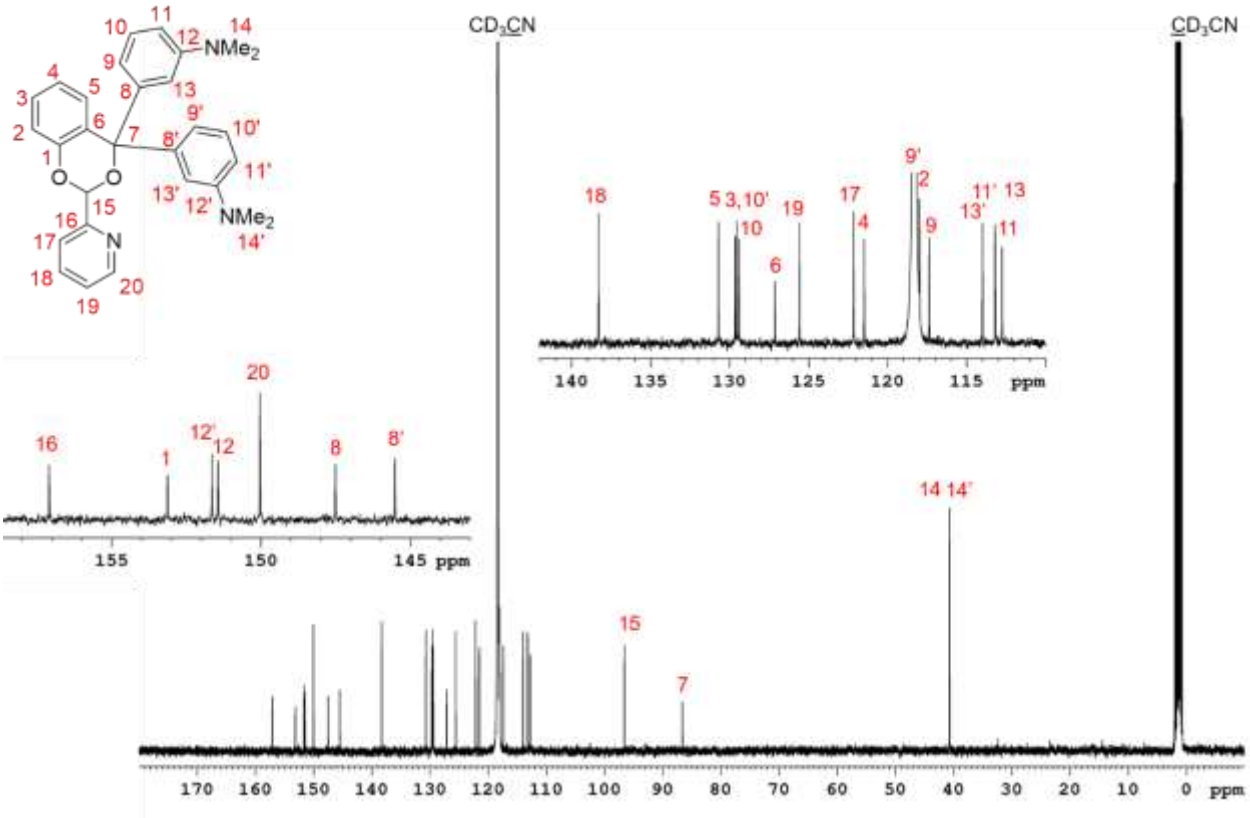

Figure S7. ^{13}C NMR spectrum (125 MHz, 298 K, CD_3CN) of masked subcomponent **A**.

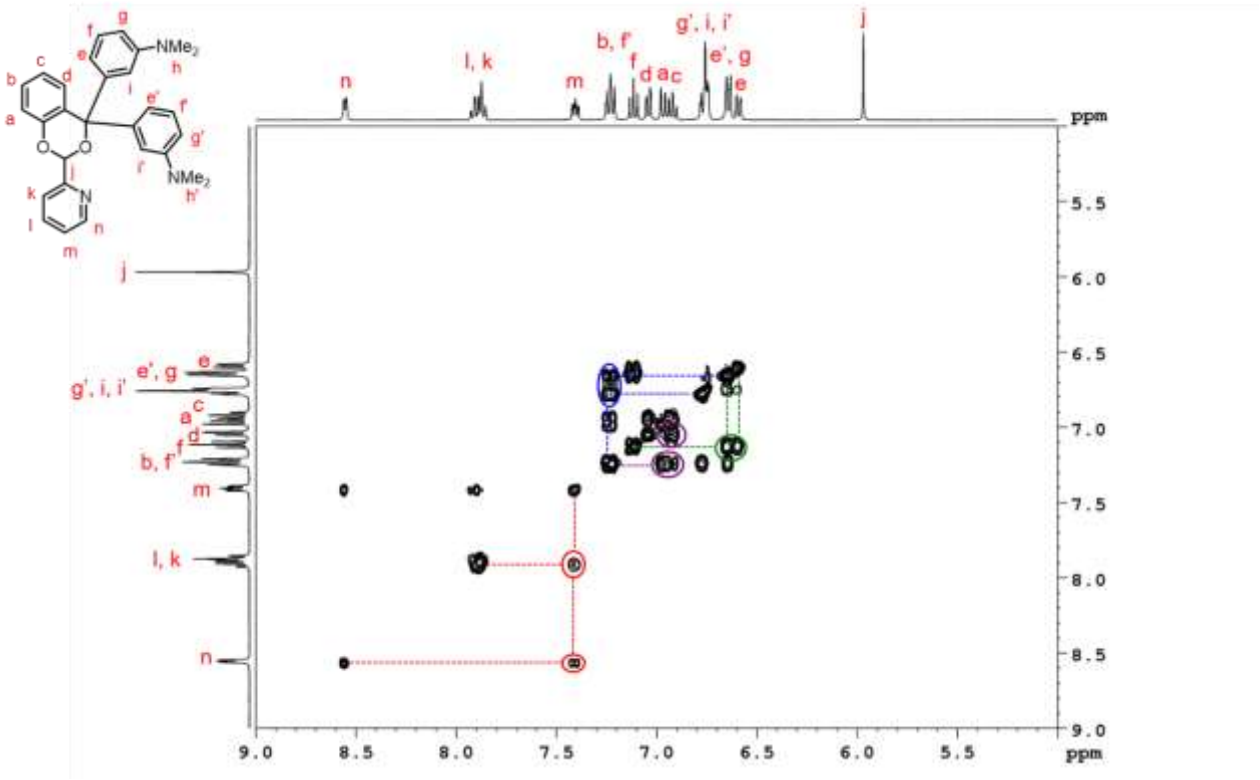

Figure S8. ^{1}H-^{1}H COSY NMR spectrum (400 MHz, 298 K, CD_3CN) of masked subcomponent **A**. Red circles show correlations between protons *k-m*, blue circles show correlations between protons *e'-g'*, blue circles show correlations between protons *e-g* and purple circles show correlations between protons *a-d*.

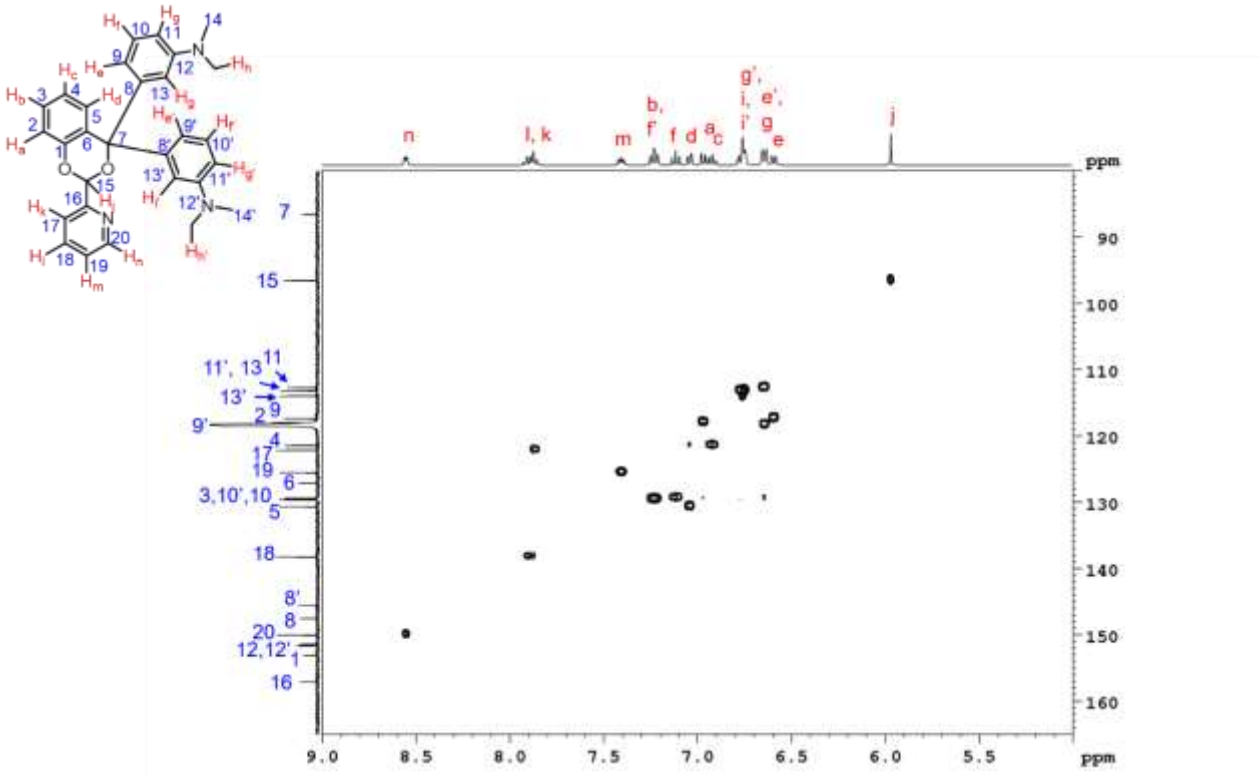

Figure S9. Partial ^{1}H-^{13}C HSQC NMR spectrum (400 MHz/101 MHz, 298 K, CD_3CN) of masked subcomponent **A**.

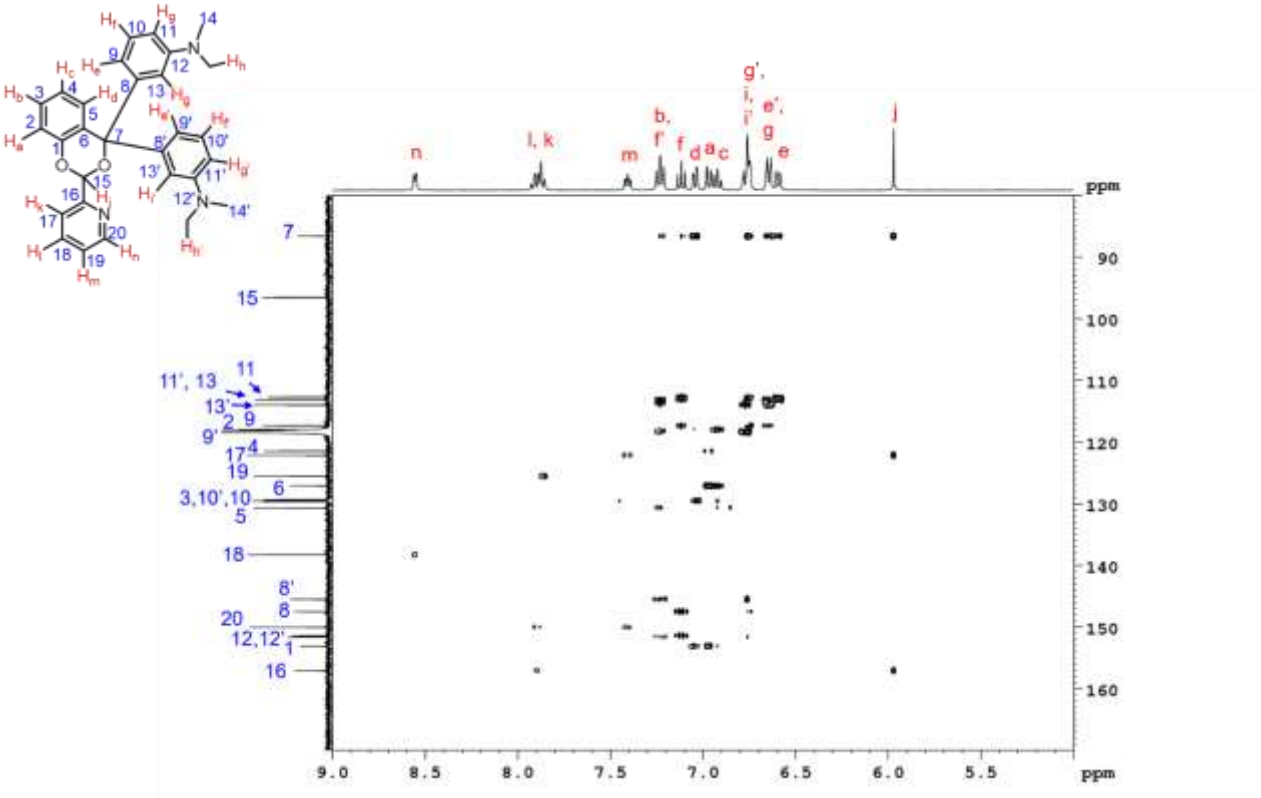

Figure S10. Partial ^{1}H-^{13}C HMBC NMR spectrum (400 MHz/101 MHz, 298 K, CD_3CN) of masked subcomponent **A**.

2.3 Masked Subcomponent B

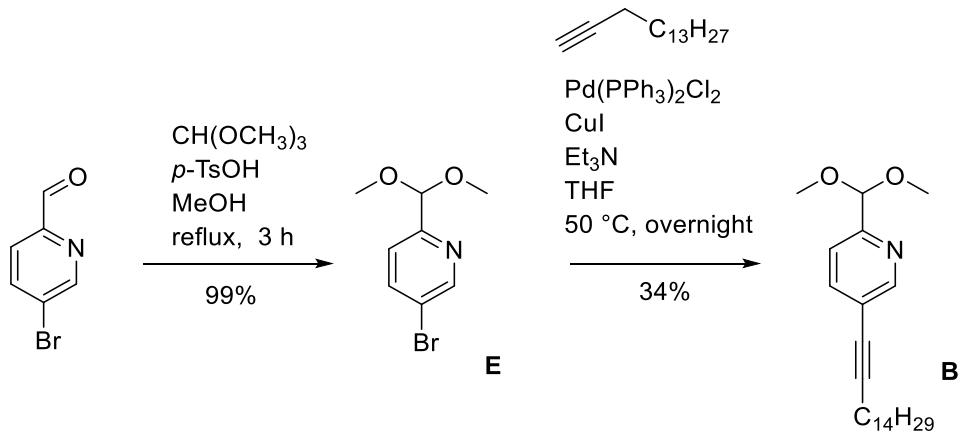

Scheme S2. Synthesis of masked subcomponent **B**.

5-Bromo-2-(dimethoxymethyl)pyridine (**E**) was synthesized according to literature procedures.[2]

A solution of **E** (1.1 g, 4.7 mmol), 1-hexadecyne (1.64 mL, 5.9 mmol), CuI (55 mg, 0.3 mmol) and Et_3N (2.0 mL, 14 mmol) was prepared in THF (20 mL) and degassed. $Pd(PPh_3)_2Cl_2$ (183 mg, 0.26 mmol) was added, and the mixture was heated to 50 °C overnight under N_2. On cooling, the crude mixture was filtered through Celite and the solvent was removed under reduced pressure. The residue was re-dissolved in 50 mL DCM, washed with 3 x 50 mL saturated aqueous NH_4Cl and dried over $MgSO_4$. The solvent was removed under reduced pressure and the crude residue was purified by column chromatography on alumina eluting with a gradient of petroleum ether (40:60)/ EtOAc from 10:0 to 9:1. Masked subcomponent **B** was isolated as a yellow oil (595 mg, 34% yield).

^{1}H NMR ($CDCl_3$, 400 MHz, 298 K) δ (ppm): 8.60 (1H, d, J = 1.5 Hz, H_e), 7.69 (1H, dd, J = 8.1 Hz, 2.2 Hz, H_d), 7.45 (1H, d, J = 8.1 Hz, H_c), 5.35 (1H, s, H_b), 3.37 (6H, s, H_a), 2.40 (2H, d, J = 7.1 Hz, H_f), 1.68–1.55 (2H, m, H_g), 1.49 – 1.36 (2H, m, H_h), 1.35–1.18 (20H, m, H_i, H_j, H_k, H_l, H_m, H_n, H_o, H_p, H_q, H_r), 0.87 (3H, t, J = 6.7 Hz, H_s).

^{13}C NMR ($CDCl_3$, 101 MHz, 298 K) δ (ppm): 155.5 (C_3), 151.8 (C_6), 139.2 (C_5), 121.1 (C_7), 120.7 (C_4), 103.7 (C_2), 94.6 (C_8), 77.4 (C_9), 53.7 (C_1), 32.1, 29.8, 29.8, 29.8, 29.7, 29.5, 29.3 (C_{13} – C_{21}), 29.1 (C_{12}), 28.7 (C_{11}), 22.8 (C_{22}), 19.6 (C_{10}), 14.3 (C_{23}).

ASAP/APCI-MS *m/z*: 372.2897 $[M - H]^+$ (calcd for $C_{24}H_{38}O_2$: 372.2897), 373.2931 $[M]^+$ (calcd for $C_{24}H_{39}O_2$ 373.2930), 374.2691 $[M + H]^+$ (calcd for $C_{24}H_{40}O_2$ 374.2961). Note that the observation of $[M – H]^+$ and $[M]^+$ ions is not uncommon in APCI-MS.[3]

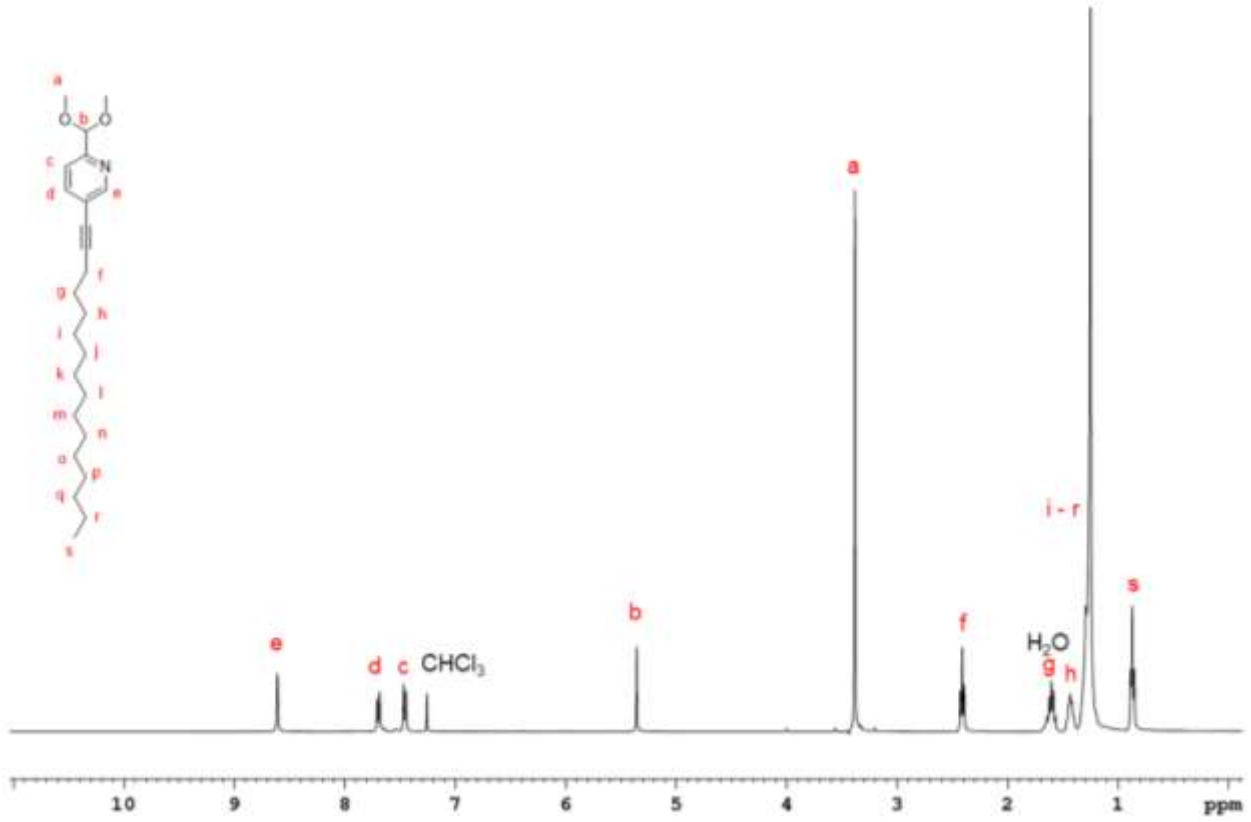

Figure S11. ^{1}H NMR spectrum (400 MHz, 298 K, $CDCl_3$) of masked subcomponent **B**.

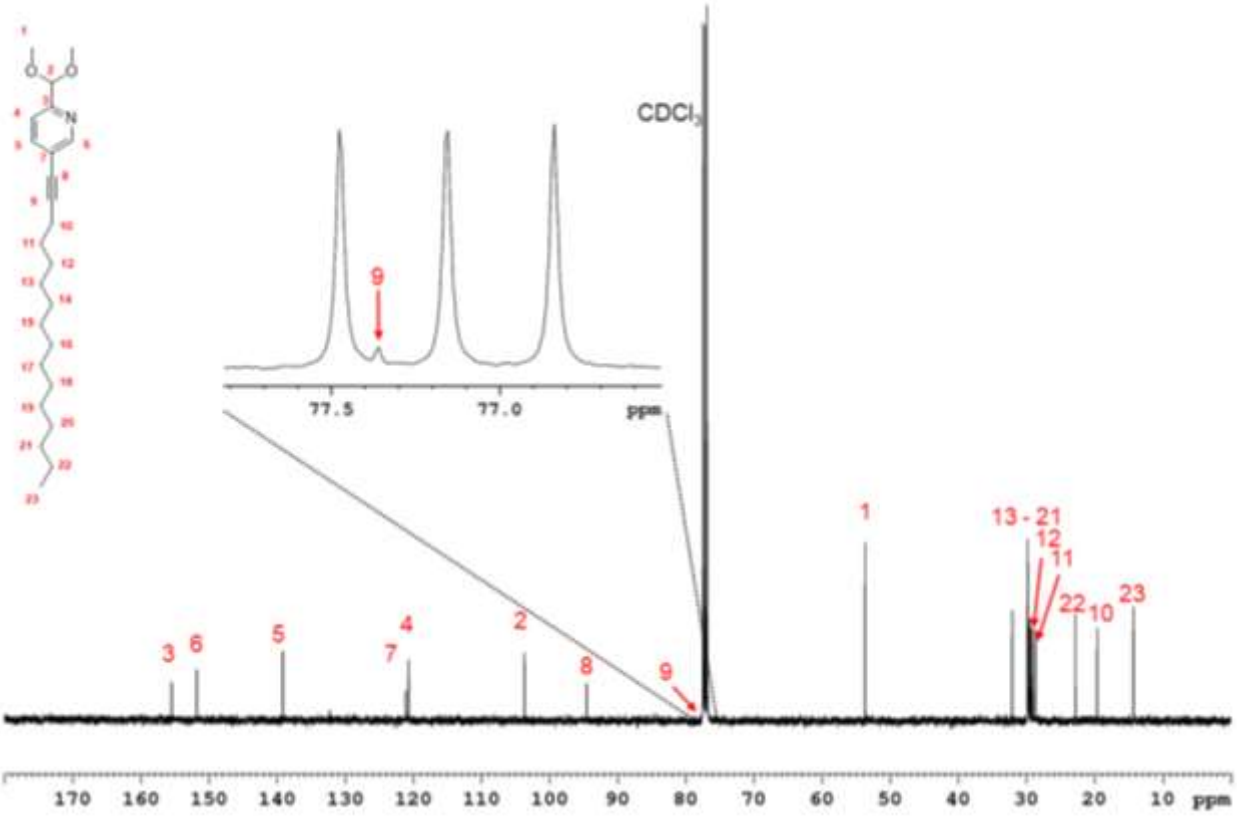

Figure S12. ^{13}C NMR spectrum (101 MHz, 298 K, $CDCl_3$) of masked subcomponent **B**.

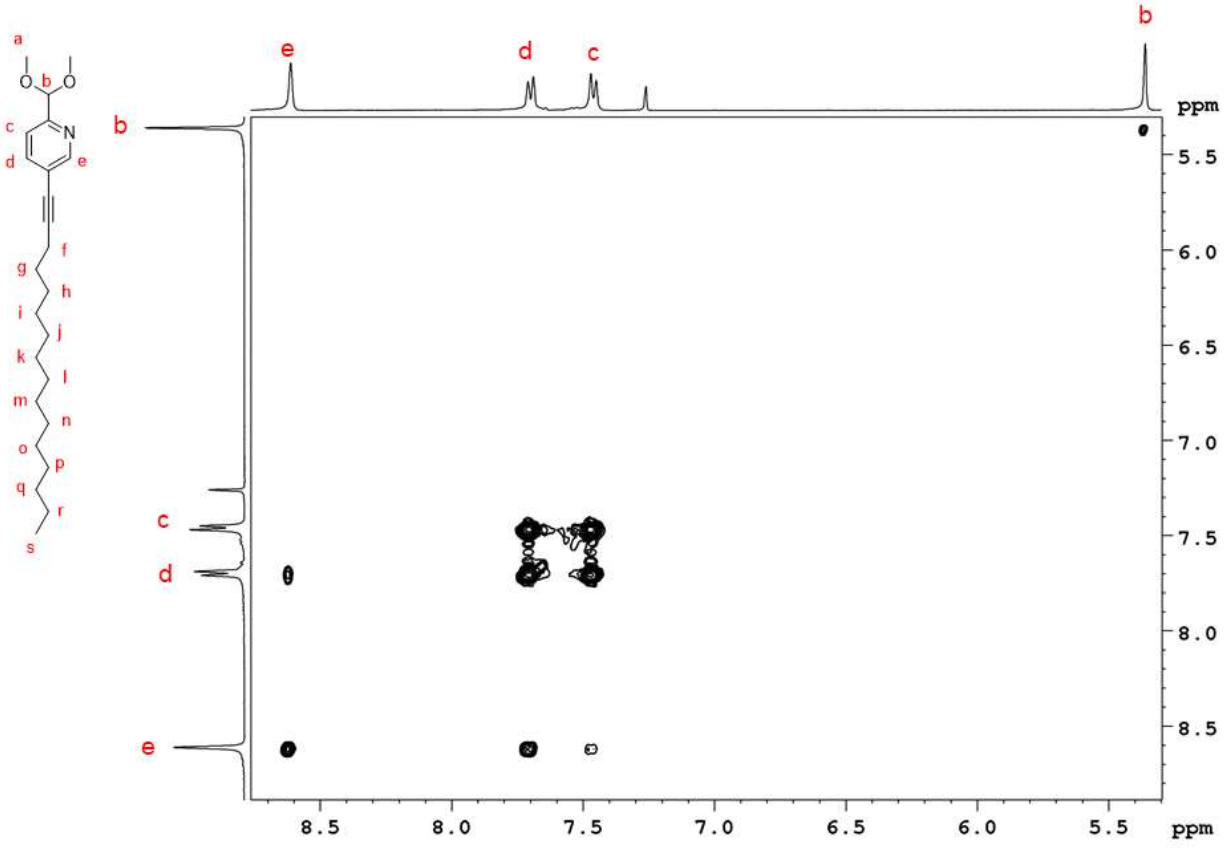

Figure S13. ^{1}H-^{1}H COSY NMR spectrum (400 MHz, 298 K, $CDCl_3$) of masked subcomponent **B**.

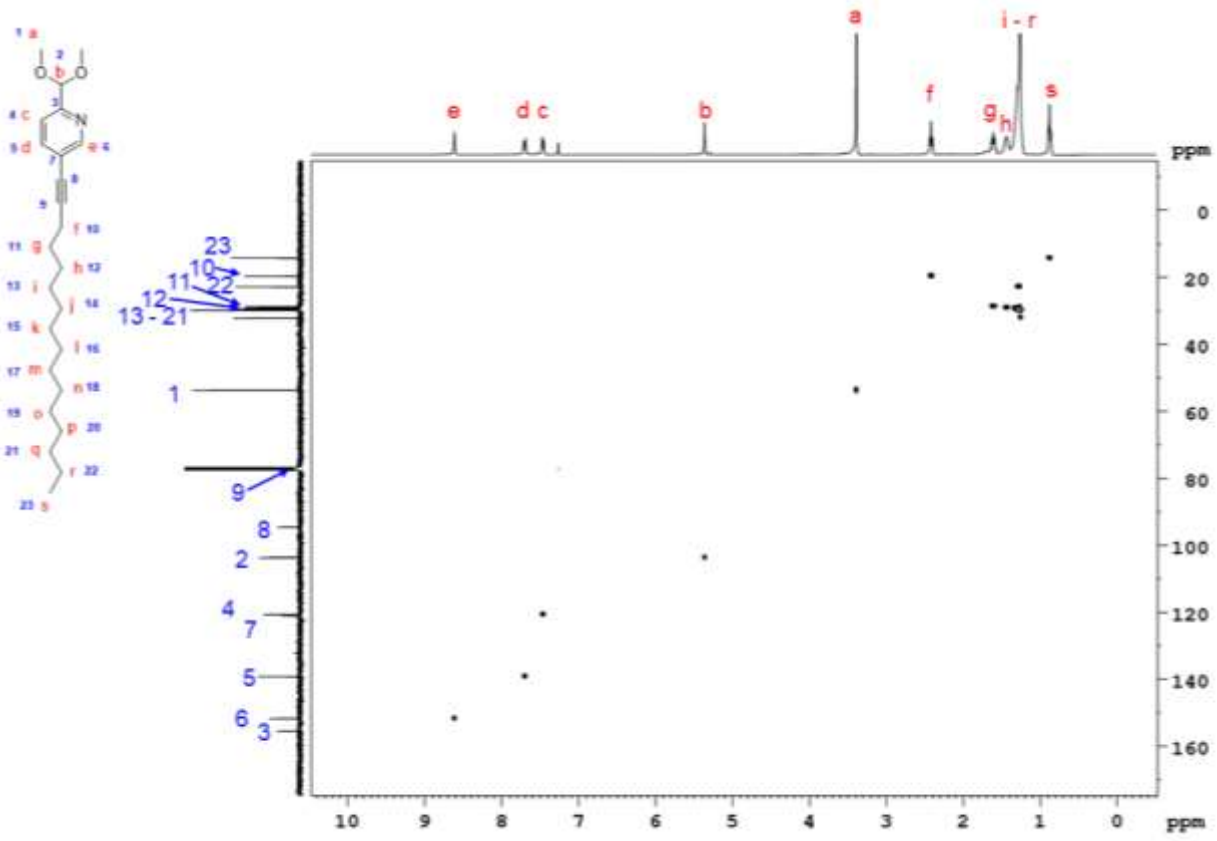

Figure S14. ^{1}H-^{13}C HSQC NMR spectrum (400 MHz/101 MHz, 298 K, $CDCl_3$) of masked subcomponent **B**.

2.4 Triamine D

Triamine **D** was prepared according to literature procedures.[4]

3 Synthesis and Host-Guest Complexes of Cages 1 and 2

3.1 Cage 1

Cage **1** was prepared according to a previously reported modified literature procedure.[4b]

3.1.1 [Adamantane ⊂ **1**]$^{8+}$

The host-guest complex was previously reported.[4a]

3.1.2 [Cyclopentane ⊂ **1**]$^{8+}$

The host-guest complex was previously reported.[4a]

3.1.3 [Benzene ⊂ **1**]$^{8+}$

Cage **1** (4.24 mg, 0.001 mmol) and benzene (1.17 mg, 0.015 mmol) were dissolved in CD_3CN (0.5 mL) and the mixture was left to equilibrate for 1 day at 298 K.

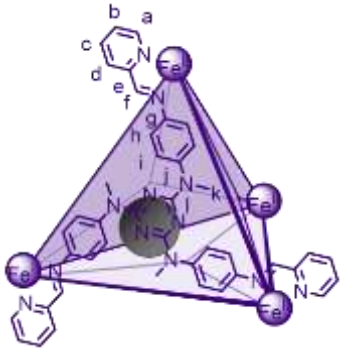

^{1}H NMR (400 MHz, CD_3CN, 298 K) δ (ppm): 8.91 (12H, s, H_f), 8.55 (12H, d, J = 7.0 Hz, H_d), 8.39 (12H, t, J = 7.0 Hz, H_c), 7.74 (12H, t, J = 7.0 Hz, H_b), 7.47 – 7.35 (36H, m, H_a, H_i), 7.07 (6H, s, encapsulated benzene) 5.09 (24H, b, H_h), 3.43 (36H, s, H_k).

Most carbons of the host-guest complex were not visible as they overlapped with the empty cage or were too small in intensity.

Only the empty cage was observed in the ESI mass spectrum.

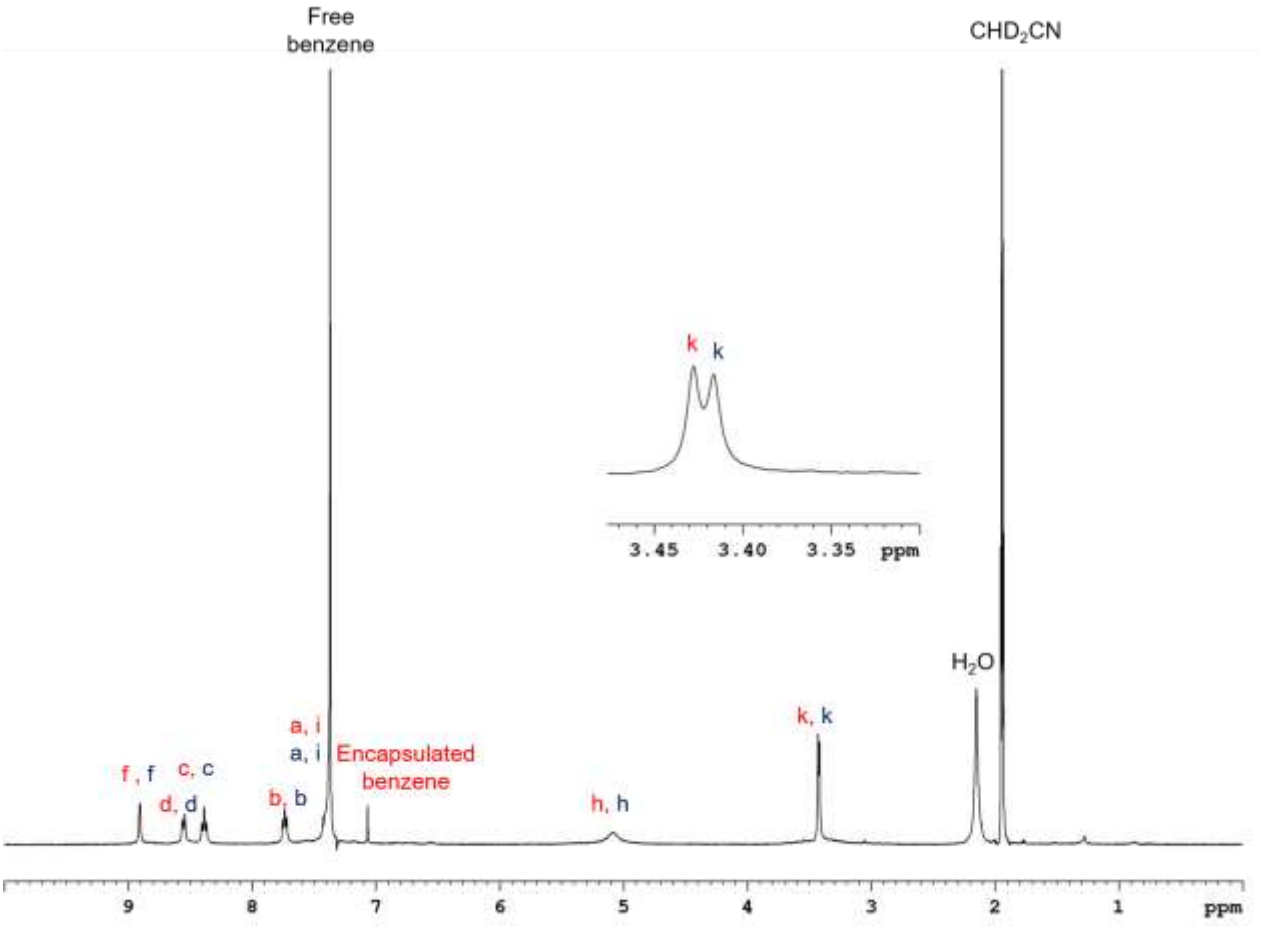

Figure S15. ^{1}H NMR spectrum (400 MHz, 298 K, CD_3CN) of [benzene ⊂ **1**]$(OTf)_8$ (red labels) and empty cage **1** (blue labels).

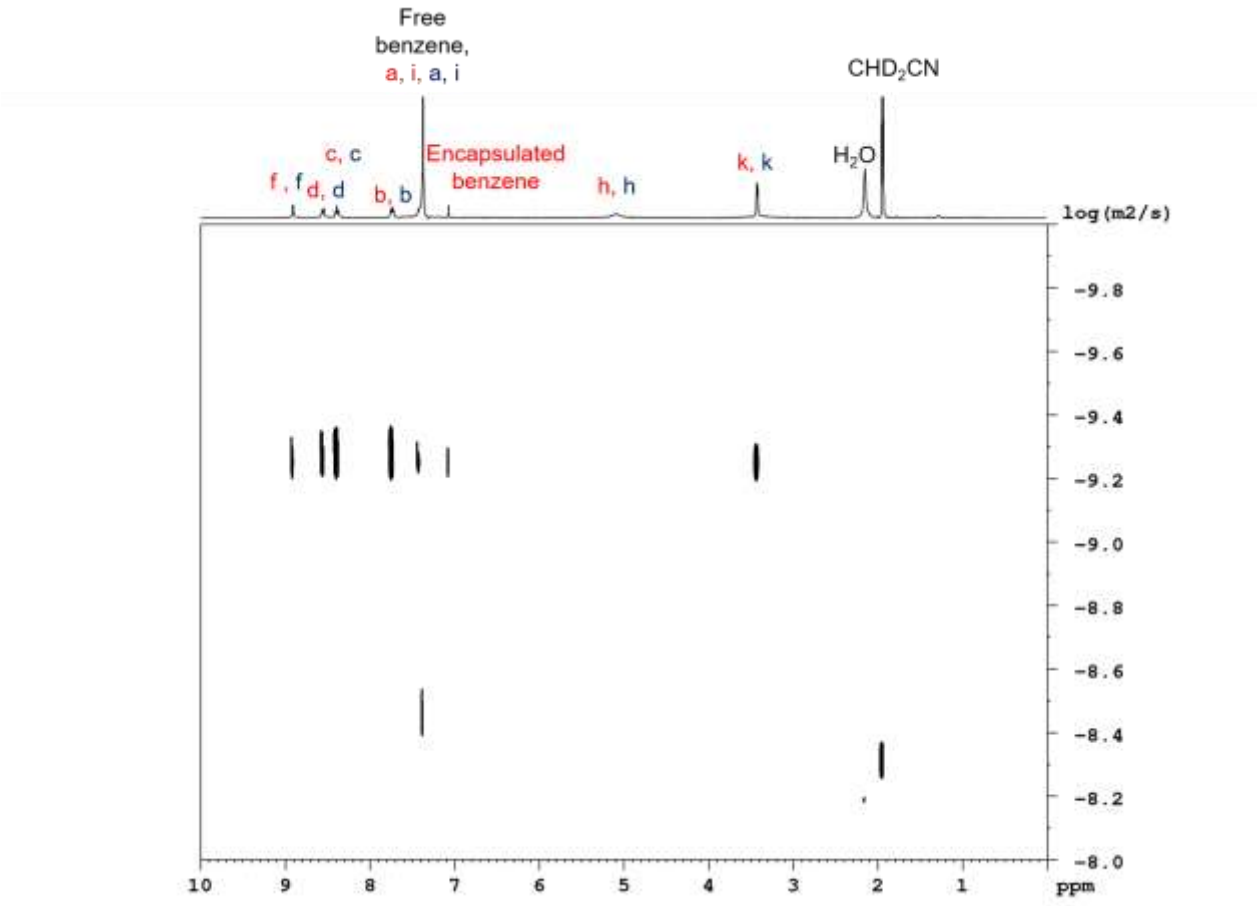

Figure S16. ^{1}H DOSY NMR spectrum (400 MHz, 298 K, CD_3CN) of [benzene ⊂ **1**](OTf)$_8$ (red labels) and empty cage **1** (blue labels).

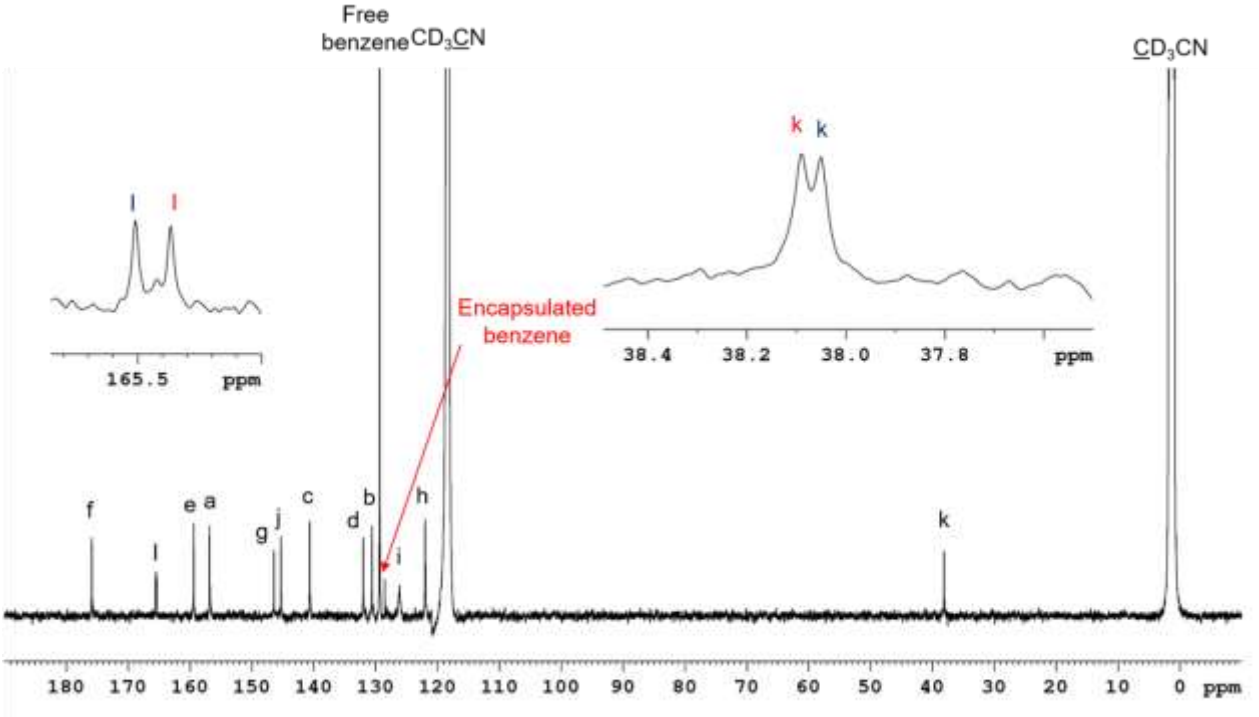

Figure S17. ^{13}C NMR spectrum (125 MHz, 298 K, CD_3CN) of [benzene ⊂ **1**](OTf)$_8$ (red labels) and empty cage **1** (blue labels). Most carbons (black labels) could not be assigned as host-guest complex or empty cage due to signal overlap.

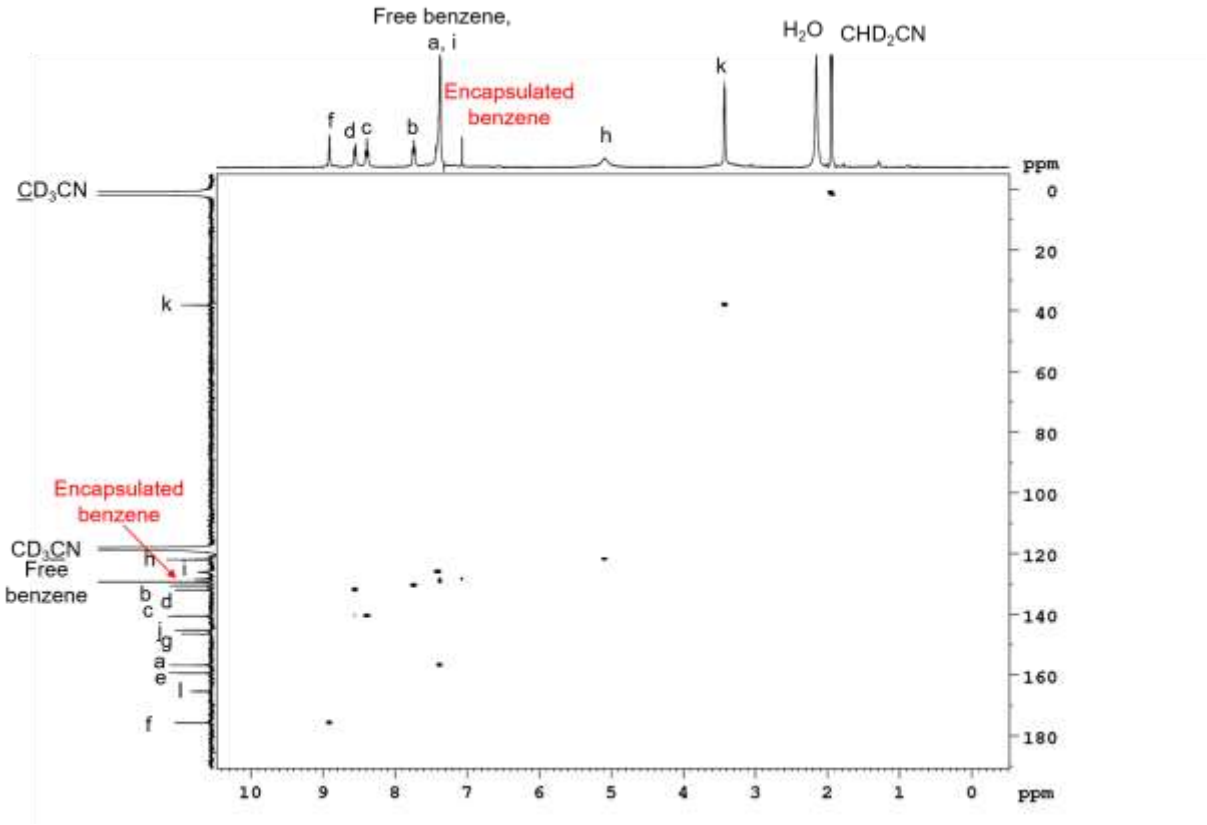

Figure S18. ^{1}H-^{13}C HSQC NMR spectrum (400 MHz/101 MHz, 298 K, CD_3CN) of [benzene ⊂ **1**](OTf)$_8$.

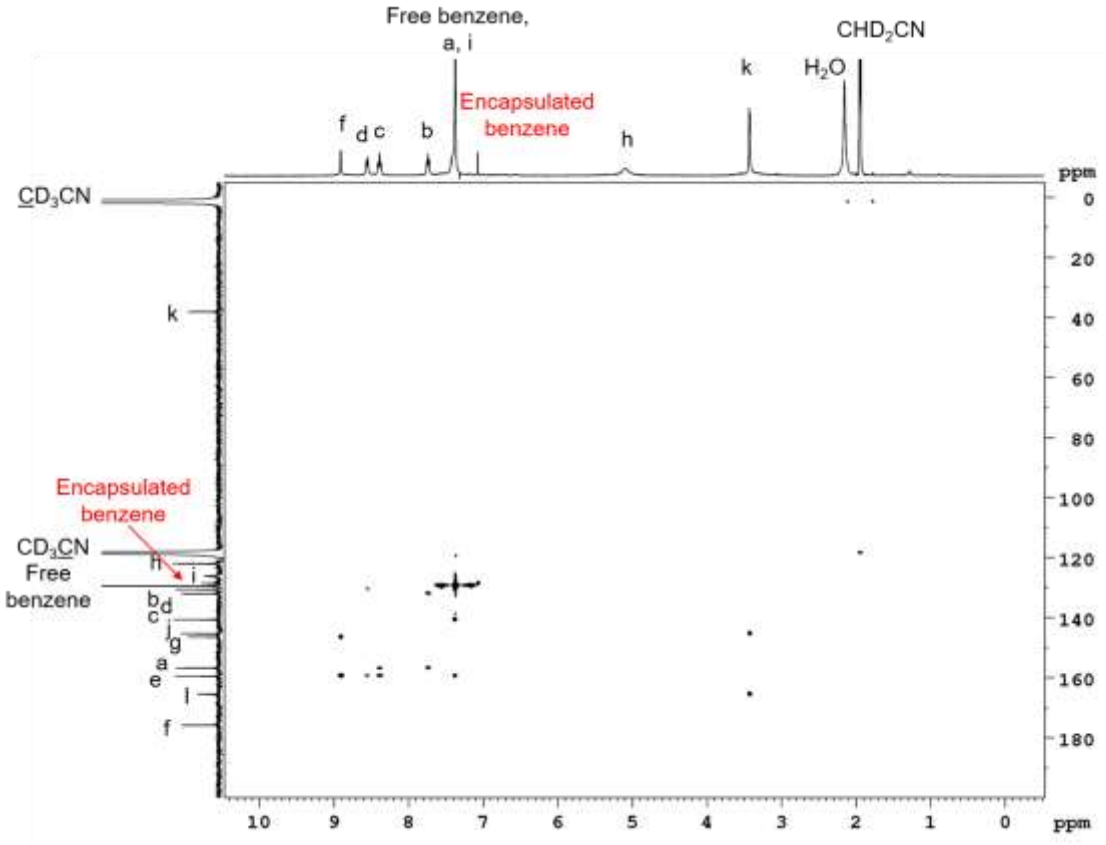

Figure S19. ^{1}H-^{13}C HMBC NMR spectrum (400 MHz/101 MHz, 298 K, CD_3CN) of [benzene ⊂ **1**](OTf)$_8$.

3.1.4 [Ferrocene ⊂ **1**]$^{8+}$

Cage **1** (4.27 mg, 0.001 mmol) and ferrocene (2.44 mg, 0.013 mmol) were dissolved in CD_3CN (0.5 mL) and the mixture was left to equilibrate for 1 day at 298 K.

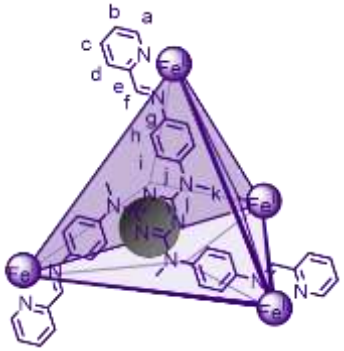

^{1}H NMR (400 MHz, CD_3CN, 298 K) δ (ppm): 8.91 (12H, bs, H_f), 8.56 (12H, b, H_d), 8.39 (12H, b, H_c), 7.74 (12H, b, H_b), 7.47 – 7.35 (m, 36H, H_a, H_i), 5.12 (24H, b, H_h), 3.92 (10H, s, encapsulated ferrocene), 3.43 (36H, bs, H_k).

^{13}C NMR (125 MHz, CD_3CN, 298 K) δ (ppm): 176.1 (C_f), 165.6 (C_l), 159.4 (C_e), 156.8 (C_a), 146.5 (C_g), 145.2 (C_j), 140.6 (C_c), 132.0 (C_d), 130.6 (C_b), 126.3 (C_i), 121.8 (C_h), 68.5 (encapsulated ferrocene), 38.3 (C_k).

Assignments of quaternary carbons are based on assignments for other host-guest complexes for cage **1**[4a] since cross-peaks in the HMBC were not observed, most likely due to the broadness of the signals in the ^{1}H NMR spectrum.

ESI-MS *m/z*: 484.5 [ferrocene ⊂ **1** + OTf]$^{7+}$, 590.4 [ferrocene ⊂ **1** + 2OTf]$^{6+}$, 738.2 [ferrocene ⊂ **1** + 3OTf]$^{5+}$, 960.2 [ferrocene ⊂ **1** + 4OTf]$^{4+}$, 1329.5 [ferrocene ⊂ **1** + 5OTf]$^{3+}$.

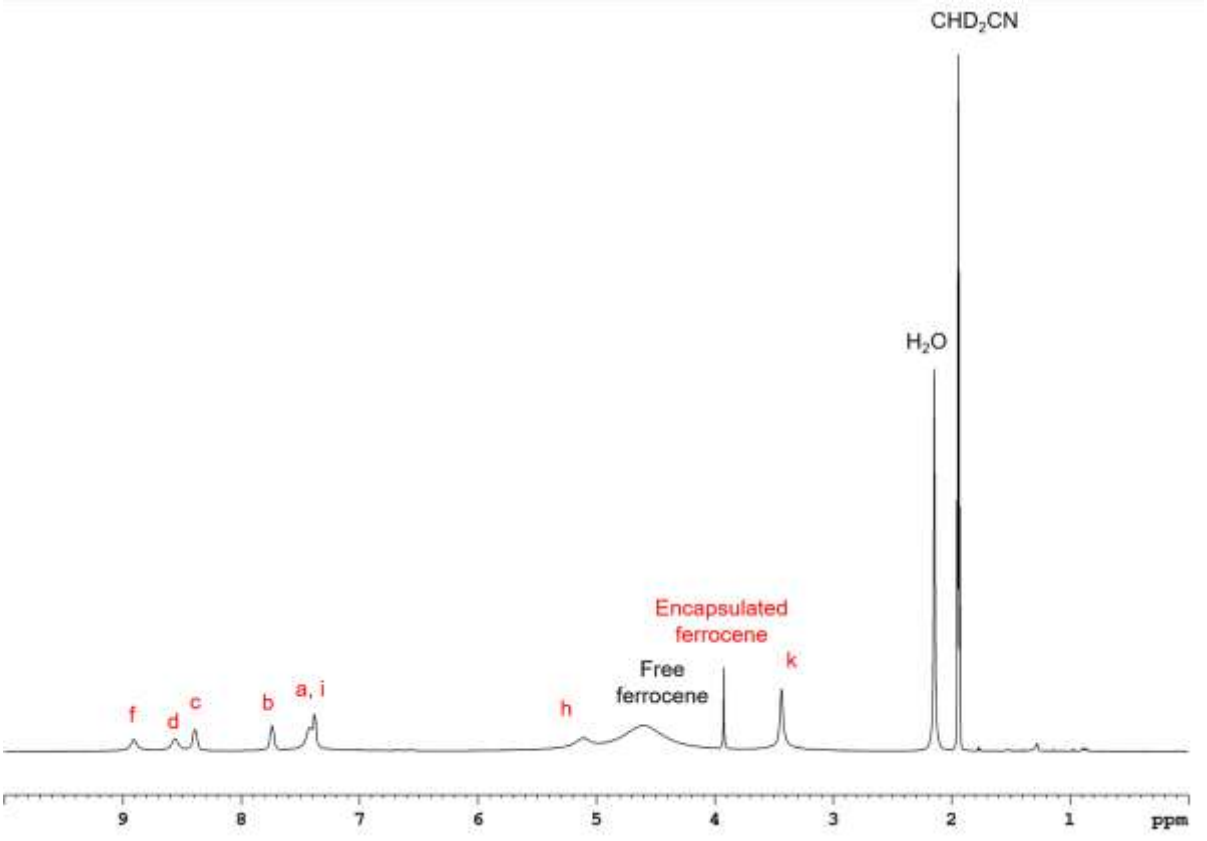

Figure S20. ^{1}H NMR spectrum (400 MHz, 298 K, CD_3CN) of [ferrocene ⊂ **1**](OTf)$_8$.

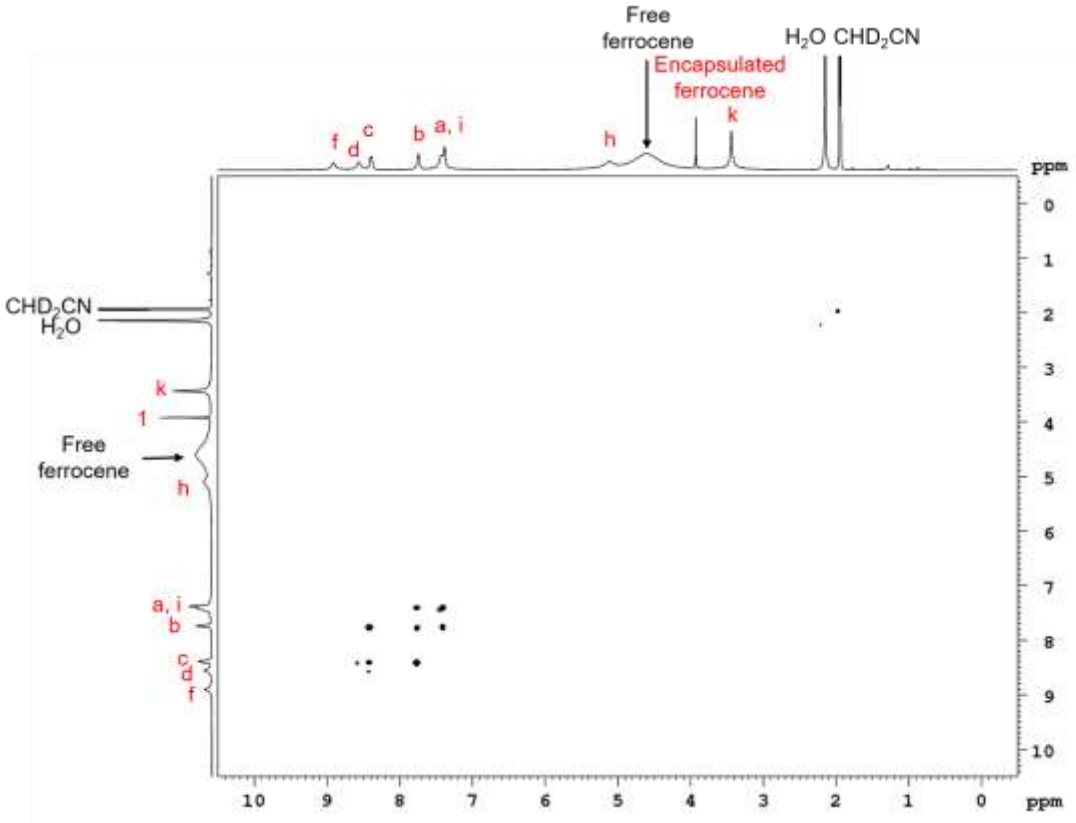

Figure S21. ^{1}H-^{1}H COSY NMR spectrum (400 MHz/400 MHz, 298 K, CD_3CN) of [ferrocene ⊂ **1**](OTf)$_8$.

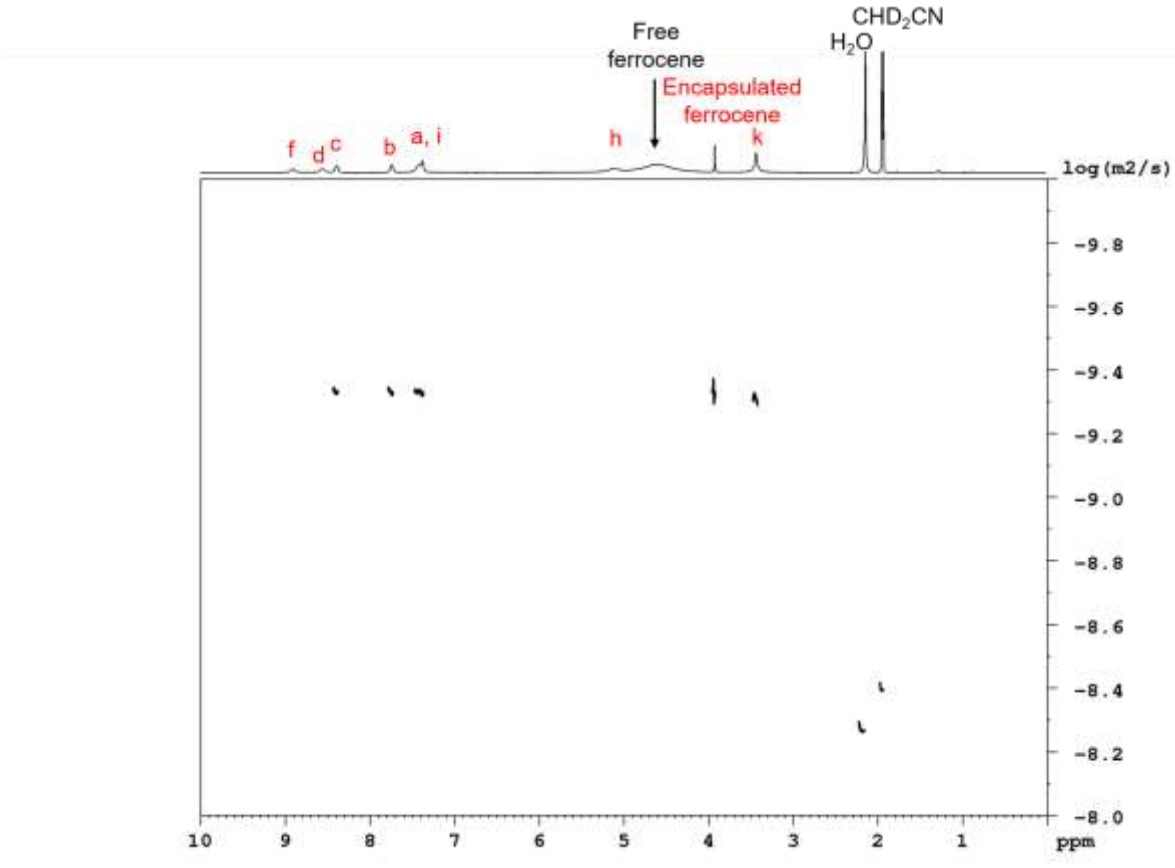

Figure S22. ^{1}H DOSY NMR spectrum (400 MHz, 298 K, CD_3CN) of [ferrocene ⊂ **1**](OTf)$_8$.

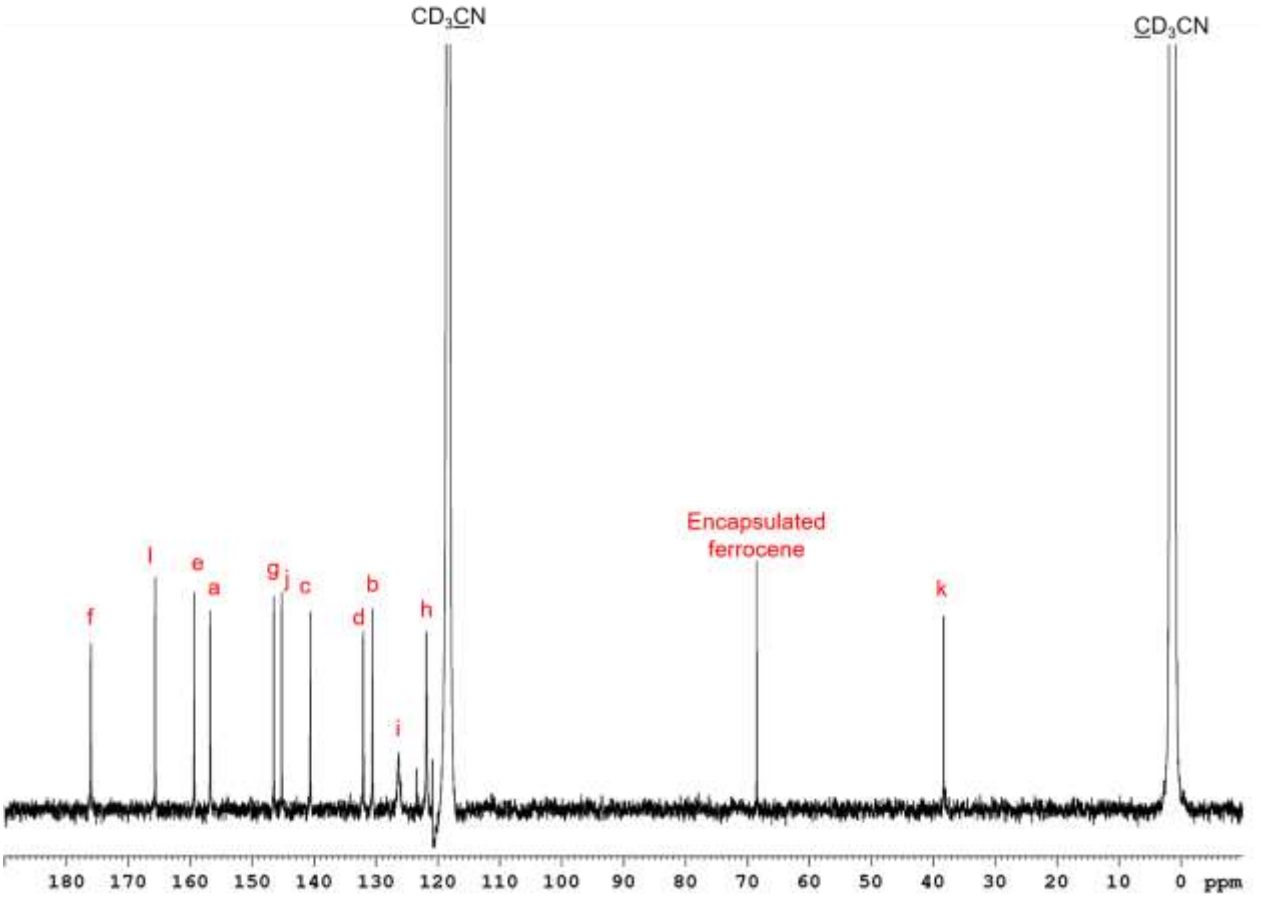

Figure S23. ^{13}C NMR spectrum (125 MHz, 298 K, CD_3CN) of [ferrocene ⊂ **1**](OTf)$_8$.

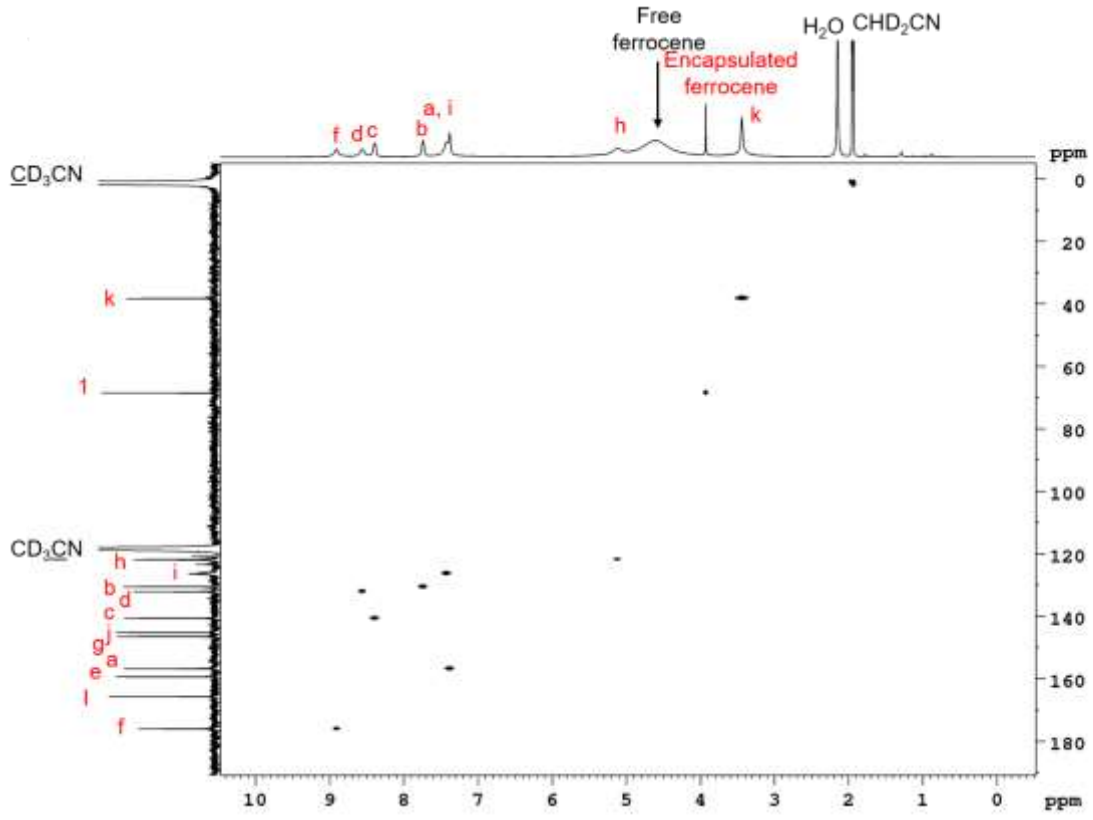

Figure S24. ^{1}H-^{13}C HSQC NMR spectrum (400 MHz/101 MHz, 298 K, CD_3CN) of [ferrocene ⊂ **1**](OTf)$_8$.

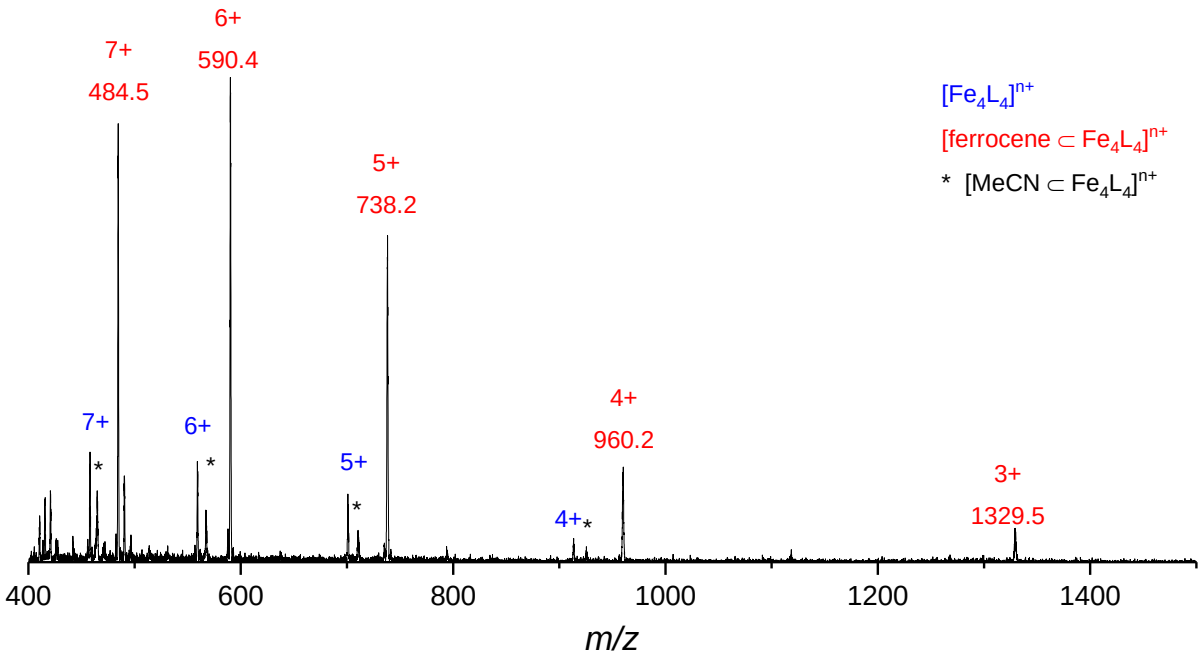

Figure S25. Low resolution ESI-mass spectrum of [ferrocene ⊂ **1**](OTf)$_8$.

3.2 Cage 2

The heat activated self-assembly of cage **2** in the presence and absence of ferrocene was carried out using analogous conditions to those optimised for the photoactivated self-assembly of cage **1** (Section 7.1.2).

In a glovebox, masked subcomponent **B** (4.7 μL, 5.4 mg, 0.012 mmol), iron(II) triflate (1.77 mg, 0.005 mmol), triamine **D** (1.77 mg, 0.004 mmol) and $LiBF_4$ (10 μL of a 1.2 M solution in CD_3CN, 0.012 mmol) were dissolved in 98:2 CD_3CN/D_2O (0.5 mL/10 μL) in a J Young tube. The tube was sealed and heated to 90 °C for 30 minutes, then allowed to equilibrate at room temperature overnight. A dark blue colour was visible after the initial heating period. The sample was filtered and the solvent removed. The blue residue was purified by size exclusion chromatography using Biobeads SX-1 eluting with DCM, and re-dissolved in CD_3CN for characterisation.

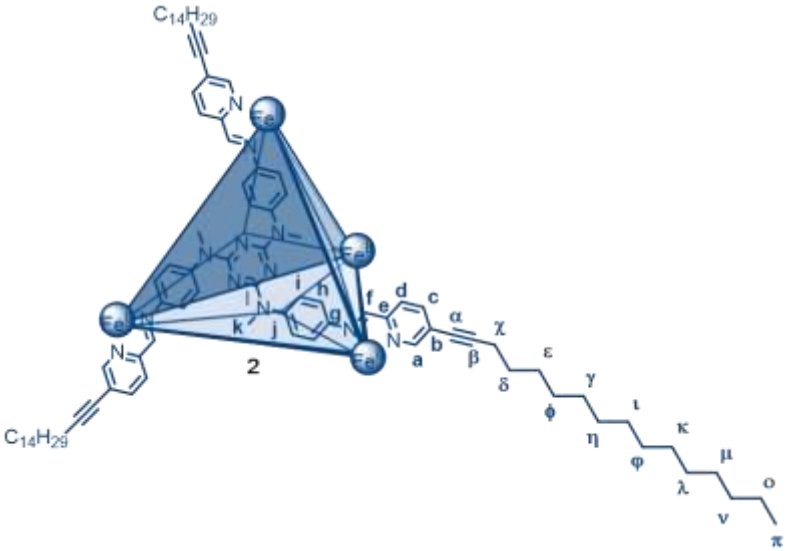

^{1}H NMR (400 MHz, CD_3CN, 298 K) δ (ppm): 8.86 (12H, bs, H_f), 8.47 (12H, d, J = 8.1 Hz, H_d), 8.27 (12H, d, J = 8.1 Hz, H_c), 7.57 – 7.37 (24H, b, H_i), 7.31 (12H, s, H_a), 5.06 (24H, bs, H_h), 3.38 (36H,

s, H_k), 2.45 (24H, t, J = 6.9 Hz, H_χ), 1.65–1.52 (24H, m, H_δ), 1.49–1.18 (264H, m, $H_{\varepsilon-o}$), 0.87 (36H, t, J = 6.5 Hz, H_π).

Assignments of quaternary carbons and carbons h and i are based on assignments for cage **1**[4a] since cross-peaks in the HSQC and HMBC were not observed, most likely due to the broadness of the signals in the ^{1}H NMR spectrum.

The ^{13}C NMR spectrum of cage **2** in the absence of a guest did not show a resonance for C_l, which was expected to appear at around 164 ppm.[4a] However, on addition of a guest such as ferrocene a new resonance was observed in this region. Additionally, the peaks assigned to C_f, C_g, C_j and C_k were found to be split in the empty cage but appear as single resonances in the host-guest complex. A comparison can be found in Figure S40. Some of these behaviours have been observed in the case of cage **1** on complexation of a flexible, aliphatic guest (2-hexylthiophene).[4a] We hypothesise that in this case, these effects could relate to the potential for the aliphatic substituents of cage **2** to fold back and become partially encapsulated within the cavity in the absence of a competing guest.

^{13}C NMR (125 MHz, CD_3CN, 298 K) δ (ppm): 175.5 (C_f), 158.9 (C_a), 157.2 (C_e), 146.6 (C_g), 145.1 (C_j), 142.4 (C_c), 131.1 (C_d), 128.6 (C_b), 127.5 (C_i), 122.1 (C_h), 102.4 (C_α), 77.1 (C_β), 50.3, 38.5 (C_k), 32.6, 30.4, 30.3, 30.2, 30.0, 29.8, 29.4, 28.7 (C_δ), 23.3, 20.0 (C_χ), 14.3 (C_π).

ESI-MS *m/z*: 712.8 [**2**]$^{8+}$, 827.0 [**2** + BF_4]$^{7+}$, 835.9 [**2** + OTf]$^{7+}$, 979.3 [**2** + $2BF_4$]$^{6+}$, 989.7 [**2** + BF_4 + OTf]$^{6+}$, 1000.1 [**2** + 2OTf]$^{6+}$, 1192.5 [**2** + $3BF_4$]$^{5+}$, 1205.0 [**2** + $2BF_4$ + OTf]$^{5+}$, 1217.4 [**2** + BF_4 + 2OTf]$^{5+}$, 1229.9 [**2** + 3OTf]$^{5+}$, 1528.0 [**2** + $3BF_4$ + OTf]$^{4+}$, 1543.5 [**2** + $2BF_4$ + 2OTf]$^{4+}$, 1559.0 [**2** + BF_4 + 3OTf]$^{4+}$, 1574.6 [**2** + 4OTf]$^{4+}$.

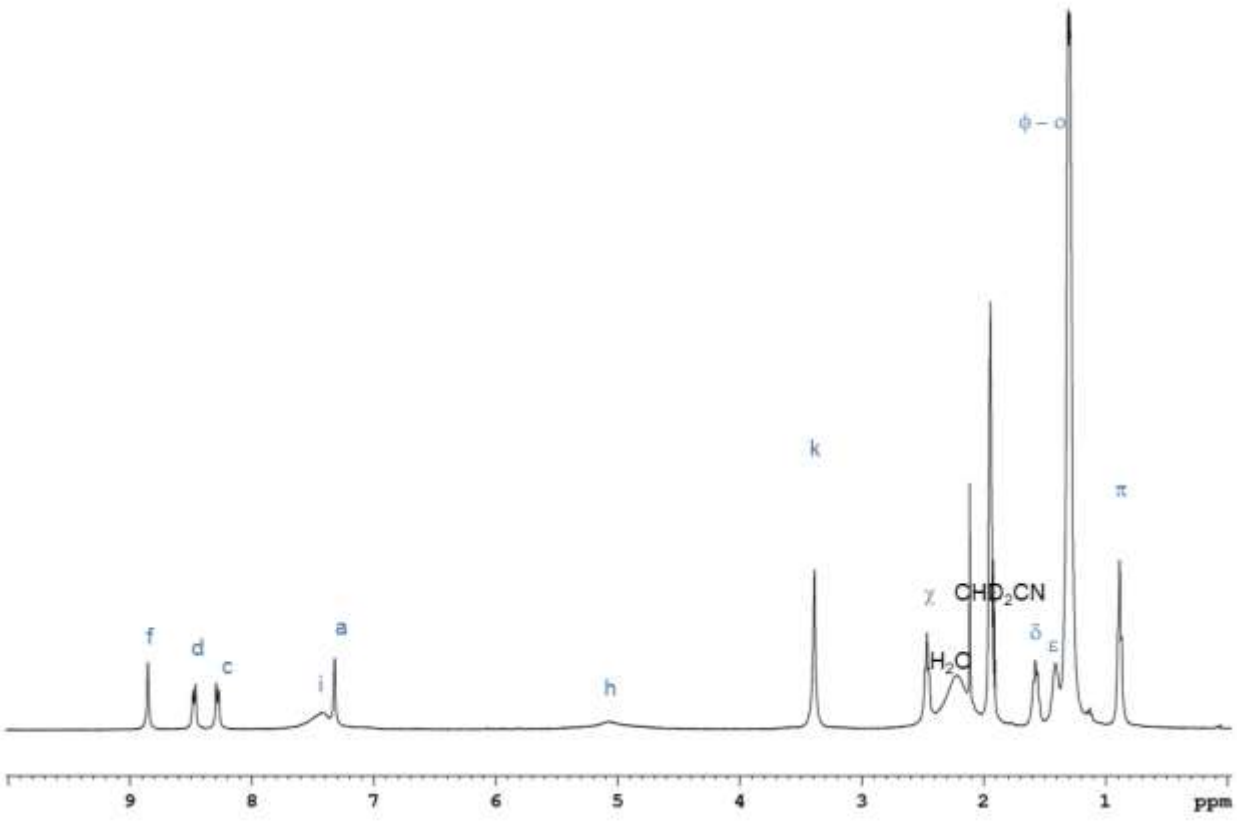

Figure S26. ^{1}H NMR spectrum of cage [**2**](X)$_8$ in CD_3CN at 298 K (X = OTf^-, BF_4^-).

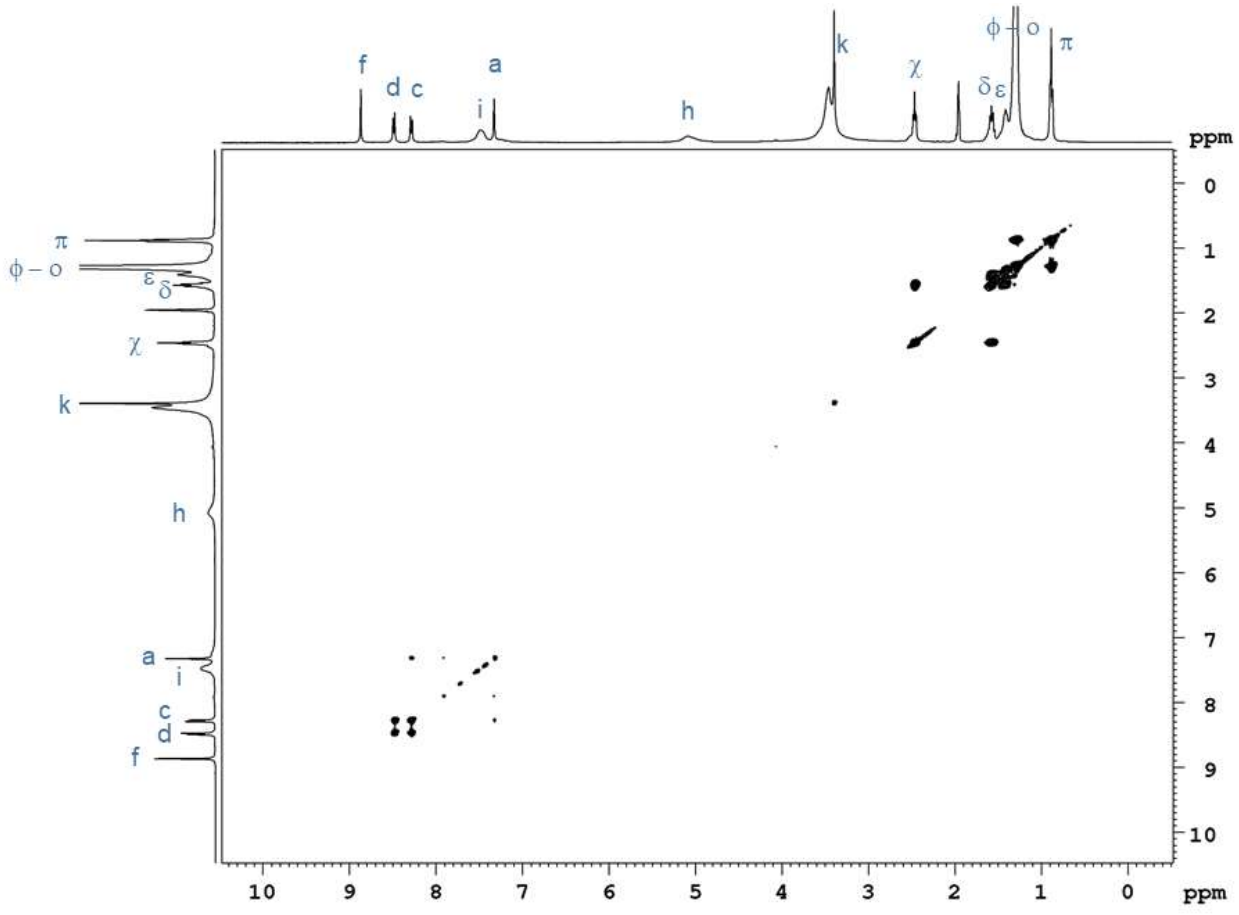

Figure S27. ^{1}H-^{1}H COSY NMR spectrum of cage [**2**](X)$_8$ in CD_3CN at 298 K (X = OTf^-, BF_4^-).

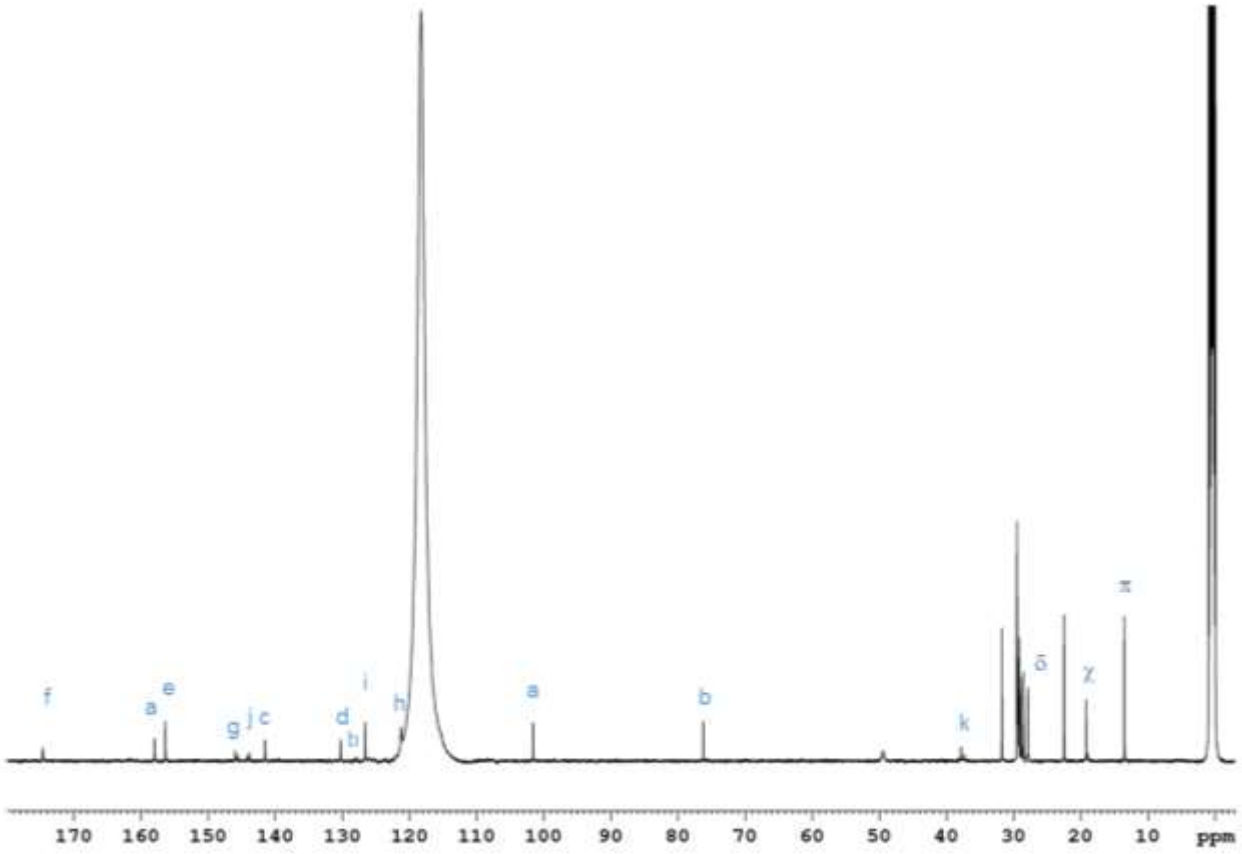

Figure S28. ^{13}C NMR spectrum of cage [**2**]$(X)_8$ in CD_3CN at 298 K (X = OTf^-, BF_4^-).

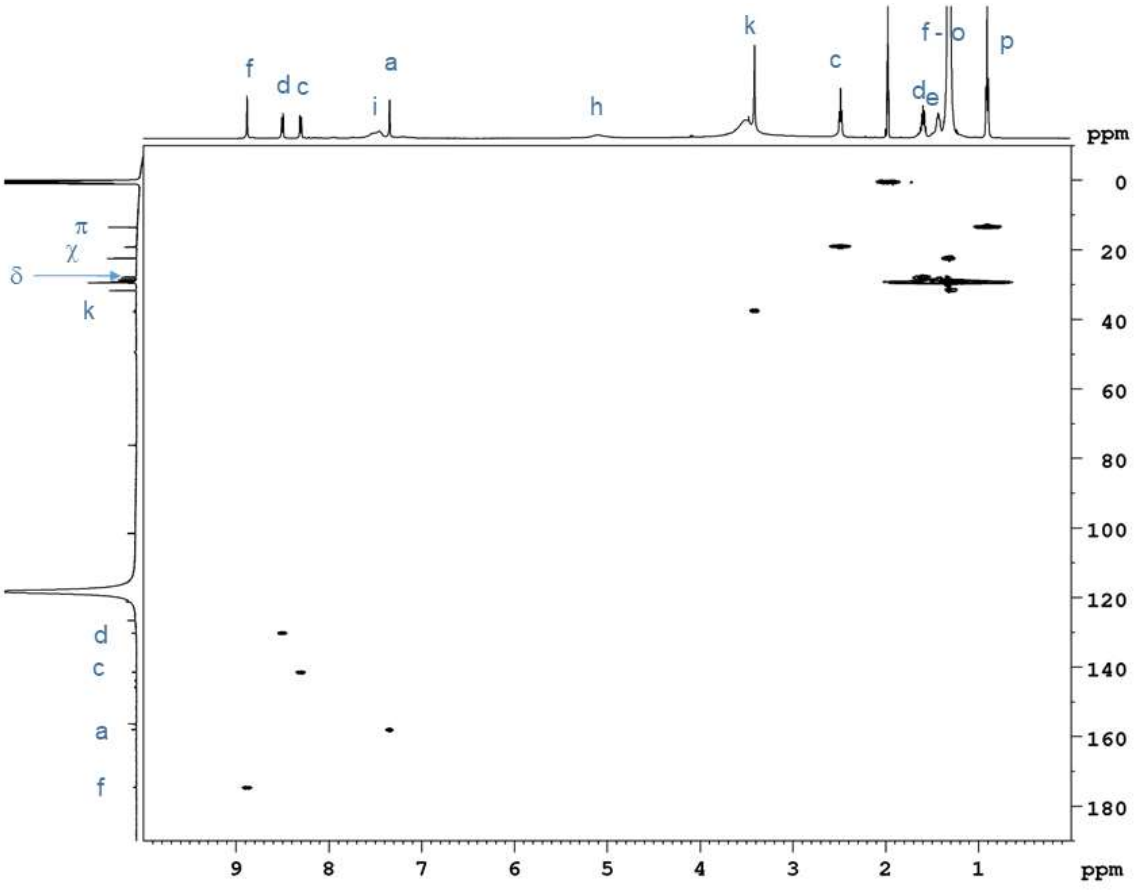

Figure S29. HSQC NMR spectrum of cage [**2**](X)$_8$ in CD_3CN at 298 K (X = OTf^-, BF_4^-).

Anion exchange was observed in the mass spectra of cage **2** due to the presence of OTf^- and BF_4^- anions in the self-assembly mixture (Figures S30-32).

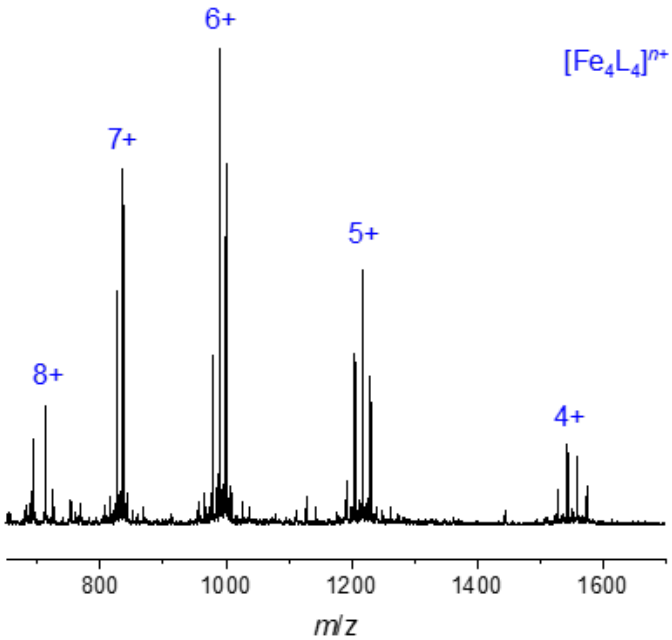

Figure S30. Low resolution ESI-mass spectrum of cage [**2**](X)$_8$ (X = OTf^-, BF_4^-).

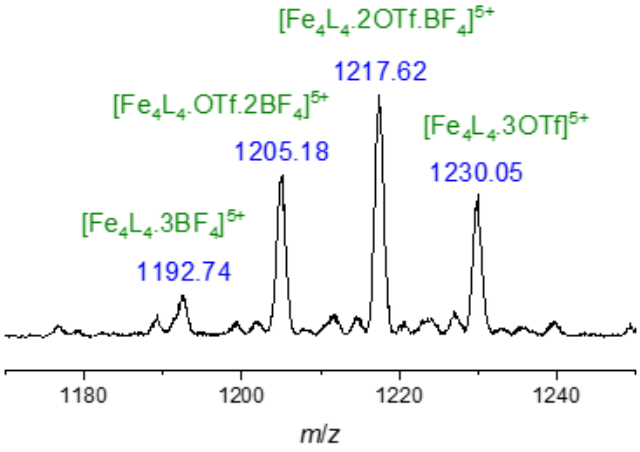

Figure S31. Selected region of the low resolution ESI-mass spectrum of cage [**2**]$(X)_8$ (X = OTf^-, BF_4^-) showing anion exchange for the $[Fe_4L_4]^{5+}$ peak.

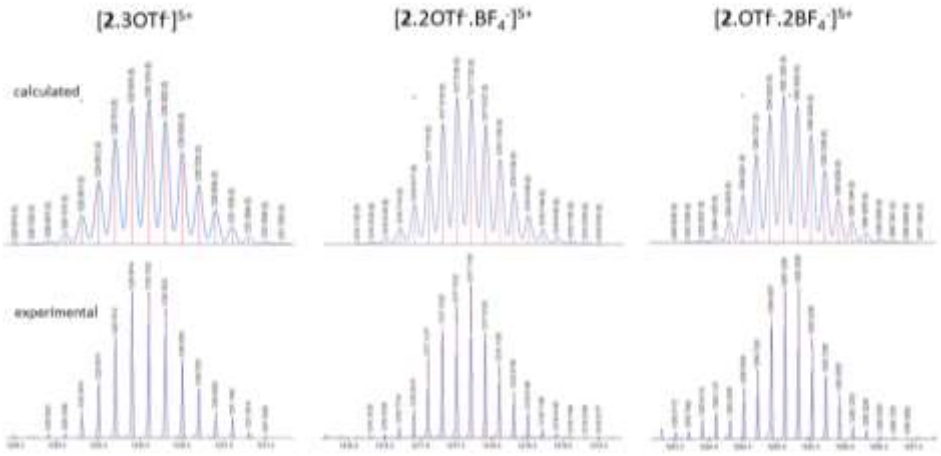

Figure S32. Selected regions of the high resolution ESI-mass spectrum of cage [**2**] for the 5+ charge with the calculated (top) and observed (bottom) isotope patterns, showing the presence of both OTf^- and BF_4^- counterions.

3.2.1 [Cyclopentane ⊂ **2**]$^{8+}$

Cage **2** (prepared in Section 3.2) was washed with 0.5 mL cyclopentane to simulate the phase transfer experiment and this was assumed to yield [cyclopentane ⊂ **2**]$^{8+}$ (Figure S33). Weak binding of cyclopentane was observed as indicated by the presence of two signals for proton f, corresponding to empty cage and [cyclopentane ⊂ **2**]$^{8+}$. However, further characterisation of the host-guest complex was not carried out due to the weakness of binding and overlapping signals for the empty cage and host-guest complex.

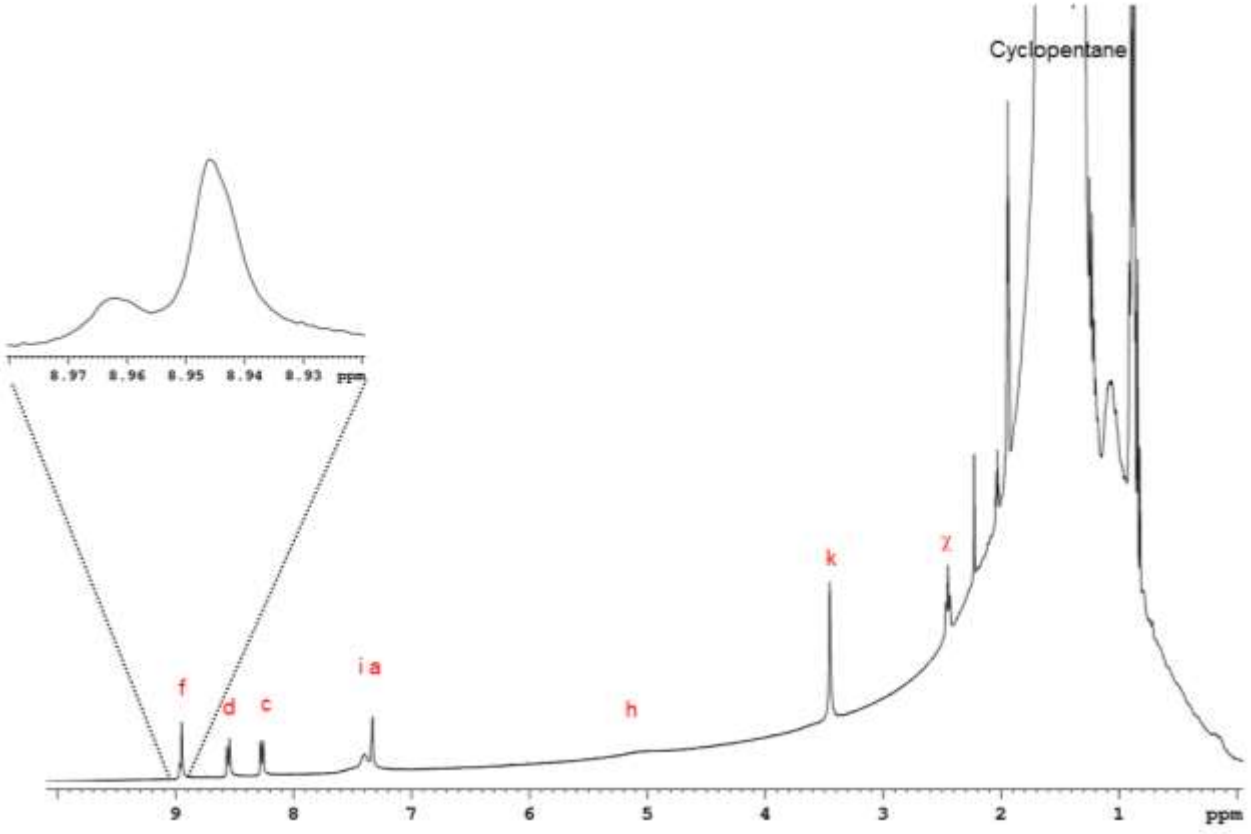

Figure S33. ^{1}H NMR spectrum of cage [**2**](X)$_8$ in CD_3CN at 298 K (X = OTf^-, BF_4^-) after washing with 0.5 mL cyclopentane.

3.2.2 [Ferrocene ⊂ **2**]$^{8+}$

In a glovebox, masked subcomponent **B** (4.7 μL, 5.4 mg, 0.012 mmol), iron(II) triflate (1.77 mg, 0.005 mmol), triamine **D** (1.77 mg, 0.004 mmol), $LiBF_4$ (10 μL of a 1.2 M solution in CD_3CN, 0.012 mmol) and ferrocene (2.44 mg, 0.013 mmol) were dissolved in 98:2 CD_3CN/D_2O (0.5 mL/10 μL) in a J Young tube. The tube was sealed and heated to 90 °C for 30 minutes, then allowed to equilibrate at room temperature overnight. A dark blue colour was visible after the initial heating period. The sample was filtered and the solvent removed. The blue residue was purified by size exclusion chromatography using Biobeads SX-1 eluting with DCM, and re-dissolved in CD_3CN for characterisation.

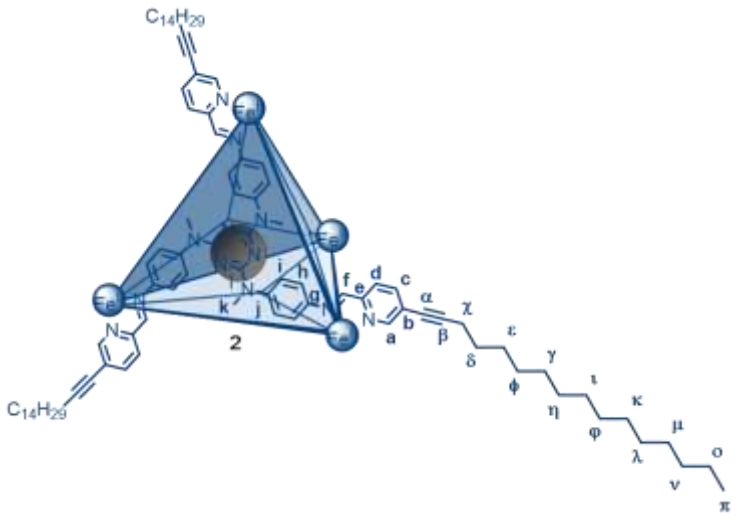

^{1}H NMR (400 MHz, CD_3CN, 298 K) δ (ppm): 8.84 (12H, s, H_f), 8.47 (12H, d, J = 8.1 Hz, H_d), 8.27 (12H, dd, J = 8.1, 1.7 Hz, H_c), 7.40 (24H, b, H_i), 7.31 (12H, d, J = 1.7 Hz, H_a), 5.09 (24H, b, H_h), 3.89 (10H, s, encapsulated ferrocene), 3.41 (36H, s, H_k), 2.45 (24H, t, J = 6.9 Hz, H_χ), 1.62–1.53 (24H, m, H_δ), 1.46–1.22 (264H, m, $H_{\varepsilon-o}$), 0.87 (36H, t, J = 6.6 Hz, H_π).

^{13}C NMR (125 MHz, CD_3CN, 298 K) δ (ppm): 175.7 (C_f), 165.6 (C_l), 158.9 (C_a), 157.3 (C_e), 146.4 (C_g), 145.3 (C_j), 142.4 (C_c), 131.2 (C_d), 127.5 (C_b), 126.3 (C_i), 121.9 (C_h), 102.6 (C_α), 77.1 (C_β), 68.4 (encapsulated ferrocene), 38.0 (C_k), 32.6, 30.4, 30.4, 30.4, 30.4, 30.3, 30.1, 29.8, 29.5, 28.8, 23.4, 20.1 (C_χ), 15.5, 14.4 (C_π).

ESI-MS *m/z*: 736.0 [ferrocene ⊂ **2**]$^{8+}$, 853.6 [ferrocene ⊂ **2** + BF_4]$^{7+}$, 862.5 [ferrocene ⊂ **2** + OTf]$^{7+}$, 1010.4 [ferrocene ⊂ **2** + 2BF_4]$^{6+}$, 1020.8 [ferrocene ⊂ **2** + BF_4 + OTf]$^{6+}$, 1031.1 [ferrocene ⊂ **2** + 2OTf]$^{6+}$, 1229.9 [ferrocene ⊂ **2** + 3BF_4]$^{5+}$, 1242.2 [ferrocene ⊂ **2** + 2BF_4 + OTf]$^{5+}$, 1254.7 [ferrocene ⊂ **2** + BF_4 + 2OTf]$^{5+}$, 1267.2 [ferrocene ⊂ **2** + 3OTf]$^{5+}$, 1558.9 [ferrocene ⊂ **2** + 4BF_4]$^{4+}$, 1574.7 [ferrocene ⊂ **2** + 3BF_4 + OTf]$^{4+}$, 1590.3 [ferrocene ⊂ **2** + 2BF_4 + 2OTf]$^{4+}$, 1605.6 [ferrocene ⊂ **2** + BF_4 + 3OTf]$^{4+}$, 1621.4 [ferrocene ⊂ **2** + 4OTf]$^{4+}$.

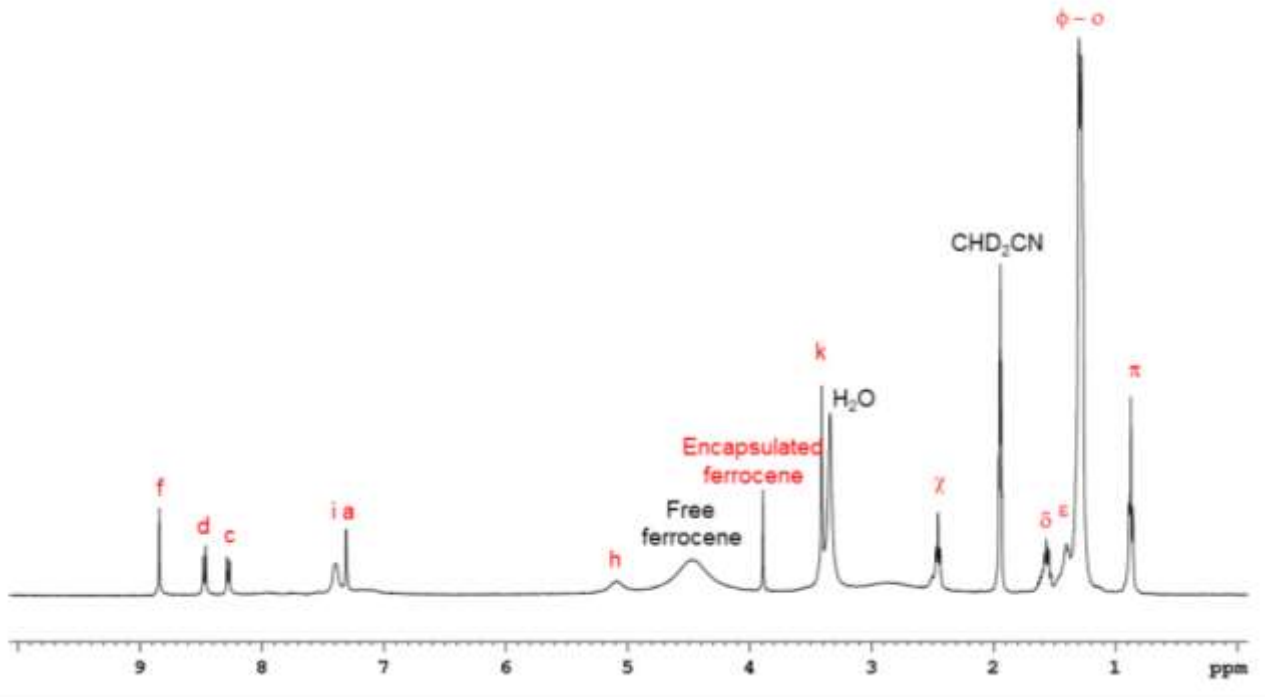

Figure S34. ^{1}H NMR spectrum of [ferrocene ⊂ **2**](X)$_8$ in CD_3CN at 298 K (X = OTf^-, BF_4^-) before purification by size exclusion chromatography.

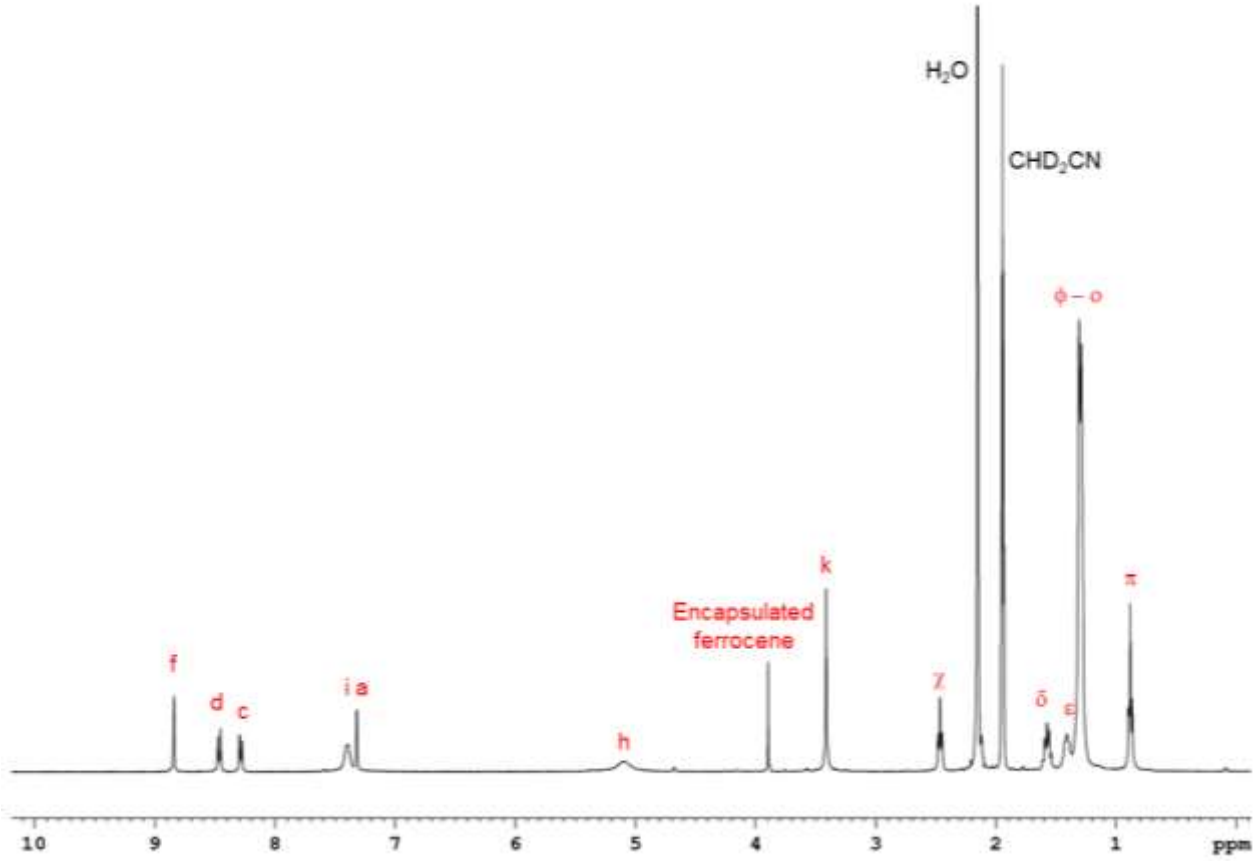

Figure S35. ^{1}H NMR spectrum of [ferrocene ⊂ **2**](X)$_8$ in CD_3CN at 298 K (X = OTf^-, BF_4^-) after purification by size exclusion chromatography.

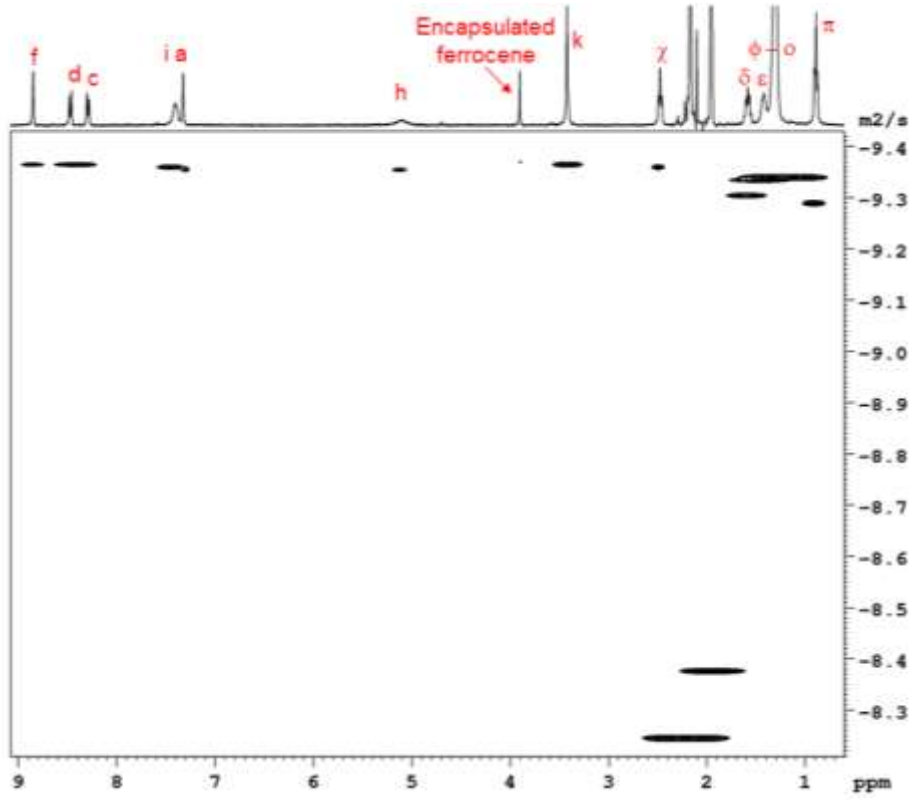

Figure S36. ^{1}H DOSY NMR spectrum of [ferrocene ⊂ **2**](X)$_8$ in CD_3CN at 298 K (X = OTf^-, BF_4^-).

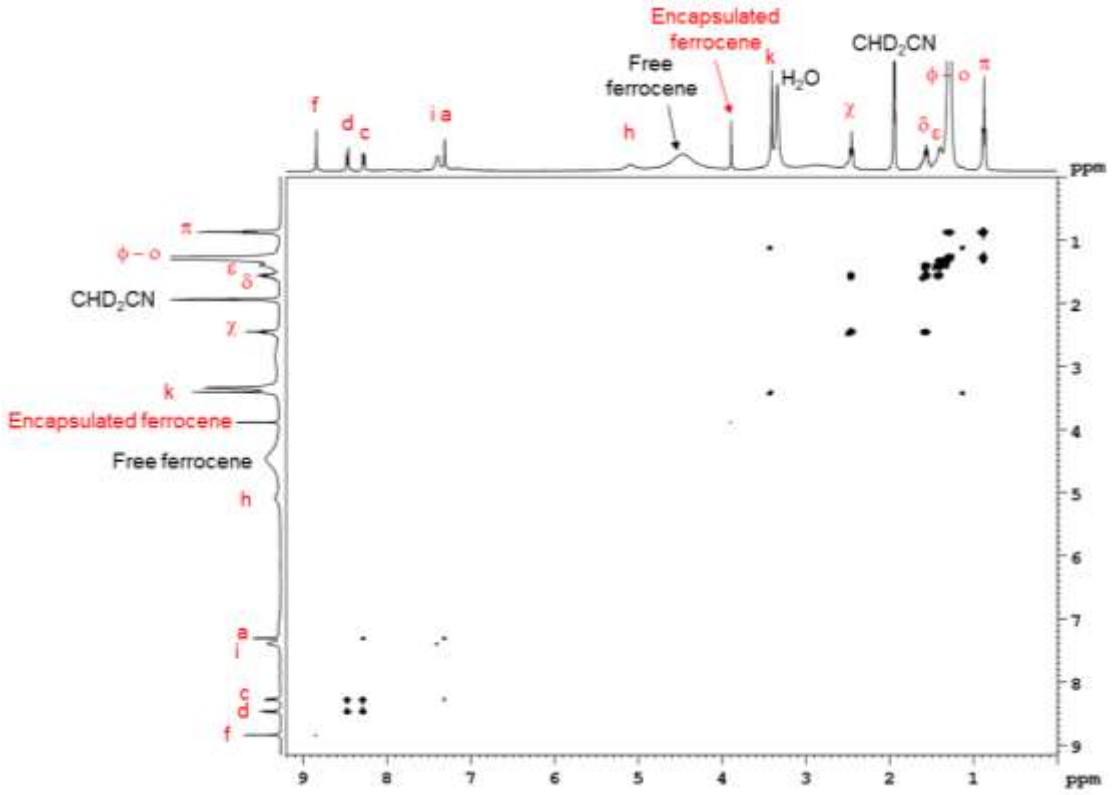

Figure S37. ^{1}H-^{1}H COSY NMR spectrum of [ferrocene ⊂ **2**](X)$_8$ in CD_3CN at 298 K (X = OTf^-, BF_4^-).

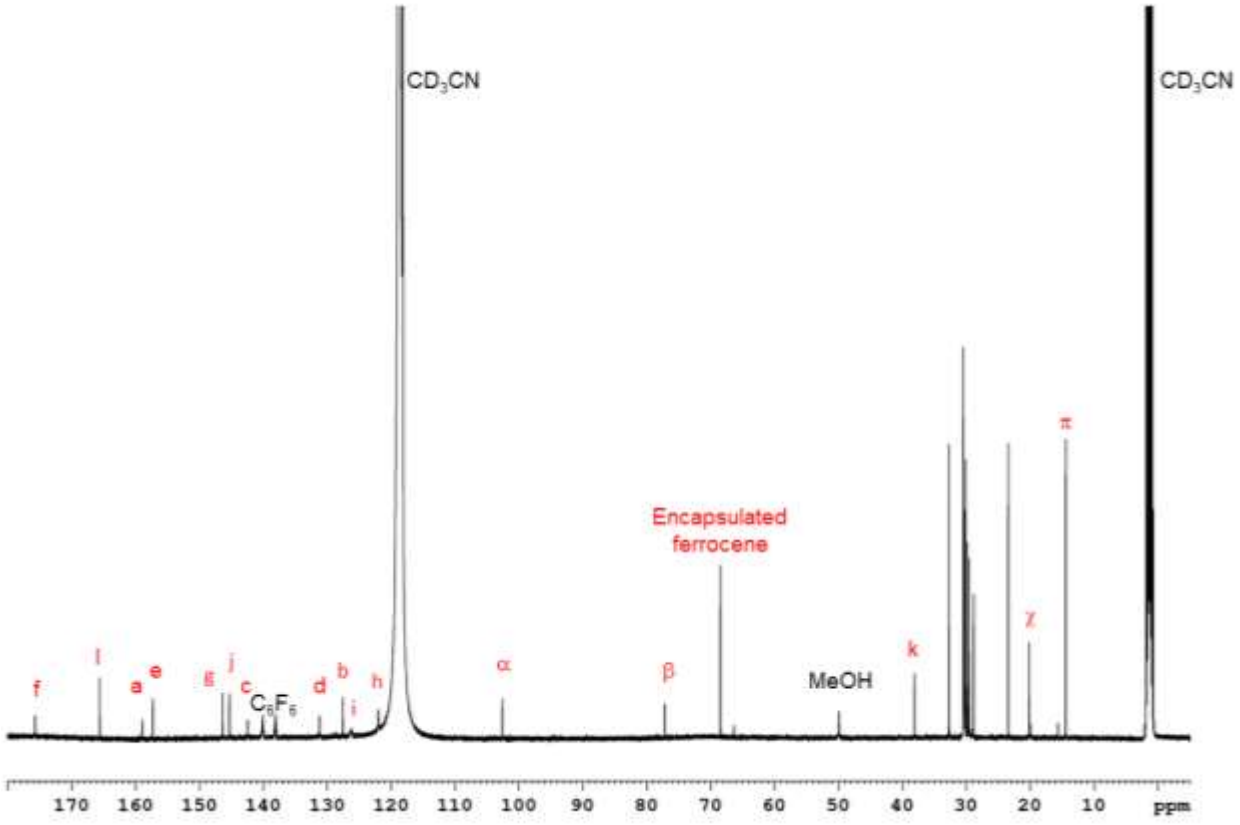

Figure S38. ^{13}C NMR spectrum of [ferrocene ⊂ **2**](X)$_8$ in CD_3CN at 298 K (X = OTf^-, BF_4^-) in the presence of a capillary containing C_6F_6 in CD_3CN.

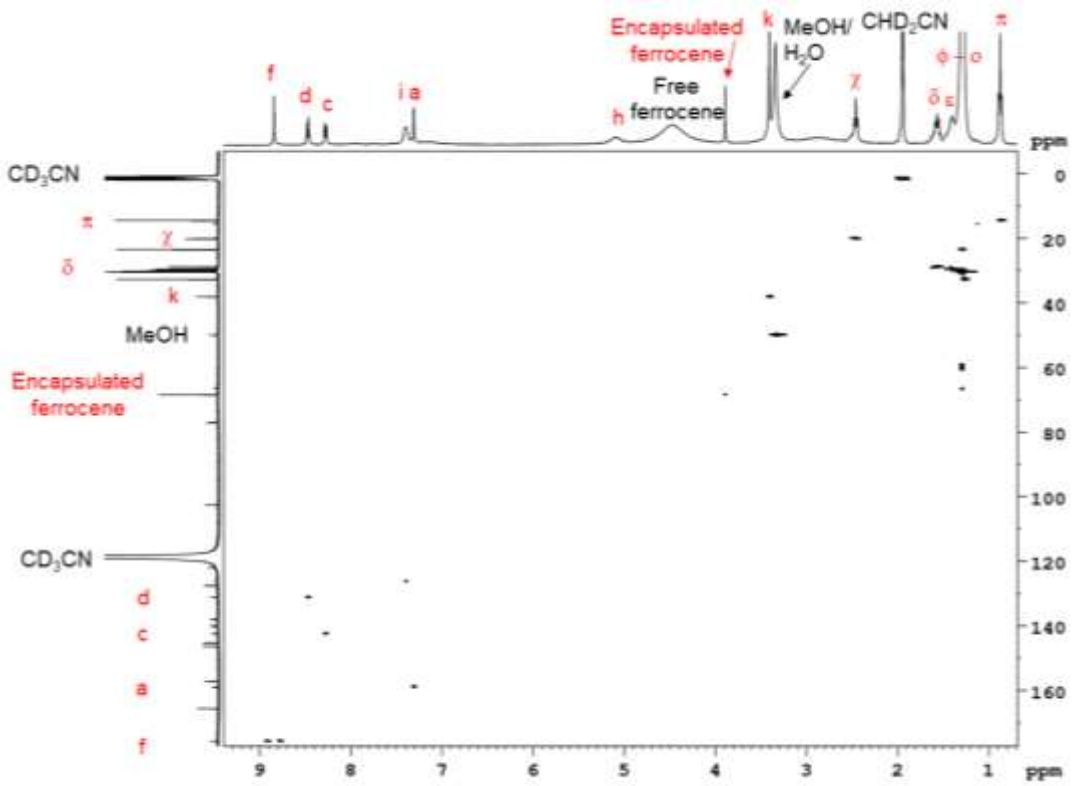

Figure S39. ^{1}H-^{13}C HSQC NMR spectrum of [ferrocene ⊂ **2**](X)$_8$ in CD_3CN at 298 K (X = OTf^-, BF_4^-).

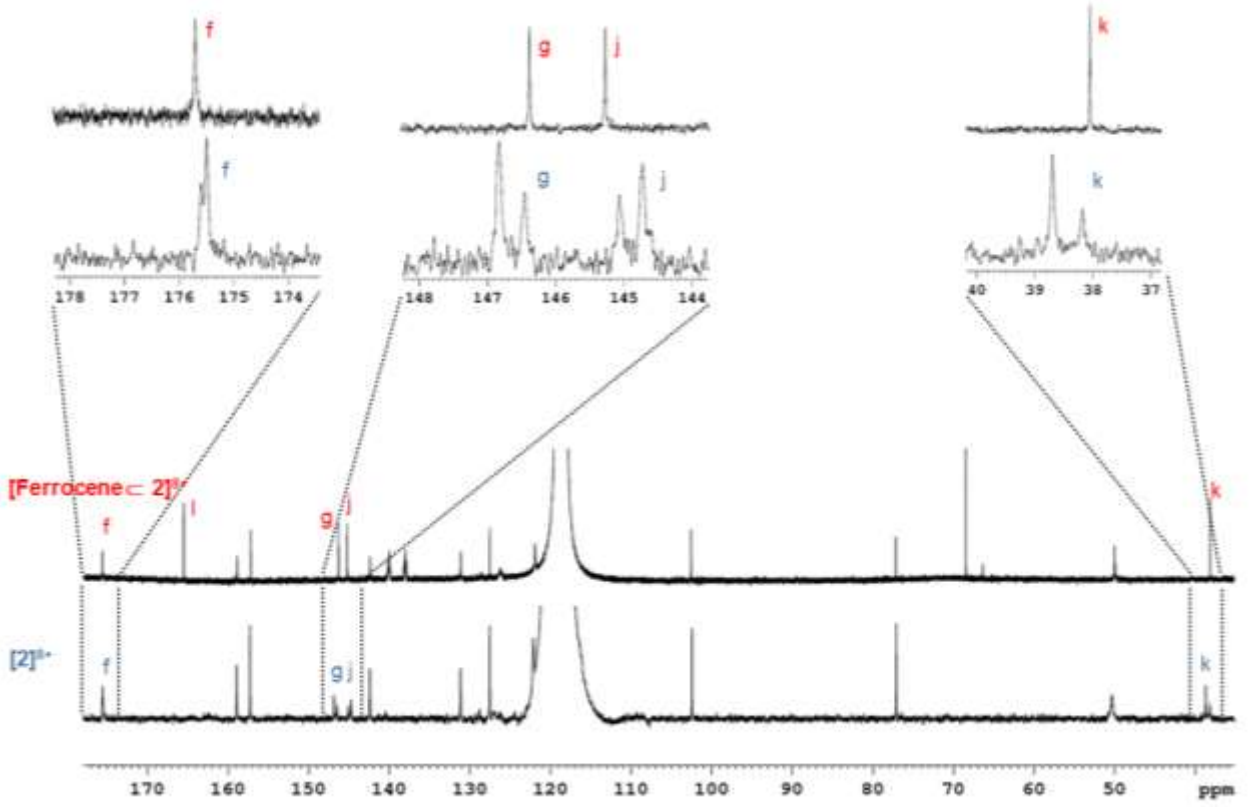

Figure S40. Comparative ^{13}C NMR spectra of [**2**](X)$_8$ (blue labels) and [ferrocene ⊂ **2**](X)$_8$ (red labels) showing the splitting of C_f, C_g, C_j and C_k and the disappearance of C_l in [**2**](X)$_8$. These resonances appear as single peaks in the spectrum of [ferrocene ⊂ **2**](X)$_8$.

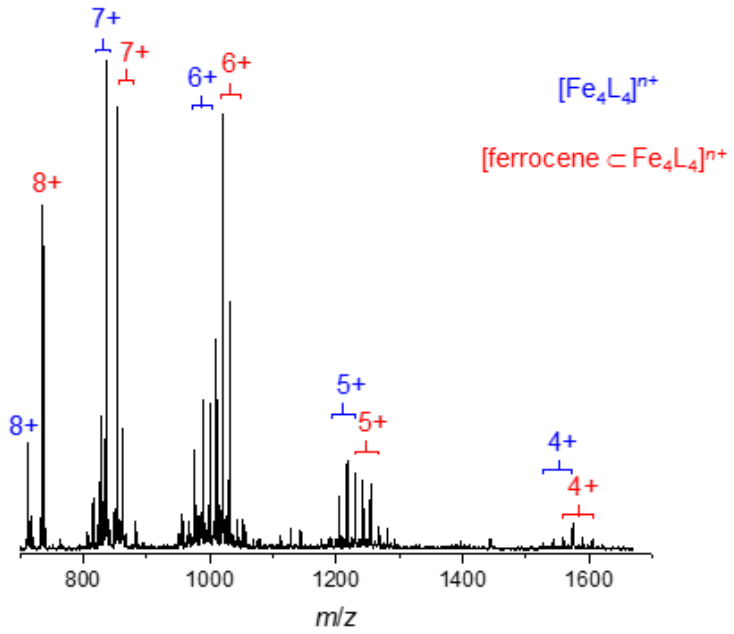

Figure S41. Low resolution ESI-mass spectrum of [ferrocene ⊂ **2**](X)$_8$ (X = OTf$^-$, BF$_4^-$). Clusters of peaks associated with the empty cage are labelled in blue, while clusters associated with the host-guest complex are labelled in red.

4 UV/visible spectroscopy

4.1 UV/visible Spectra of Masked Subcomponent A and Protecting Group C

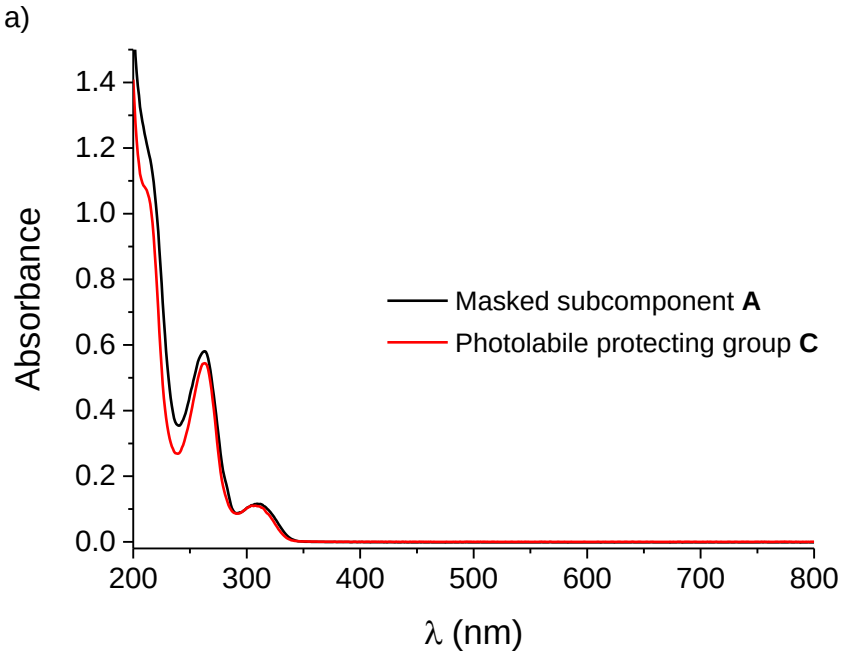

Figure S42. UV/visible spectra of masked subcomponent **A** (20 μM) and photolabile protecting group **C** (20 μM) in CH_3CN.

4.2 Photostability of Masked Subcomponent A and Protecting Group C

The photodeprotection of masked subcomponent **A** was initially investigated by UV/visible spectroscopy. The photocleavage of **C** from **A** is inferred to proceed via benzylic C-O bond

cleavage,[5] facilitated by electron-donating groups in the *meta* position due to the excited state *meta* effect.[6] Following bond cleavage, a zwitterionic intermediate forms that breaks down to release the aldehyde and the protecting group is regenerated following hydrolysis of an intermediate species. A wavelength of 300 nm was chosen for deprotection as the UV-Vis spectrum of **A** in CH_3CN had a peak at 310 nm, attributed to absorbance of the 3-(dimethylamino)phenyl groups (Figure S42).[5a]

A broad absorption around 450 nm was observed following irradiation at 300 nm for 1 min (Figure S43a). This feature is attributed to a transient product of deprotection, since it disappeared following further irradiation. Illumination of the photolabile protecting group **C** produced a similar band over the same irradiation time (Figure S43b). Continued photolysis of **A** over 30 min led to a loss of the peaks at 310 nm and at 263 nm. However, these spectral changes did not correspond to the release of protecting group **C**, which has a similar UV/visible spectrum to that of **A** (Figure S42). The similarity of the spectral changes to those following the irradiation of **C** (Figure S43a) suggested that the released photolabile protecting group underwent degradation upon further irradiation. Thus, ^{1}H NMR spectroscopy was used instead of UV/visible spectroscopy to monitor deprotection of the masked subcomponent **A**.

Method: Masked subcomponent **A** (20 μM) or protecting group **C** (20 μM) in CH_3CN (3 mL) was irradiated at 300 nm in a quartz cuvette for 1, 5, 15 and 30 minutes.

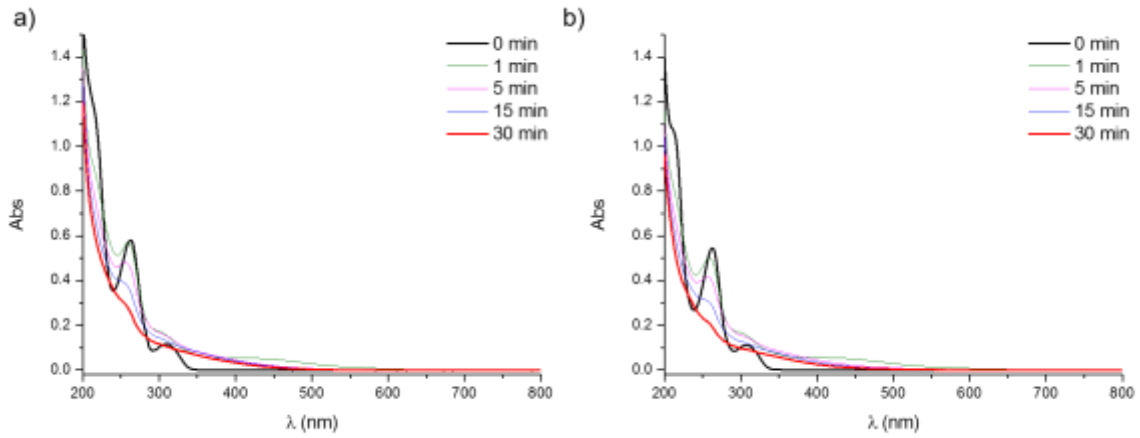

Figure S43. UV/visible spectra of a) masked subcomponent **A** (20 μM) and b) protecting group **C** (20 μM) upon irradiation at 300 nm in CH_3CN.

4.3 Cage 1

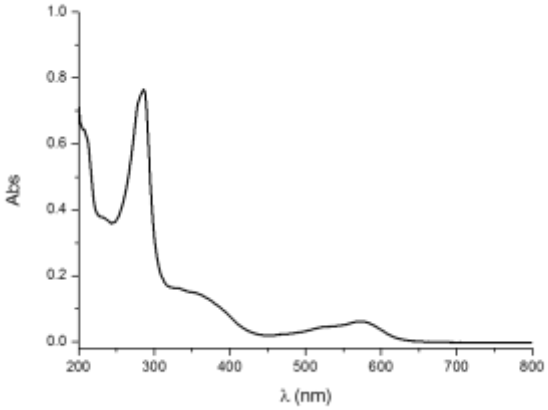

Figure S44. UV/visible spectra of cage **1** (3 μM) in CH_3CN.

4.4 Cage 2

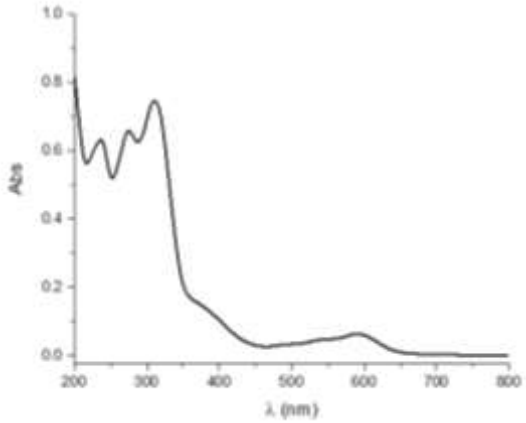

Figure S45. UV/visible spectra of cage **2** (3 μM) in CH_3CN.

5 Photostability Experiments

5.1 Protecting Group C

Control experiments using ^{1}H NMR spectroscopy confirmed that the photolabile protecting group **C** decomposed upon irradiation at 300 nm. The complete disappearance of **C** was observed within 15 min of irradiation and new signals appeared in the ^{1}H NMR spectrum (Figure S46).

Method: Protecting group **C** (4.35 mg, 0.012 mmol) was dissolved in CD_3CN (0.5 mL) in a J Young tube and the solution was degassed by 3 freeze/pump/thaw cycles and refilled with N_2. The solution was irradiated at 300 nm and ^{1}H NMR spectra were recorded after 1, 2, 3, 4, 5, 7, 9, 11, 13, 15, 19, 23 and 28 minutes of irradiation.

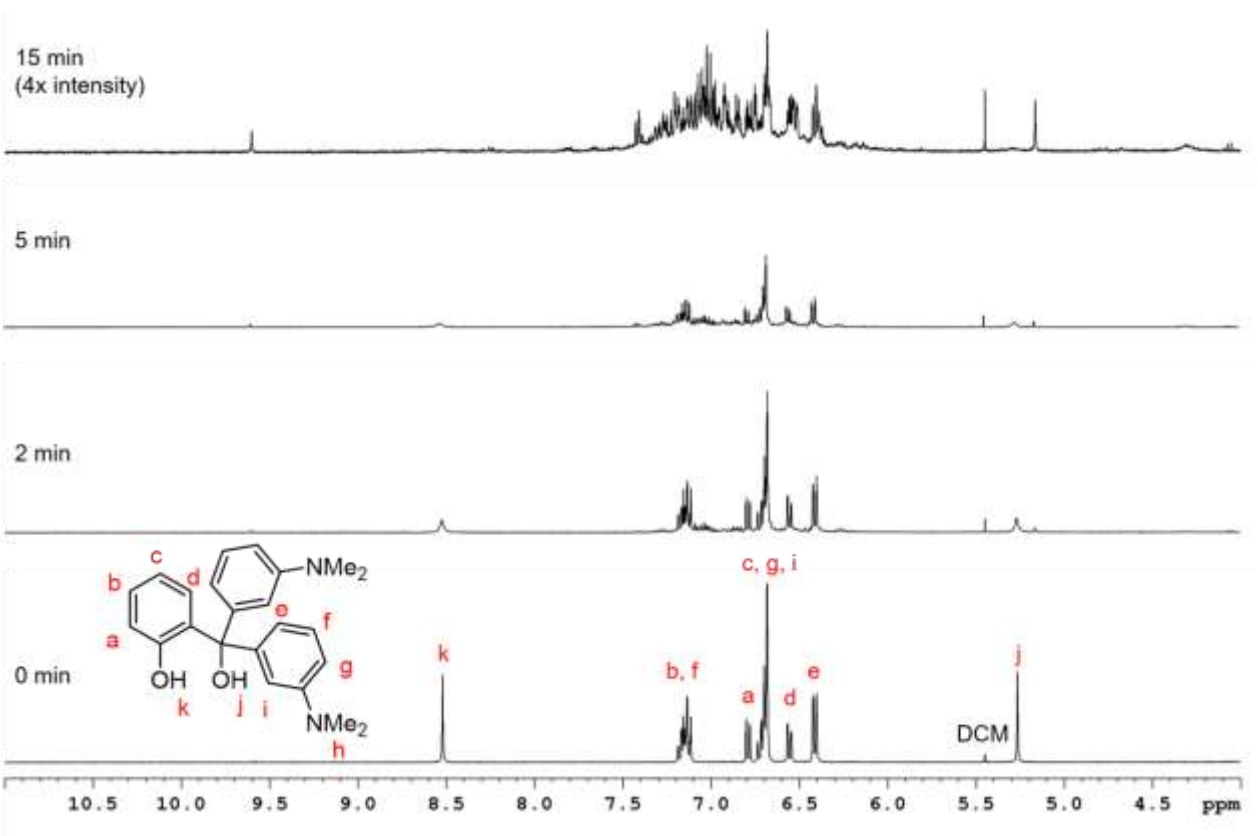

Figure S46. Aromatic region of ^{1}H NMR spectra of the protecting group **C** upon irradiation at 300 nm for 0, 2, 5 and 15 minutes showing photodegradation.

5.2 2-Formylpyridine

2-Formylpyridine was also not stable to irradiation at 300 nm (Figure S47).

Method: 2-Formylpyridine (1.1 µL, 0.012 mmol) was dissolved in CD_3CN (0.5 mL) in a J Young tube and the solution was degassed by 3 freeze/pump/thaw cycles and refilled with N_2. The solution was irradiated at 300 nm and ^1H NMR spectra were recorded after 1, 5, 15, 30 and 40 minutes of irradiation.

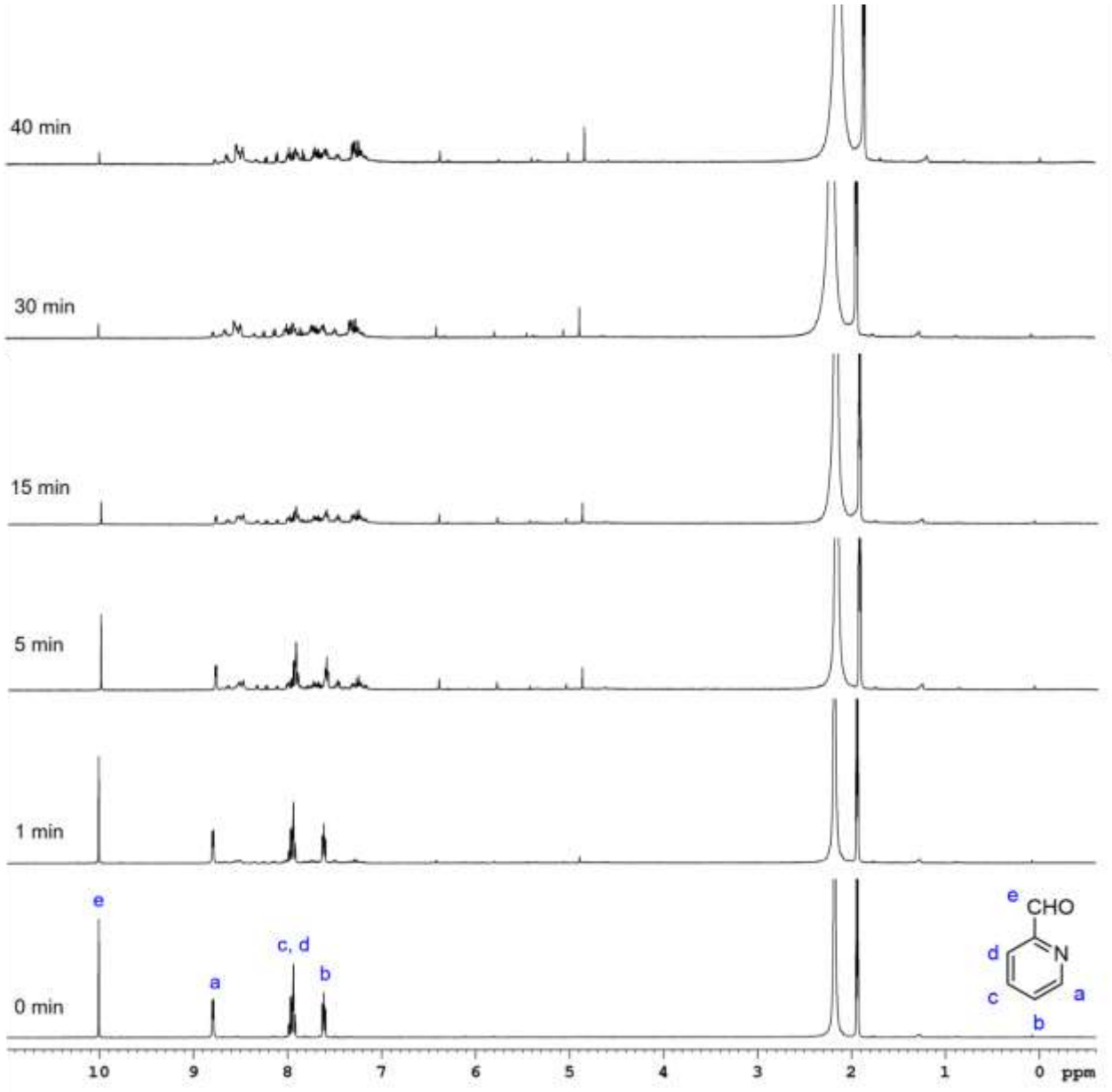

Figure S47. ^1H NMR spectra of 2-formylpyridine upon irradiation at 300 nm for 0-40 minutes showing photodegradation in CD_3CN.

5.4 Cages 1 and 2

Although cages **1** and **2** absorb light at 300 nm (Figures S44, S45), no degradation of the cages was observed upon irradiation for 40 min at 300 nm (Figure S48).

Method: Cage **1** (4.42 mg, 0.001 mmol) or cage **2** (6.90 mg, 0.01 mmol) was dissolved in CD_3CN (0.5 mL) in a J Young tube and the solution was degassed by 3 freeze/pump/thaw cycles and refilled with N_2. The solution was irradiated at 300 nm and ^1H NMR spectra were recorded after 40 minutes of irradiation.

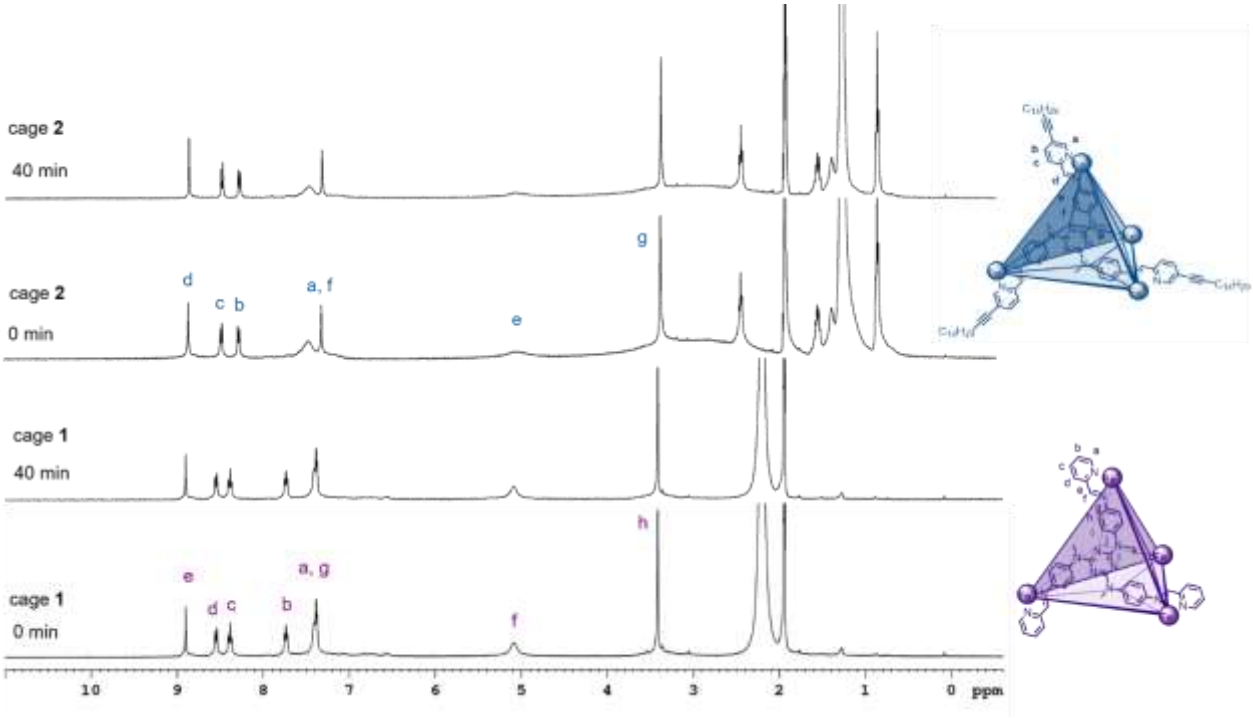

Figure S48. ^1H NMR spectra of cages **1** (bottom) and **2** (top) (2 mM in CD_3CN) upon irradiation at 300 nm for 0 and 40 minutes showing no degradation.

5.5 Masked Subcomponent A

The masked subcomponent **A** was stable under lab lighting conditions for 3 days and also to the heat generated upon irradiation at 300 nm for 30 min when protected by an opaque aluminum foil sheath (Figure S49). Subsequent irradiations at different wavelengths, each for 30 min, were undertaken to monitor photostability. Irradiation at 575 nm and 419 nm showed minimal deprotection (Figure S49). Larger quantities of 2-formylpyridine were released upon irradiation at 350 nm and 253 nm, wavelengths closer to the absorption bands of **A**, but photodeprotection was incomplete within 30 min.

Method: Masked subcomponent **A** (5.46 mg, 0.012 mmol) was dissolved in CD_3CN (0.5 mL) in a J Young tube and the solution was degassed by 3 freeze/pump/thaw cycles and refilled with N_2. The solution was left under lab lighting for 3 days, irradiated for 30 minutes at 300 nm in foil (heat control), and irradiated for 30 minutes each at 575 nm, 419 nm, 350 nm and 253 nm. ^1H NMR spectra were recorded to monitor the stability of masked subcomponent **A** under each condition as indicated by the release of 2-formylpyridine (Scheme S3).

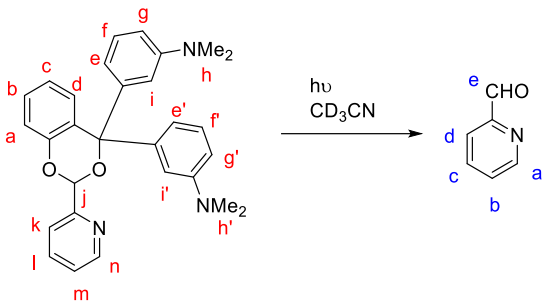

Scheme S3. Photodeprotection of masked subcomponent **A** upon irradiation releasing 2-formylpyridine.

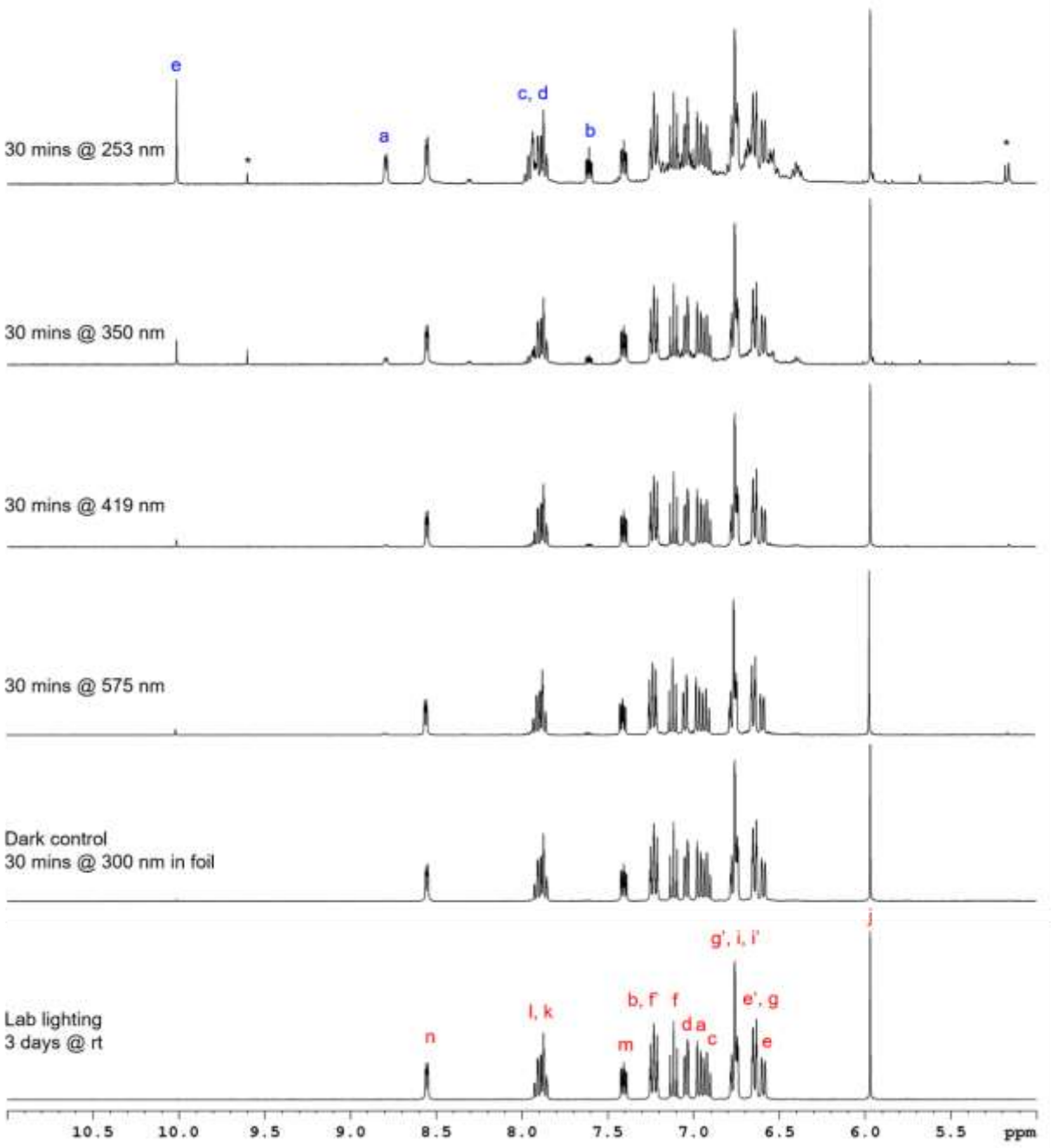

Figure S49. ^{1}H NMR spectra of masked subcomponent **A** (red labels) in various irradiation conditions monitoring the release of 2-formylpyridine (blue labels) in CD_3CN. See Scheme S3 for proton assignments; * marks peaks assigned to a derivative of the released protecting group.

5.6 Masked Subcomponent A + $Fe(OTf)_2$ + Triamine D

To ensure the compatibility of masked subcomponent **A** with the other constituents of cage **1**, further investigations of its stability were undertaken. Compound **A** did not react with either triamine **D** or iron(II) triflate in the dark at room temperature overnight (Figure S50). A mixture of **A**, **D** and iron(II) triflate also showed no reaction in a control experiment involving irradiation at 300 nm for 30 min of a vessel covered with opaque aluminum foil followed by subsequent exposure to lab lighting conditions for 5 h (Figure S51).

5.6.1 Dark Controls

J Young tubes containing solutions of: a) masked subcomponent **A** (0.012 mmol); b) masked subcomponent **A** (0.012 mmol) and triamine **D** (0.004 mmol); c) masked subcomponent **A** (0.012 mmol) and $Fe(OTf)_2$ (0.004 mmol); d) masked subcomponent **A** (0.012 mmol), triamine **D** (0.004 mmol) and $Fe(OTf)_2$ (0.004 mmol) in CD_3CN (0.5 mL) were degassed by 3 freeze/pump/thaw cycles and refilled with N_2. The solutions were kept overnight at room temperature in the dark and their ^1H NMR spectra were recorded to monitor the stability of masked subcomponent **A** in the presence of the other subcomponents for cage self-assembly.

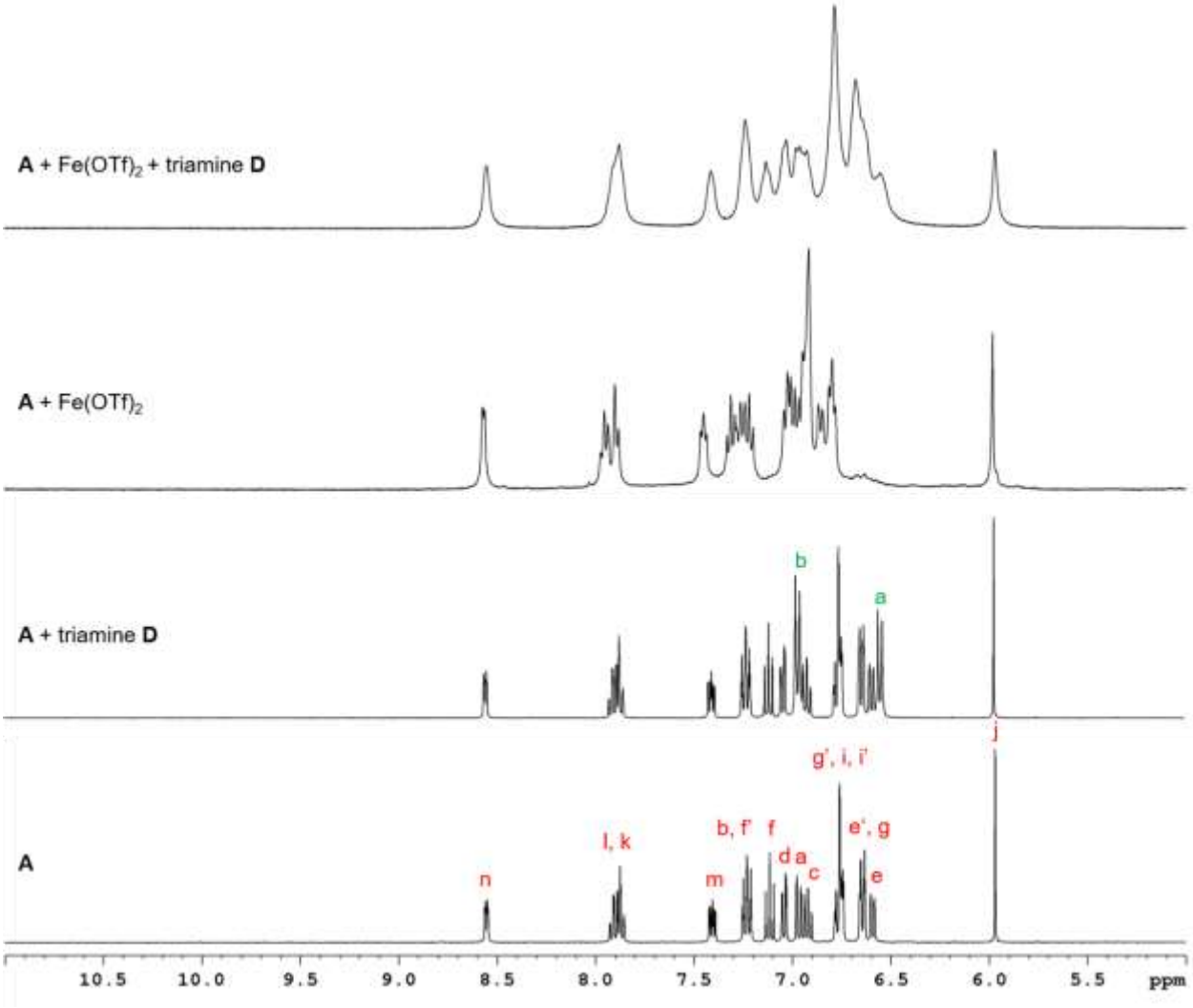

Figure S50. ^1H NMR spectra of masked subcomponent **A** (red labels), **A** + triamine **D** (green labels), **A** + $Fe(OTf)_2$ and **A** + $Fe(OTf)_2$ + triamine **D** following equilibration overnight at room temperature in the dark in CD_3CN. See Scheme S3 for proton assignments.

5.6.2 Light and Heat Controls

A J Young tube containing a solution of masked subcomponent **A** (0.012 mmol), triamine **D** (0.004 mmol) and $Fe(OTf)_2$ (0.004 mmol) in CD_3CN (0.5 mL) was degassed by 3

freeze/pump/thaw cycles and refilled with N_2. The solution was kept in the dark (dark control), irradiated for 40 minutes at 300 nm in foil (heat control) then left to equilibrate at room temperature overnight in the dark before being left in lab lighting for 5 h at room temperature. ^{1}H NMR spectra were recorded to monitor the stability of masked subcomponent **A** in the presence of the other subcomponents for cage self-assembly.

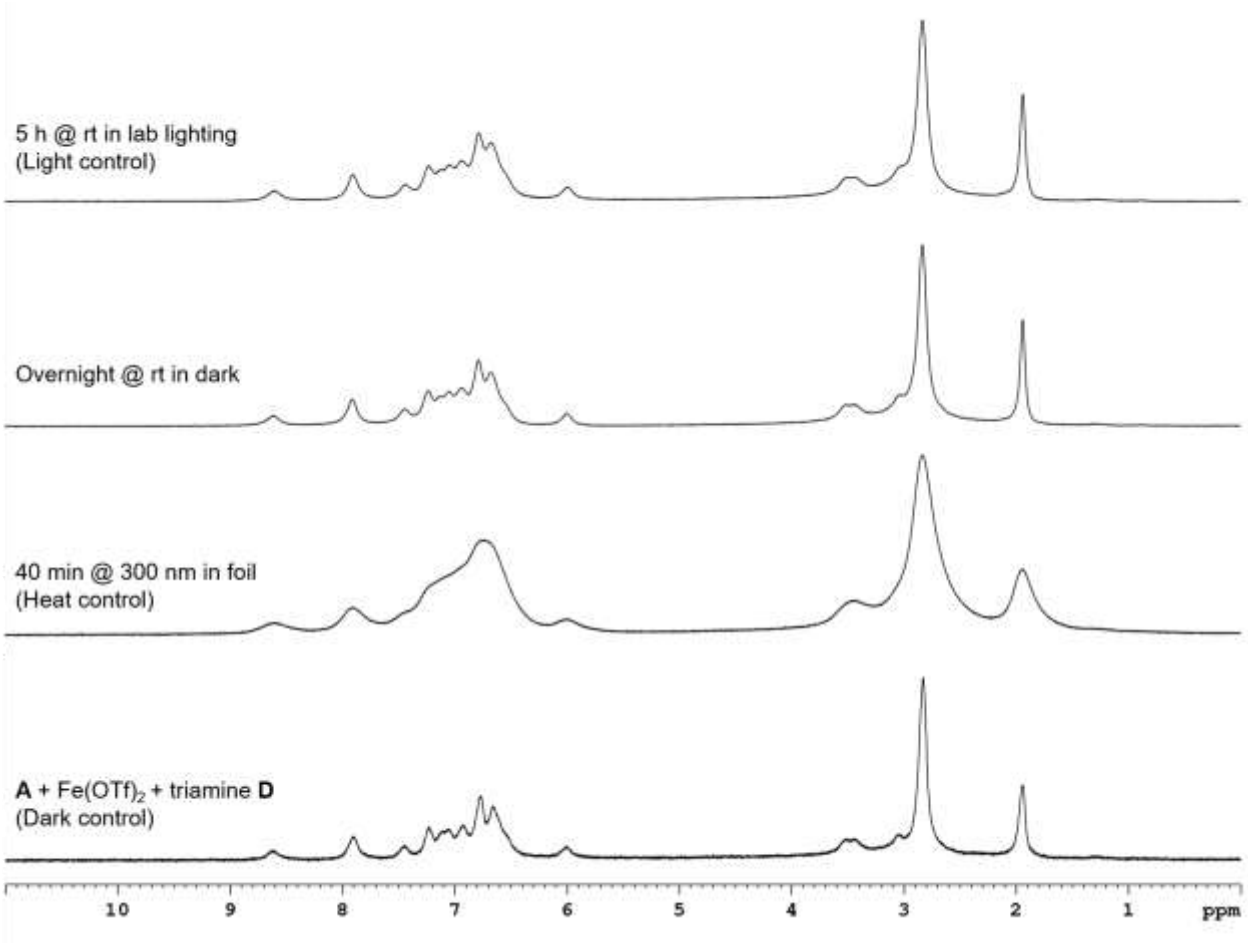

Figure S51. ^{1}H NMR spectra of **A** + $Fe(OTf)_2$ + triamine **D** following equilibration overnight at room temperature in the dark in CD_3CN. See Scheme S3 for proton assignments.

6 Photodeprotection Time Course Experiments

Time-course ^{1}H NMR experiments monitored the conversion of **A** to 2-formylpyridine upon irradiation at 300 nm in various control experiments.

6.1 Color Changes

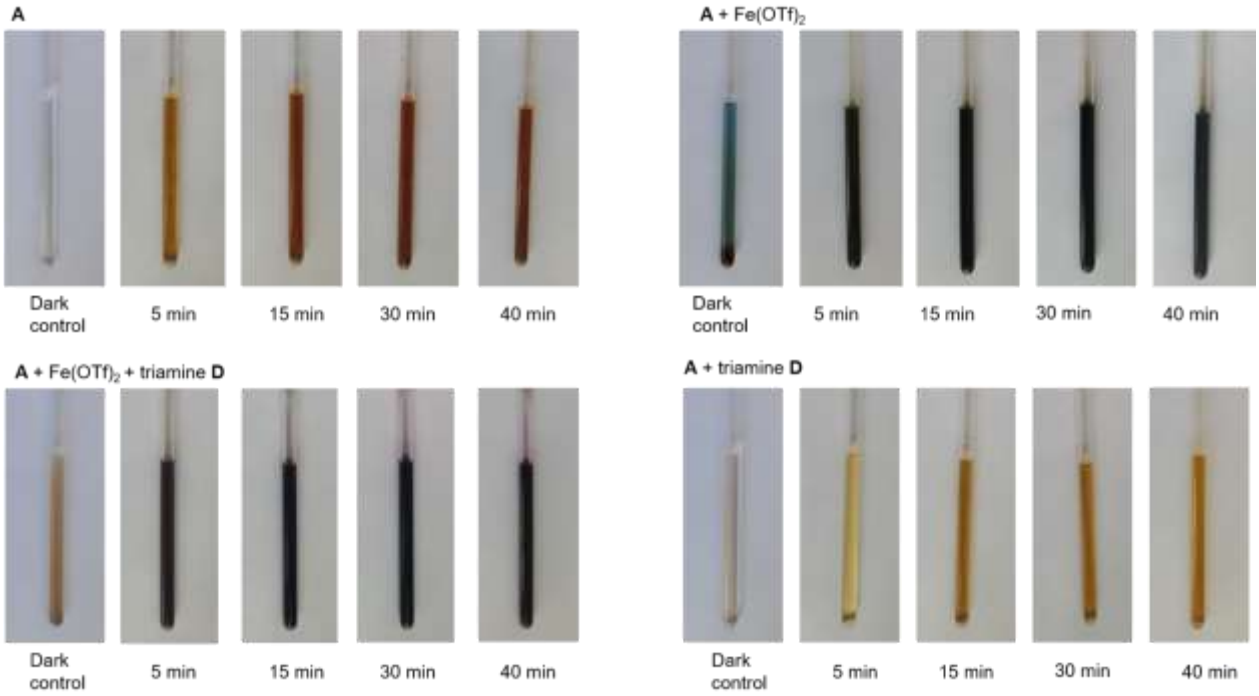

Figure S52. Colour changes observed by the naked eye upon irradiation at 300 nm for 0 (dark control), 5, 15, 30 and 40 minutes.

6.2 Masked Subcomponent A

Photodeprotection of **A** alone proceeded cleanly as the major products detected were 2-formylpyridine and a derivative of the protecting group formed following degradation with light. The amount of released 2-formylpyridine was quantified by integrating proton signal *j* of **A** and the proton signal *e* of 2-formylpyridine (Figure S53) and degradation of the released 2-formylpyridine by light appeared to be minimal over the course of the 40 min irradiation.

Method: A J Young tube containing a solution of masked subcomponent **A** (5.43 mg, 0.012 mmol) in CD_3CN (0.5 mL) was degassed by 3 freeze/pump/thaw cycles and refilled with N_2. The solution was equilibrated at room temperature overnight in the dark and then irradiated at 300 nm. ^{1}H NMR spectra were recorded after 1, 2, 3, 4, 5, 7, 9, 11, 13, 15, 19, 23, 30 and 40 minutes of irradiation.

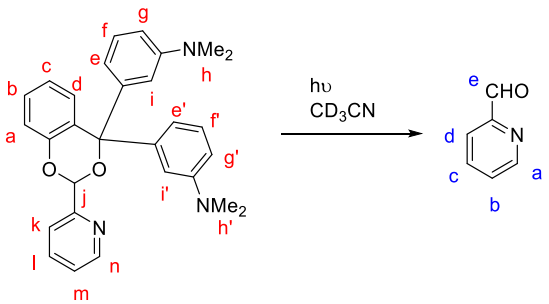

Scheme S4. Photodeprotection of masked subcomponent **A** upon irradiation releasing 2-formylpyridine.

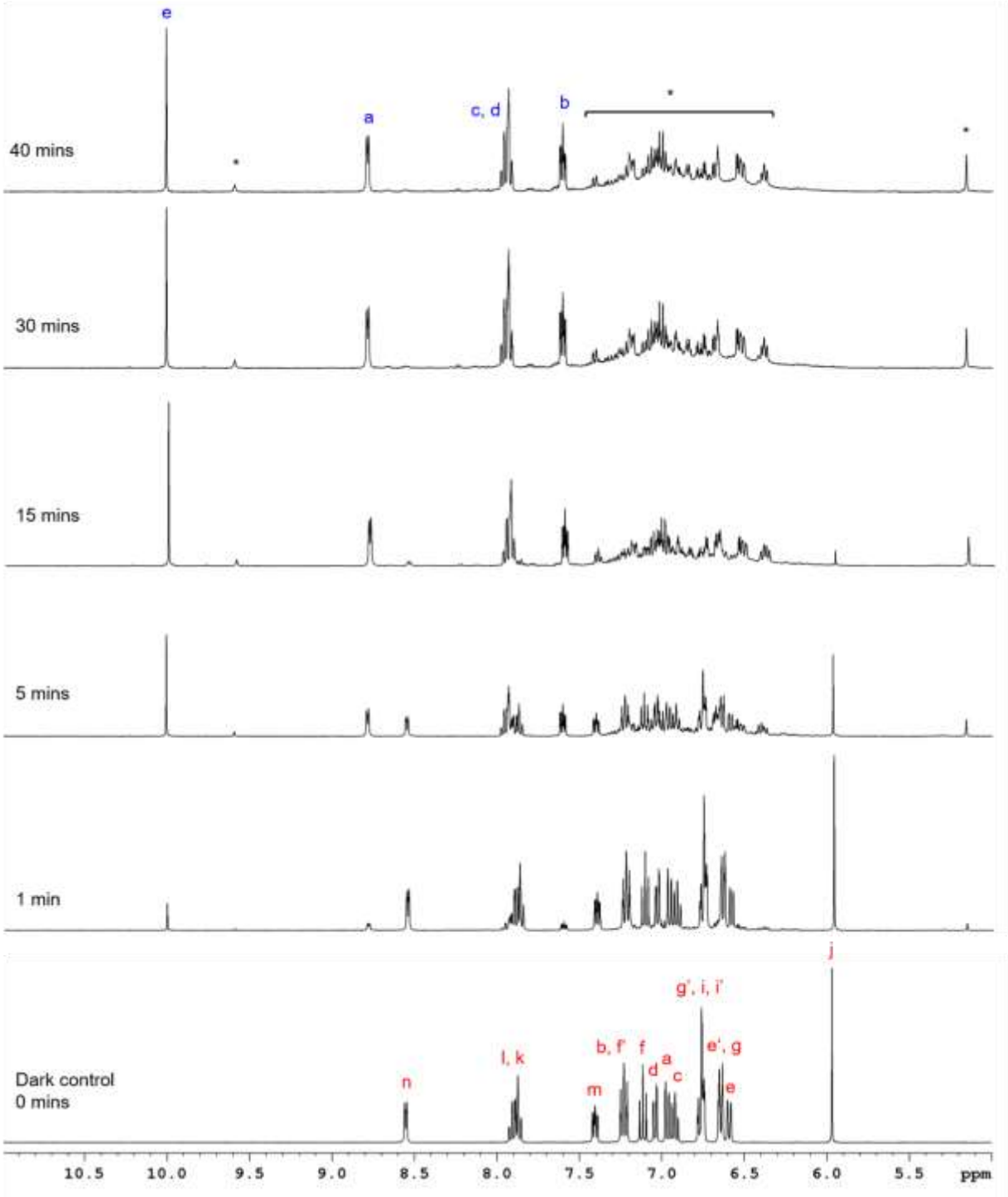

Figure S53. ^{1}H NMR spectra of masked subcomponent **A** upon irradiation at 300 nm showing the release of 2-formylpyridine after various irradiation times in CD_3CN. See Scheme S4 for proton assignments; * marks peaks assigned to a derivative of the released protecting group.

6.2.1 Quantification of 2-Formylpyridine Release

Relaxation delays (D1) of $5T_1$ are recommended to ensure complete relaxation of each signal between pulses and therefore, accurate integration of the signals. The T_1 relaxation value for proton *j* of masked subcomponent **A** and the aldehyde proton *e* of 2-formylpyridine was investigated using the t1ir1d pulse program by varying the delay d7. These protons have long T_1 relaxation values of greater than 6 s in degassed CD_3CN (Figures S54, S55). A relaxation delay

(D1) of over 30 s between scans was not feasible for time-course ^{1}H NMR experiments and therefore, a value of 3 s was chosen as a compromise between a long relaxation delay for increased integration accuracy and experiment time.

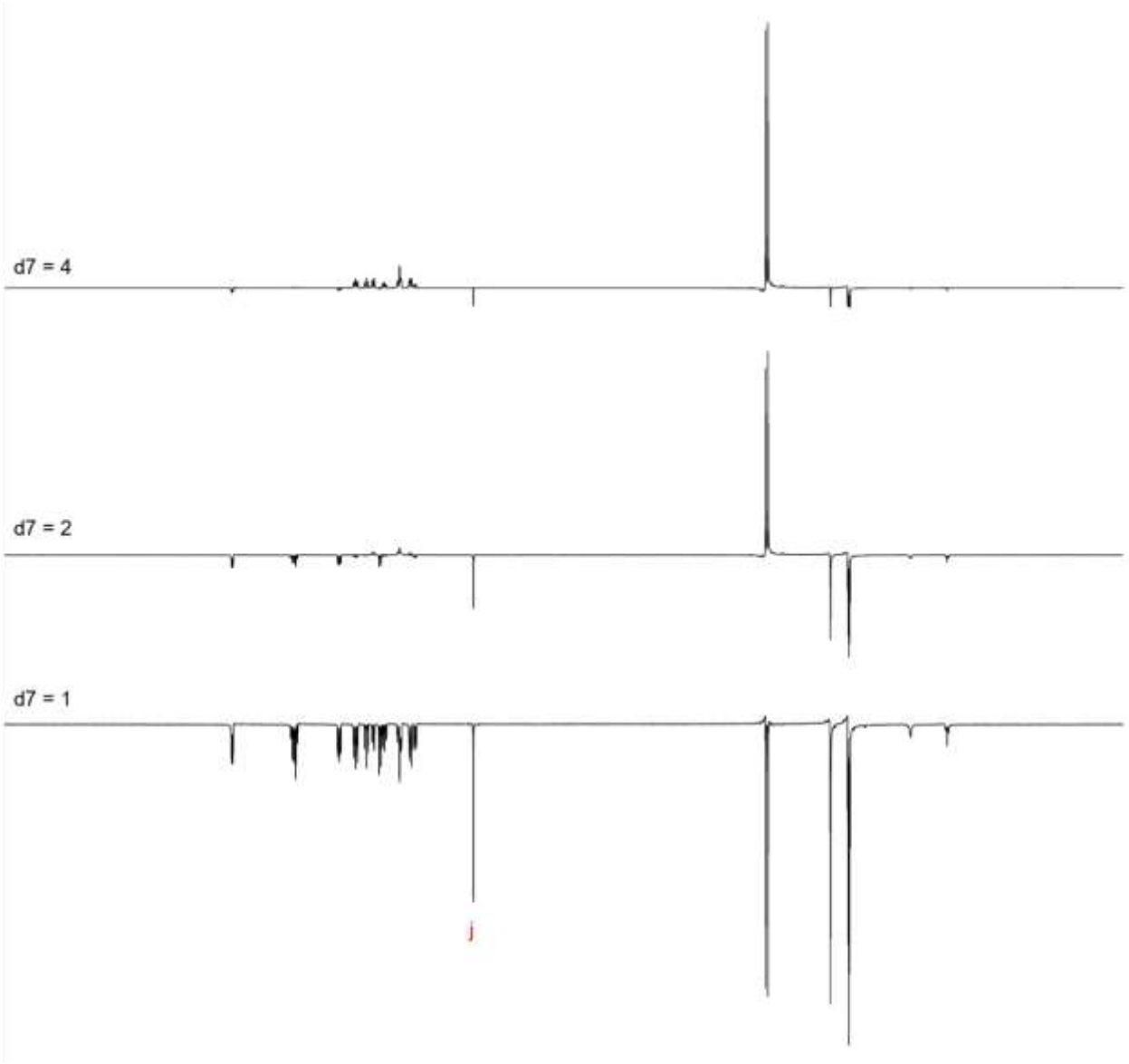

Figure S54. ^{1}H NMR spectra of masked subcomponent **A** in CD_3CN with different d7 delays showing the long T_1 relaxation value for the proton *j* signal.

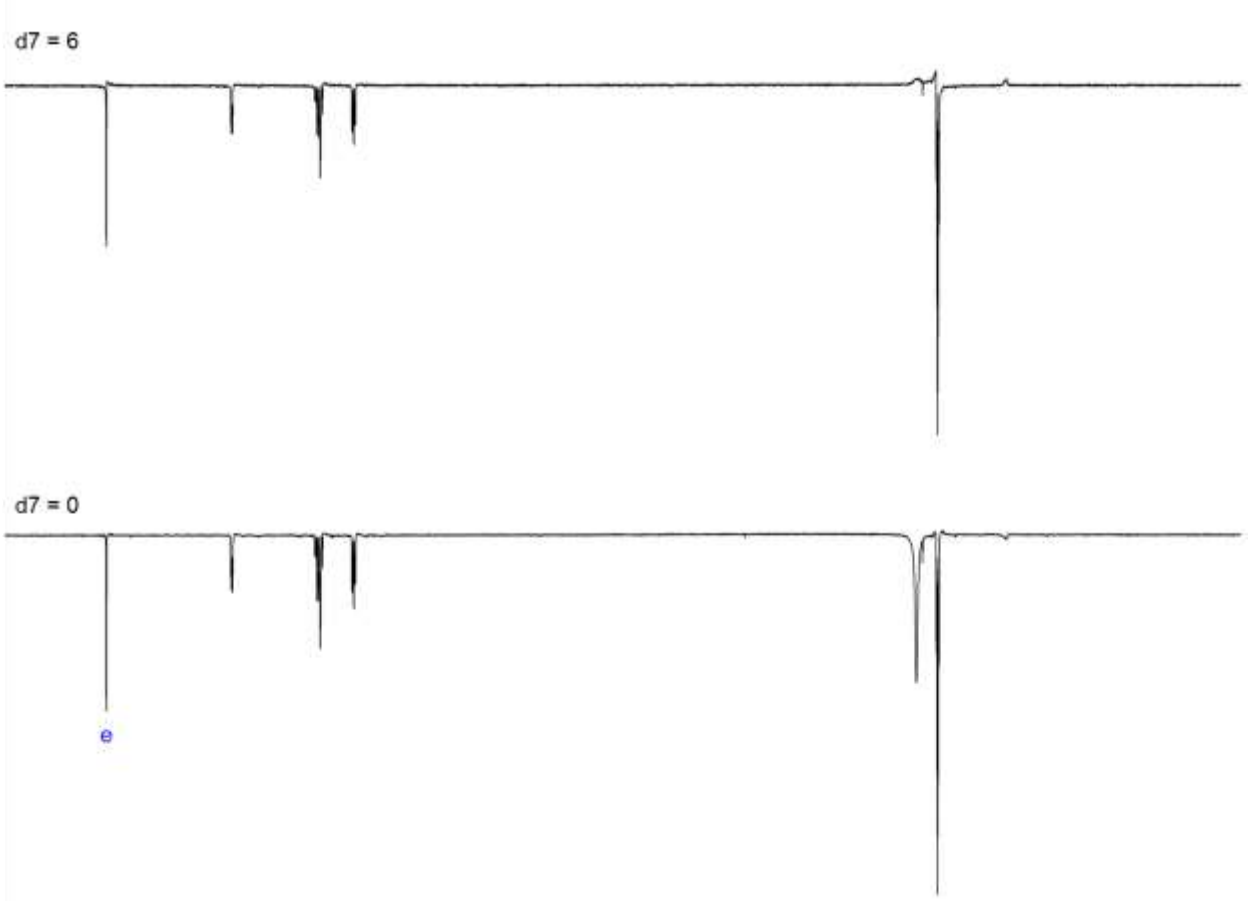

Figure S55. ^{1}H NMR spectra of 2-formylpyridine in CD_3CN with different d7 delays showing the long T_1 relaxation value for the proton *e* signal.

Control experiments with masked subcomponent **A** varying D1 from 0 s to 25 s showed minimal variation in the integrals of the aromatic proton signals which have long but slightly different T_1 relaxation values. Therefore, any difference in the integrals of proton *j* of masked subcomponent **A** and the aldehyde proton *e* of 2-formylpyridine due to the shortened D1 value was assumed to be minimal and a systematic error.

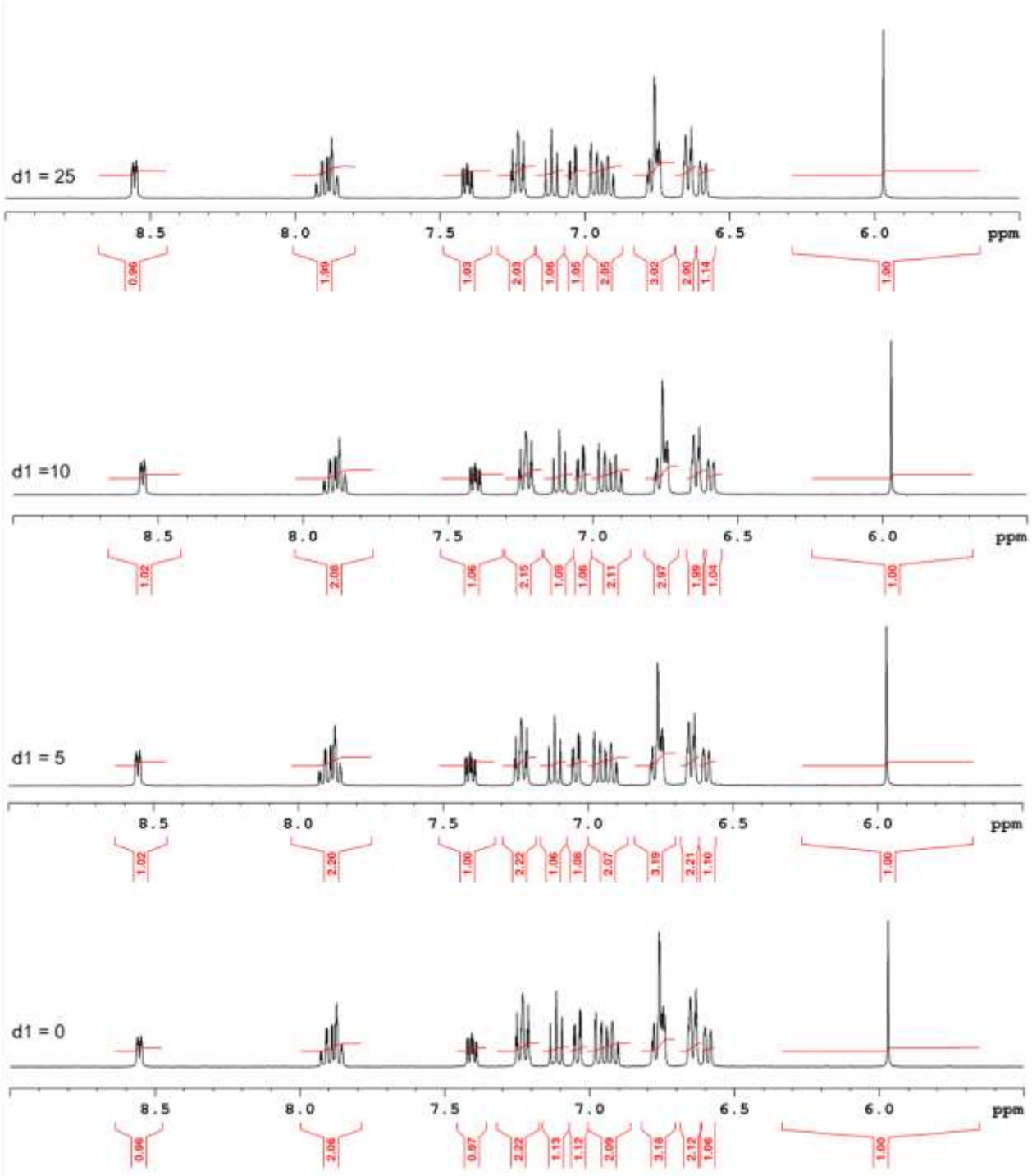

Figure S56. ^{1}H NMR spectra of masked subcomponent **A** in CD_3CN with different d1 delays showing minimal variation of the integrals of the aromatic proton signals.

The photodeprotection experiment described in Section 5.2 was carried out in triplicate. Each ^{1}H NMR spectrum was recorded for 16 scans with a relaxation delay of 3 s. The spectra were phased and the baselines were corrected before integrating the signals for proton *j* of masked subcomponent **A** and the aldehyde proton *e* of 2-formylpyridine. The integrals were converted to a 2-formylpyridine mole fraction according to Equation 1 for each irradiation time. From the three replicates, the average mole fraction (black squares) and standard deviation (red error bars) were calculated for each irradiation time and plotted in Figure S21. Variation between replicates is attributed to small variation in temperature between experiments, integration errors and the use of different J Young tubes.

$$Mole\ fraction = \frac{\int proton\ e}{\int proton\ e + \int proton\ j}$$ Equation 1

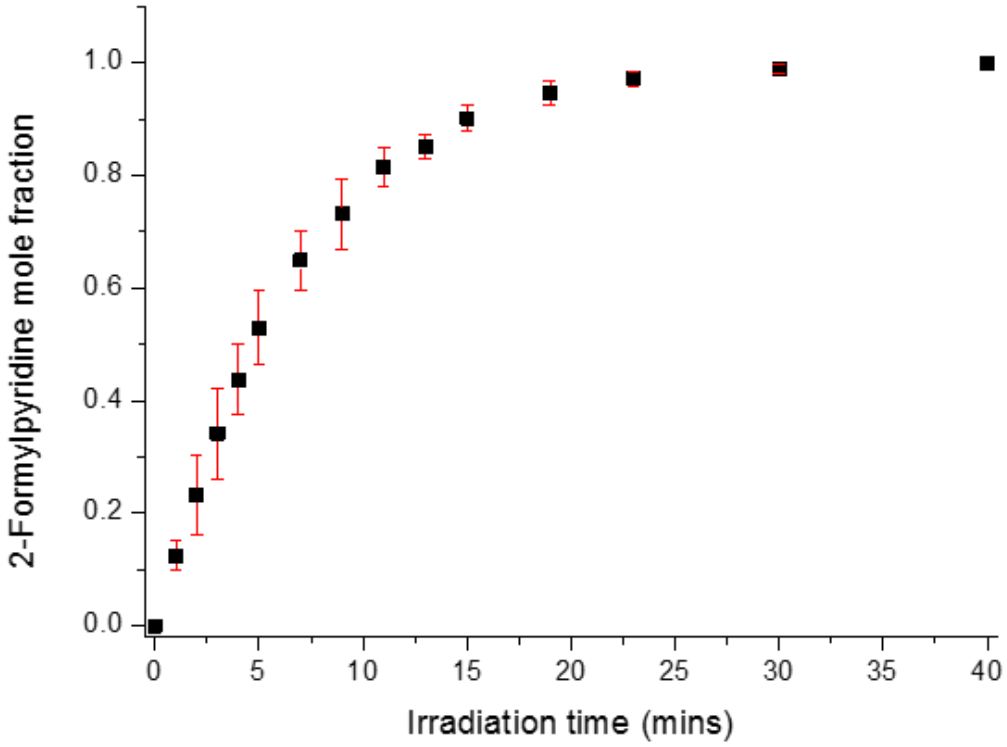

Figure S57. Photodeprotection of masked subcomponent **A** releasing 2-formylpyridine following irradiation at 300 nm in CD_3CN. The mole fraction of 2-formylpyridine was calculated according to Equation 1 and the graph shows the average of three replicates (black squares) with standard deviation (red error bars).

6.3 Masked Subcomponent A + Fe^{2+}

Release of 2-formylpyridine was also observed upon photodeprotection of **A** in the presence of iron(II) triflate (Figure S58). However, the broad signals in the ^1H NMR spectra prevented the quantification of the deprotection over time.

Method: A J Young tube containing a solution of masked subcomponent **A** (5.43 mg, 0.012 mmol) and $Fe(OTf)_2$ (1.42 mg, 0.004 mmol) in CD_3CN (0.5 mL) was degassed by 3 freeze/pump/thaw cycles and refilled with N_2. The solution was equilibrated at room temperature overnight in the dark and then irradiated at 300 nm. ^1H NMR spectra were recorded after 1, 2, 3, 4, 5, 7, 9, 11, 13, 15, 19, 23, 30 and 40 minutes of irradiation. The formation of a precipitate prevented automatic shimming of the sample and led to broad signals in the ^1H NMR spectra.

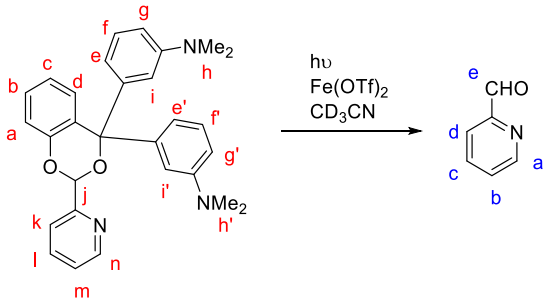

Scheme S5. Photodeprotection of masked subcomponent **A** in the presence of iron(II) triflate upon irradiation releasing 2-formylpyridine.

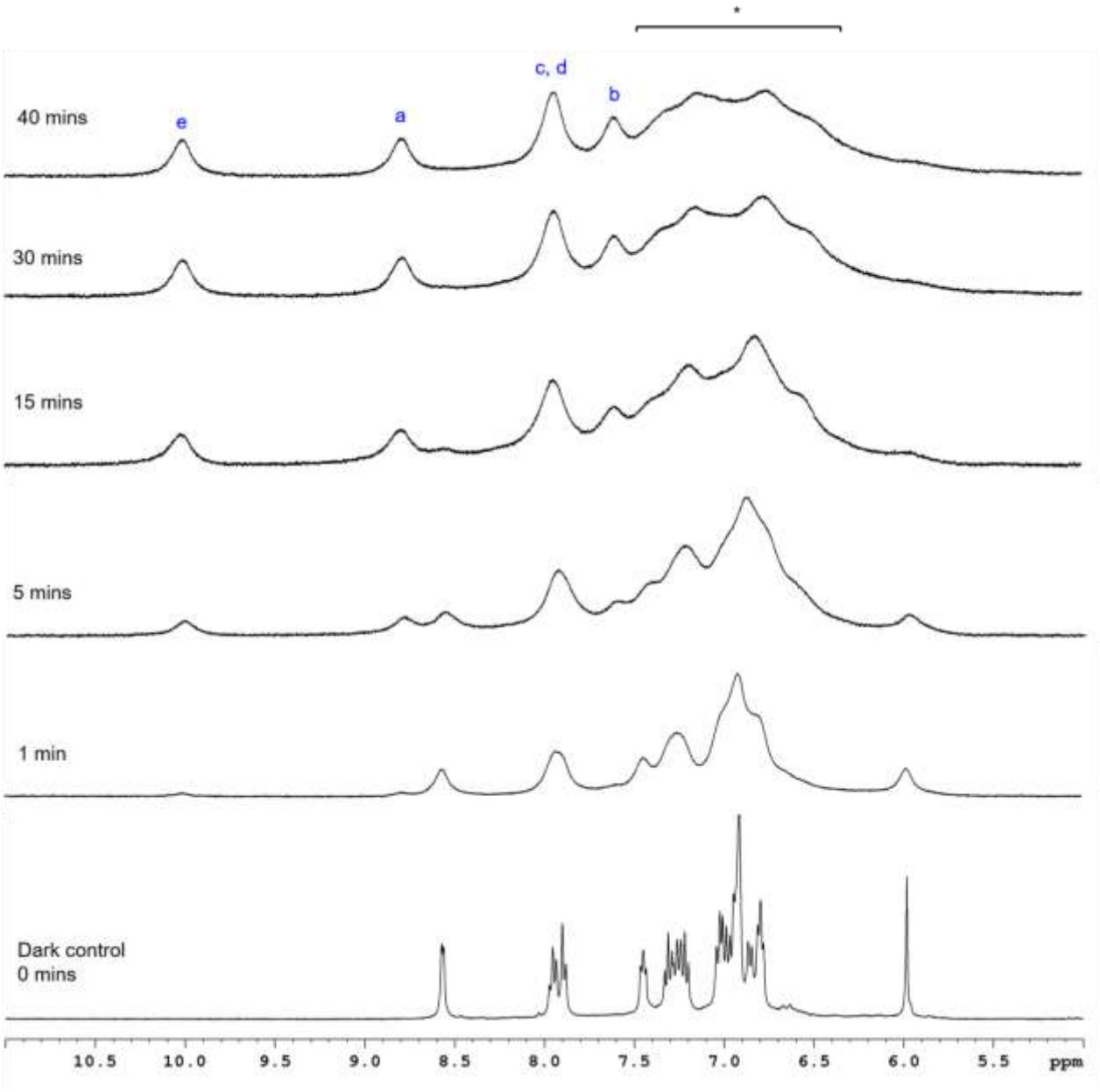

Figure S58. ^{1}H NMR spectra of a mixture of masked subcomponent **A** and iron(II) triflate upon irradiation at 300 nm showing the release of 2-formylpyridine after various irradiation times in CD_3CN. See Scheme S5 for proton assignments; * marks peaks assigned to a derivative of the released protecting group.

6.5 Masked Subcomponent A + Triamine D

Release of 2-formylpyridine was also observed upon photodeprotection of **A** in the presence of triamine **D** (Figure S59). However, the formation of side-products with triamine **D** prevented the quantification of the deprotection over time.

Method: A J Young tube containing a solution of masked subcomponent **A** (5.43 mg, 0.012 mmol) and triamine **D** (1.79 mg, 0.004 mmol) in CD_3CN (0.5 mL) was degassed by 3 freeze/pump/thaw cycles and refilled with N_2. The solution was equilibrated at room temperature overnight in the dark and then irradiated at 300 nm. ^1H NMR spectra were recorded after 1, 2, 3, 4, 5, 7, 9, 11, 13, 15, 19, 23, 30 and 40 minutes of irradiation.

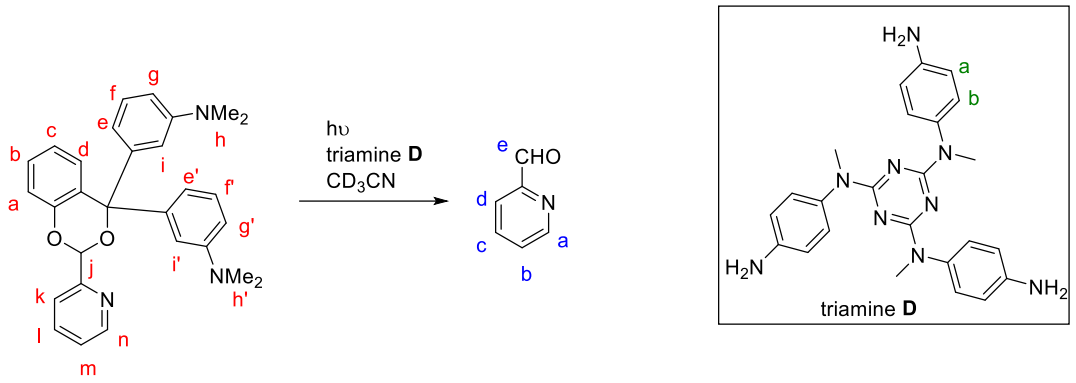

Scheme S6. Photodeprotection of masked subcomponent **A** in the presence of triamine **D** releasing 2-formylpyridine upon irradiation.

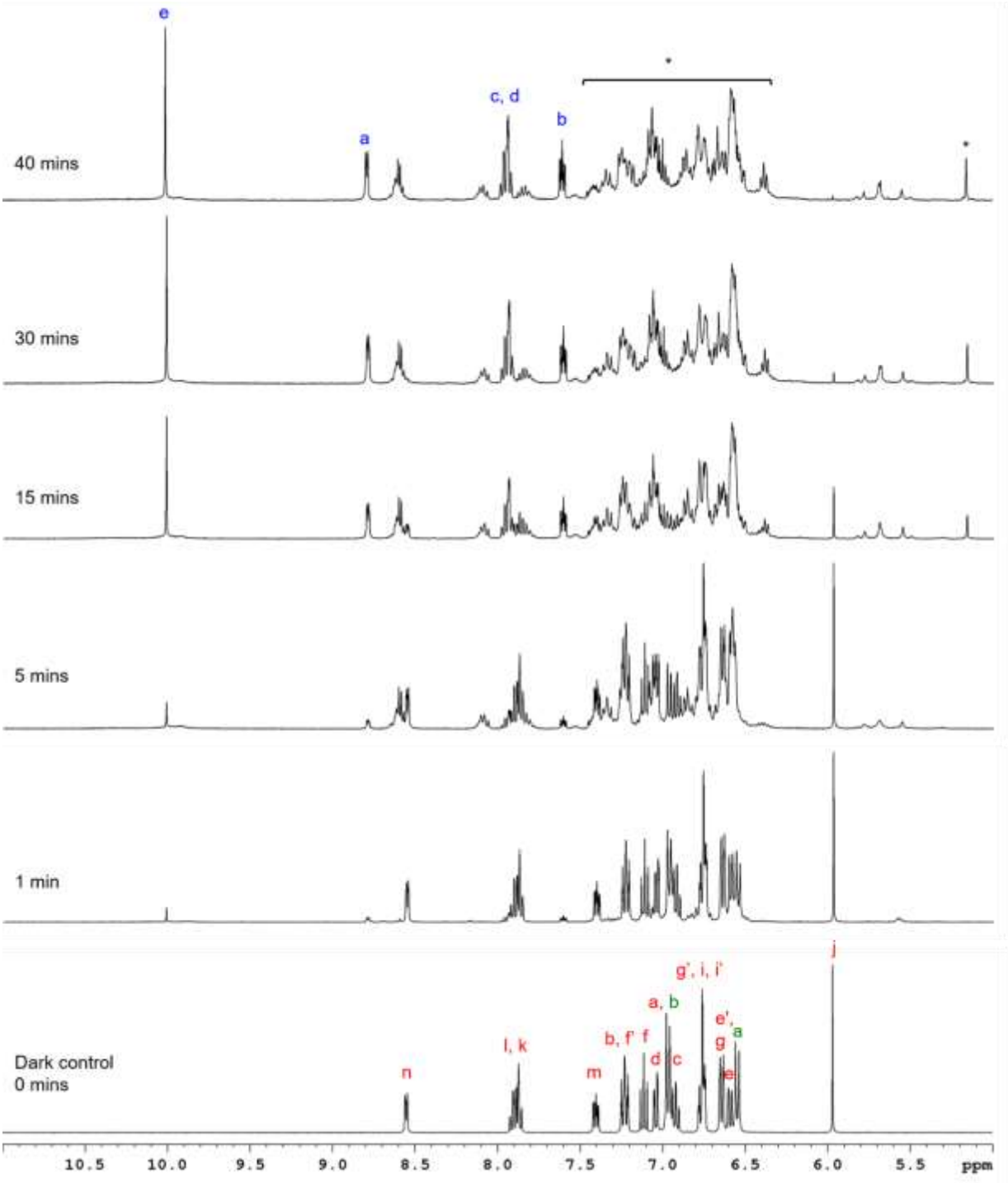

Figure S59. ^{1}H NMR spectra of a mixture of masked subcomponent **A** (red labels) and triamine **D** (green labels) upon irradiation at 300 nm showing the release of 2-formylpyridine (blue labels) after various irradiation times in CD_3CN. See Scheme S6 for proton assignments; * marks peaks assigned to a derivative of the released protecting group.

6.6 Cage 1

A mixture of masked subcomponent **A**, triamine **D** and iron(II) triflate in a 3:1:1 ratio in CD_3CN was irradiated for 40 min, and the photodeprotection was monitored by ^{1}H NMR spectroscopy (Figure S60). During the first 15 min, peaks in the ^{1}H NMR spectra were broad but they began to sharpen after 15 min of irradiation and a color change to purple was observed (Figure S52). Despite the potential for absorbance of cage **1** (Figure S44) or intermediate iron(II) complexes at 300 nm to interfere with photodeprotection, peaks corresponding to cage **1** were observed in the

^{1}H NMR spectrum after 30 min of irradiation (Figure S60). These peaks increased in intensity following equilibration at room temperature over 24 h. Some 2-formylpyridine was still present after equilibrium was reached (Figure S61), which we infer to be a consequence of side-reactions with triamine **D** or iron(II) triflate during the photodeprotection, as discussed above. The excess 2-formylpyridine could be removed along with residues of the released protecting group **C** by precipitation of the cage with diethyl ether (Figure S61). Figure S62 shows a comparison of the ^{1}H NMR spectrum after 40 min irradiation for the self-assembly of cage **1** with the control experiments (masked subcomponent **A** alone and in the presence of iron(II) triflate or triamine **D**).

Method: A J Young tube containing a solution of masked subcomponent **A** (5.48 mg, 0.012 mmol), iron(II) triflate (1.45 mg, 0.004 mmol) and triamine **D** (1.79 mg, 0.004 mmol) in CD_3CN (0.5 mL) was degassed by 3 freeze/pump/thaw cycles and refilled with N_2. The solution was equilibrated at room temperature overnight in the dark and then irradiated at 300 nm. ^{1}H NMR spectra were recorded after 1, 2, 3, 4, 5, 7, 9, 11, 13, 15, 19, 23, 30 and 40 minutes of irradiation. The mixture was left to equilibrate at room temperature for 1 day and another ^{1}H NMR spectra was recorded. The cage was purified by filtering through glass fibre filter paper and adding the filtrate dropwise to diethyl ether (~9 mL) to precipitate the cage. Following centrifugation, the supernatant was decanted and the purple solid was washed twice with diethyl ether and dried *in vacuo* to give **1**.

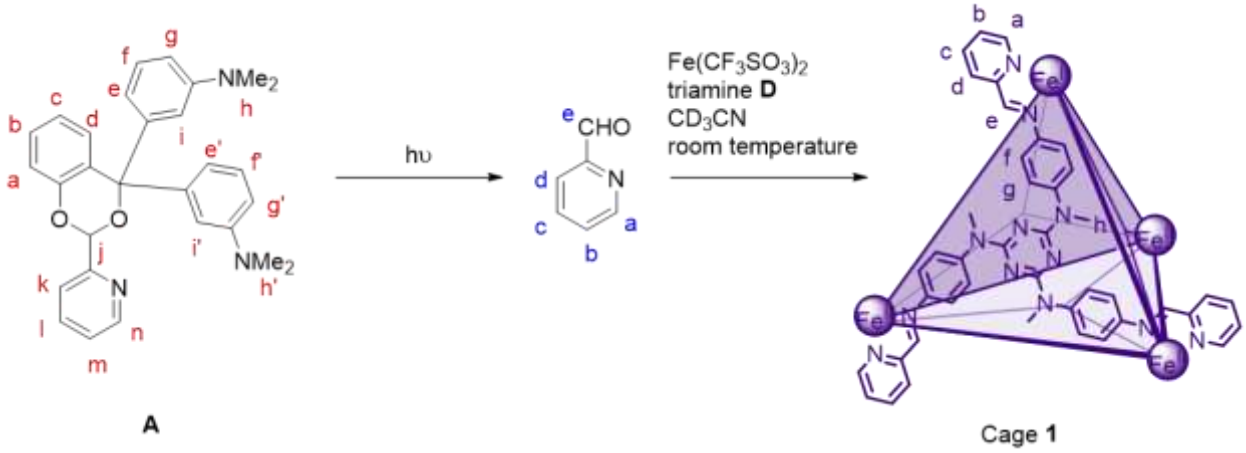

Scheme S7. Photoactivated self-assembly of cage **1** from photodeprotection of masked subcomponent **A** and equilibration with iron(II) triflate and triamine **D** in CD_3CN.

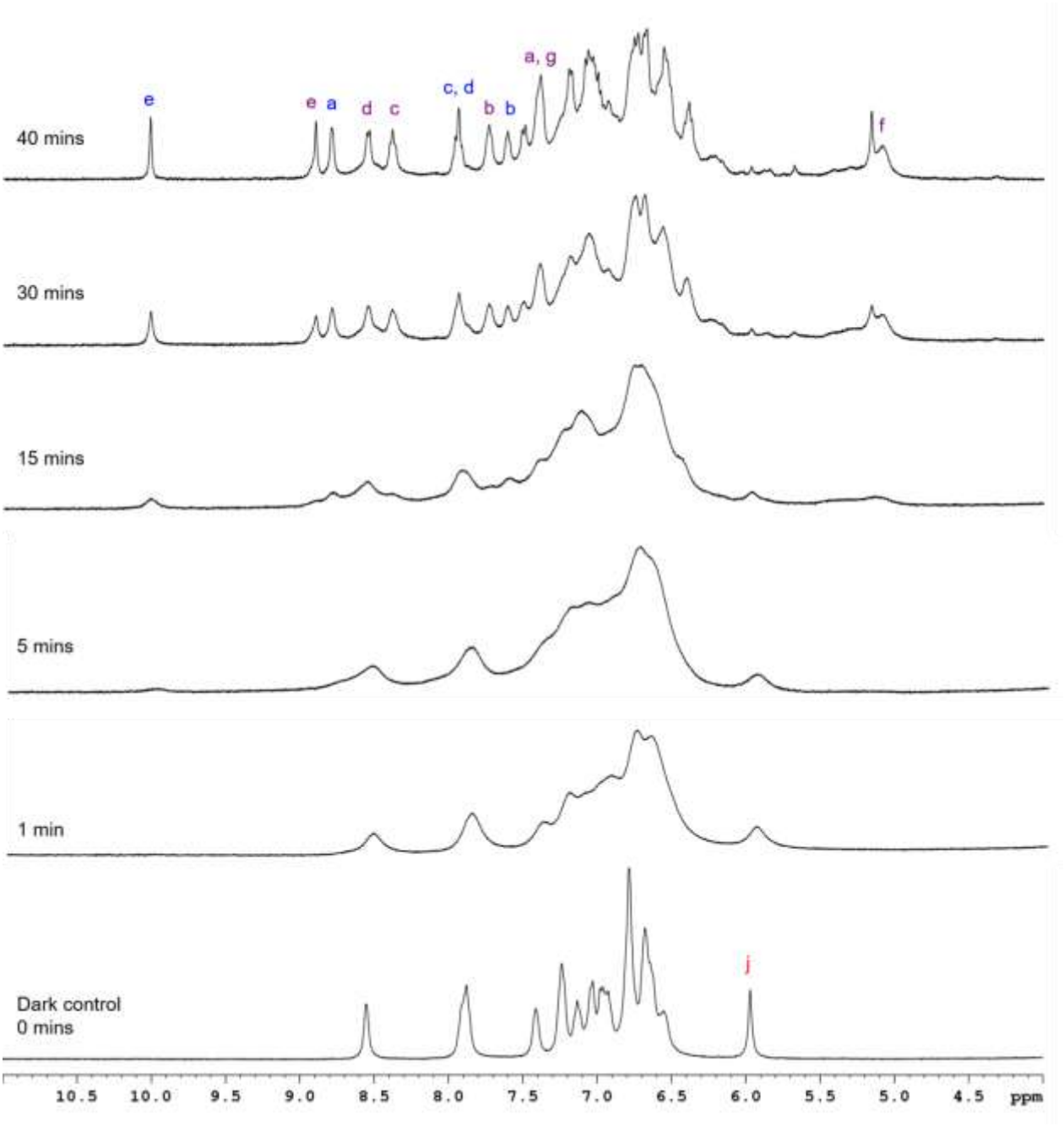

Figure S60. ^{1}H NMR spectra of a mixture of masked subcomponent **A** (red labels), triamine **D** and iron(II) triflate upon irradiation at 300 nm showing the release of 2-formylpyridine (blue labels) and formation of cage **1** (purple labels) after various irradiation times in CD_3CN. See Scheme S7 for proton assignments.

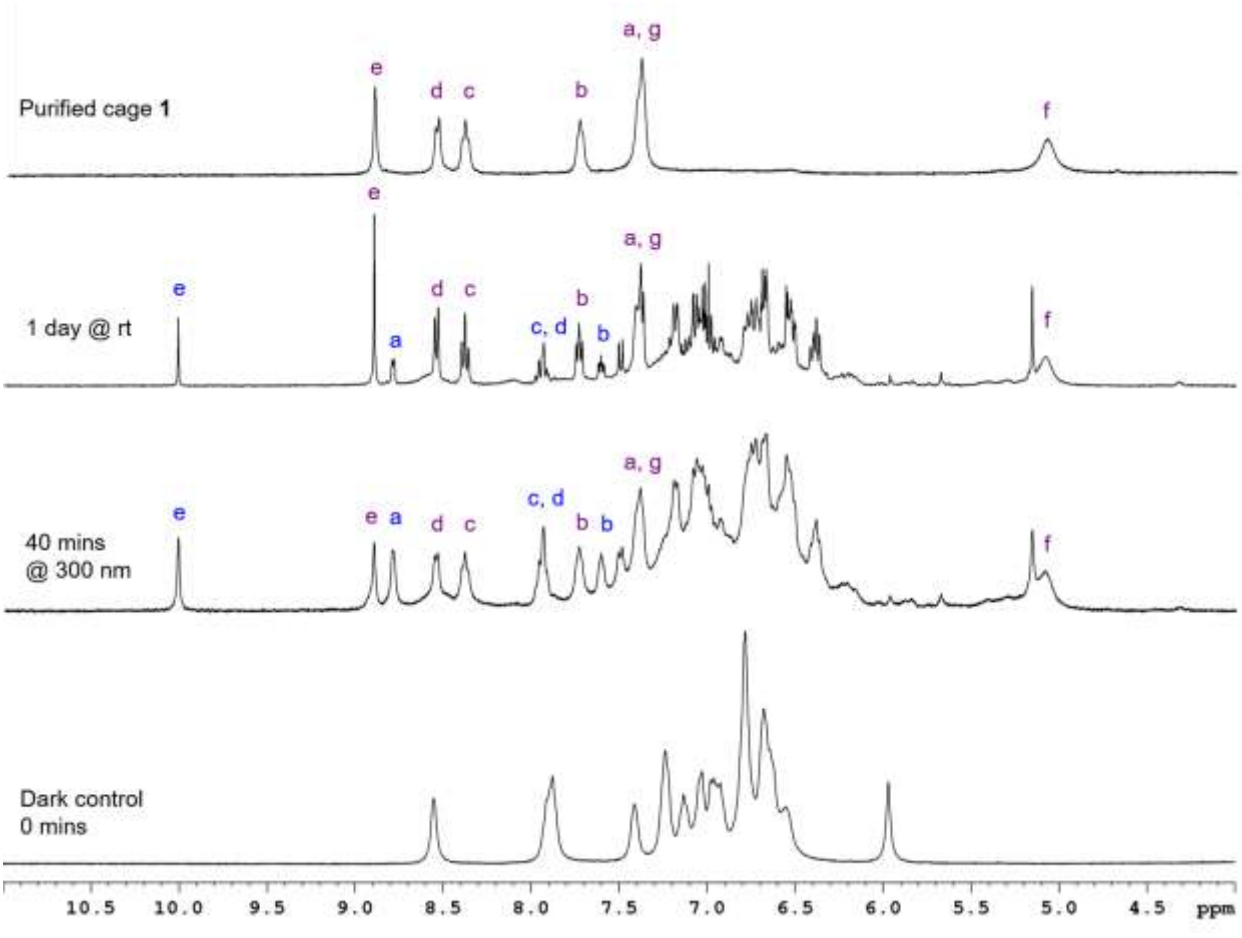

Figure S61. ^{1}H NMR spectra of the reaction mixture upon irradiation at 300 nm showing the release of 2-formylpyridine (blue labels) and formation of cage **1** (purple labels) following equilibration at room temperature in CD_3CN. The cage was purified by precipitation to remove the excess 2-formylpyridine and released photolabile protecting group. See Scheme S7 for proton assignments.

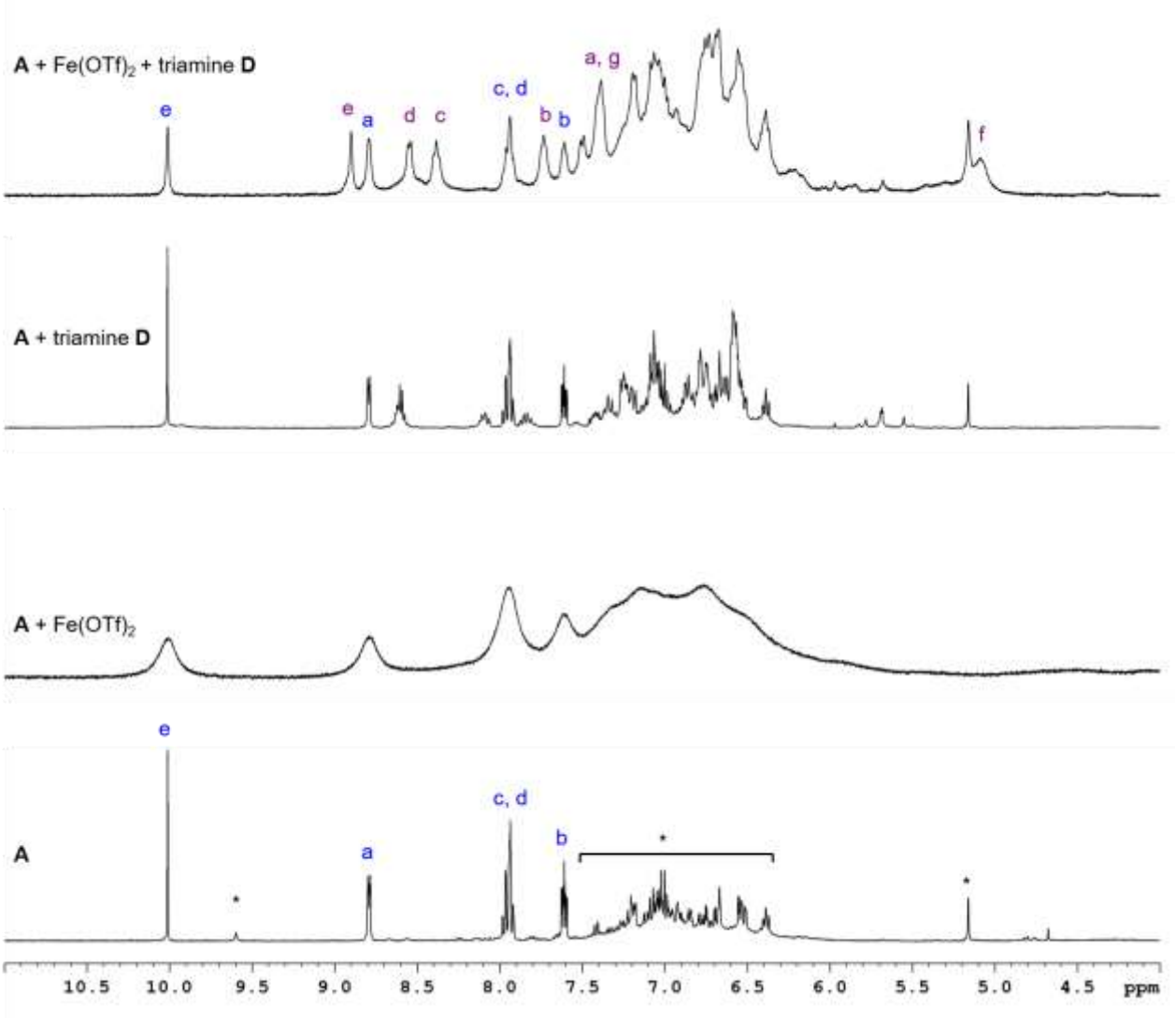

Figure S62. Comparison of ^{1}H NMR spectra after 40 minutes of irradiation at 300 nm in CD_3CN for photodeprotections of: **A**, **A** + $Fe(OTf)_2$, **A** + triamine **D**, and **A** + $Fe(OTf)_2$ + triamine **D**. See Scheme S7 for proton assignments; * marks peaks assigned to a derivative of the released protecting group.

7 Photoactivated Self-Assembly of Cage 1 and Guest Uptake

The following optimizations were found to maximize the yield and purity of cage **1** prepared *via* photodeprotection of **A**. First, a slight excess of iron(II) triflate (5 equiv instead of 4 per cage) was used (Figure S63) in order to rebalance the reaction stoichiometry away from excess 2-formylpyridine. Second, the reaction was carried out in 98:2 CD_3CN:D_2O in order to help ensure that the released **C** residue reacted with water and not **D**. Third, the irradiation time was increased to 55 min. These conditions minimized the amount of insoluble precipitate observed and gave minimal decomposition of the released protecting group while maximizing the amount of **1** observed by ^{1}H NMR spectroscopy (Figure S63).

7.1 Cage 1

7.1.1 Optimisation

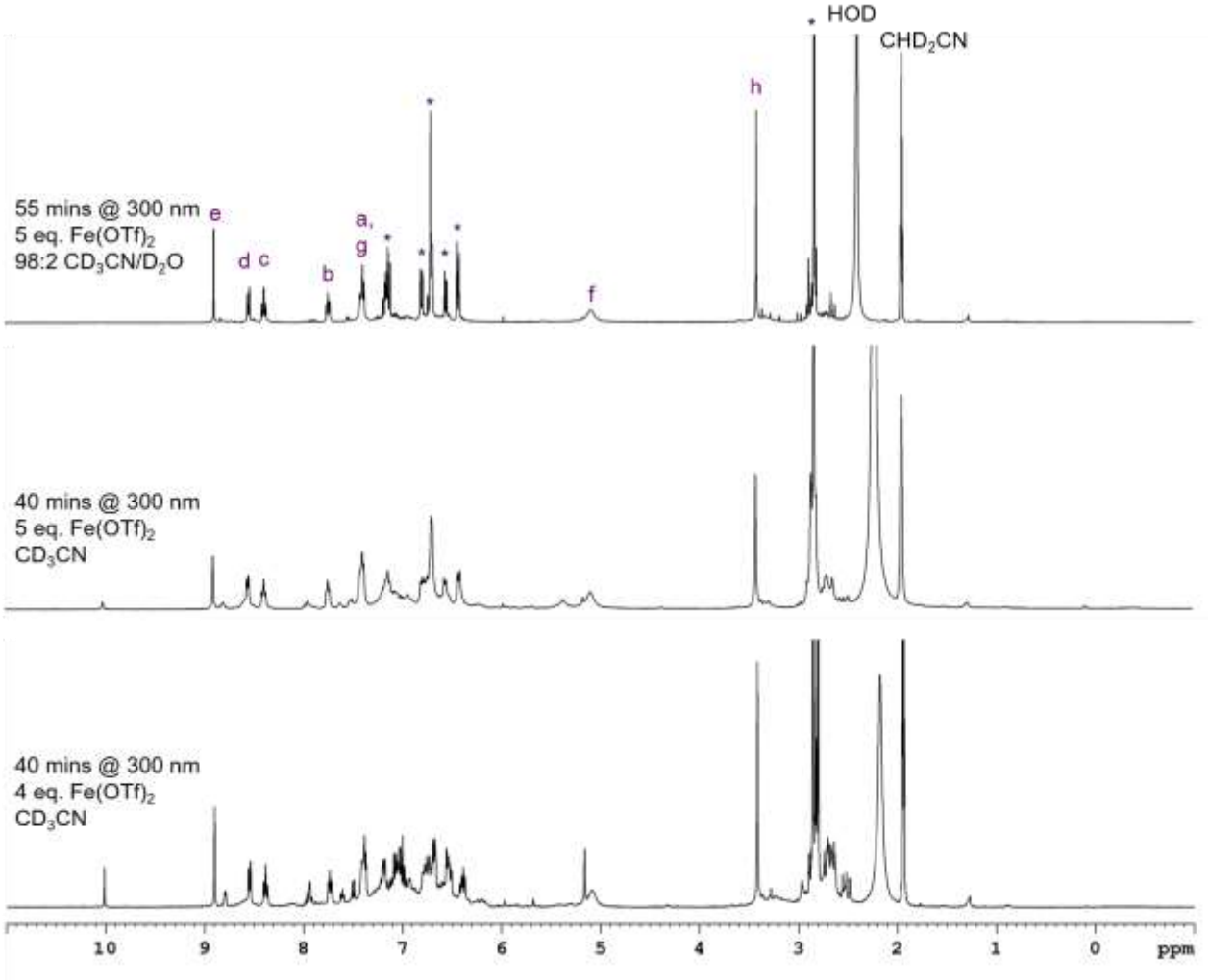

Figure S63. Comparison of ^{1}H NMR spectra for optimisation of the light-triggered self-assembly of cage **1** (purple labels) varying the number of equivalents of iron(II) triflate, solvent composition and irradiation time. See Scheme S7 for proton assignments; * marks peaks assigned to a derivative of the released protecting group.

7.1.2 Optimised Method

In a glovebox, masked subcomponent **A** (5.42 mg, 0.012 mmol), iron(II) triflate (1.77mg, 0.005 mmol) and triamine **D** (1.77 mg, 0.004 mmol) were dissolved in 98:2 CD_3CN/D_2O (0.5 mL/10 µL) in a J Young tube. The solution was irradiated for 55 minutes at 300 nm then left to equilibrate at 298 K for several days. ^{1}H NMR spectra were recorded periodically to monitor the equilibration progress.

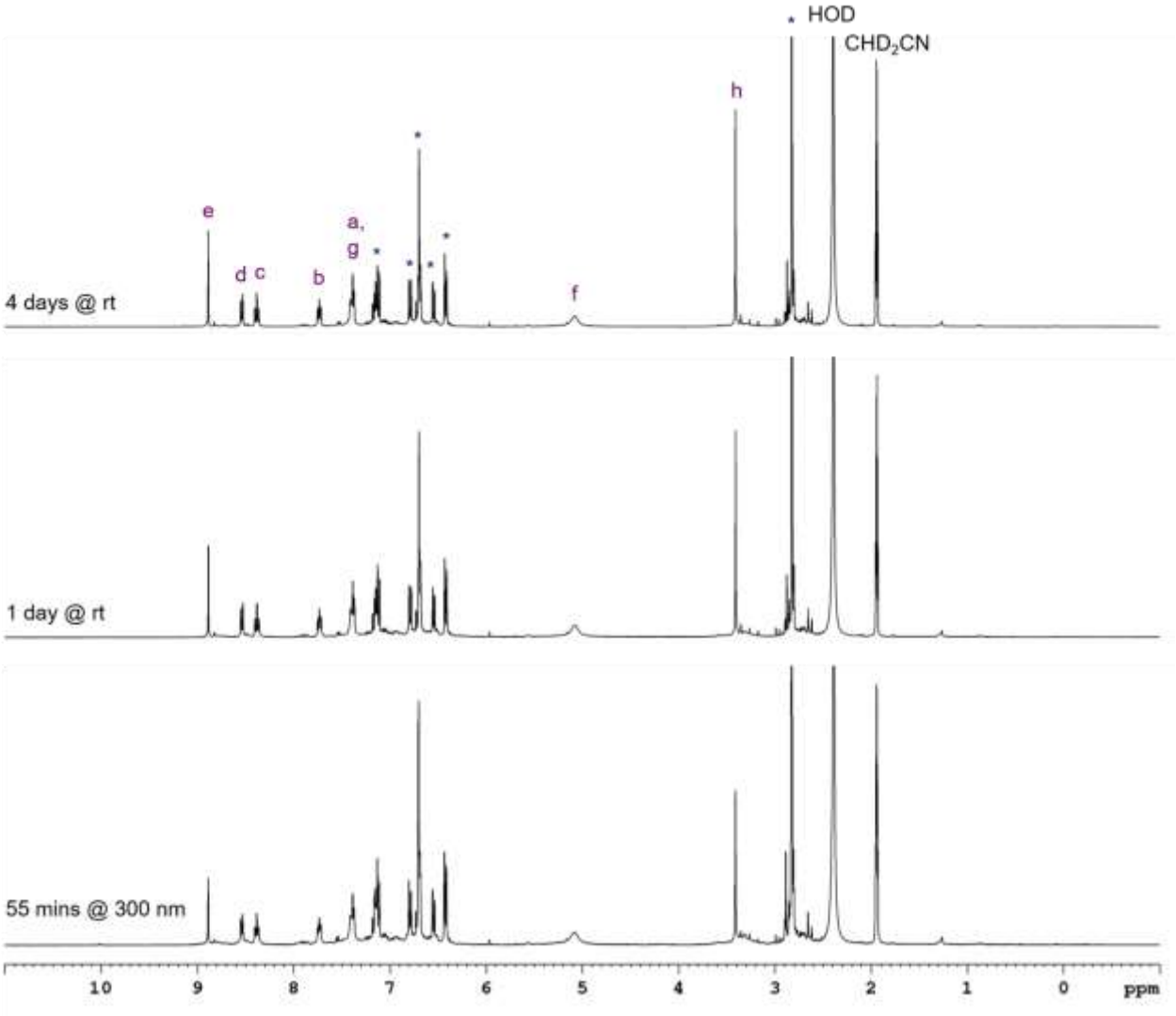

Figure S64. ^{1}H NMR spectra of the reaction mixture upon irradiation at 300 nm and equilibration at room temperature showing the formation of cage **1** (purple labels) and release of the photolabile protecting group (*) in 98:2 CD_3CN/D_2O. See Scheme S7 for proton assignments.

7.2 [Adamantane ⊂ 1]$^{8+}$

In a glovebox, masked subcomponent **A** (5.42 mg, 0.012 mmol), iron(II) triflate (1.77 mg, 0.005 mmol), triamine **D** (1.77 mg, 0.004 mmol) and adamantane (1.47 mg, 0.01 mmol) were dissolved in 98:2 CD_3CN/D_2O (0.5 mL/10 µL) in a J Young tube. The solution was irradiated for 55 minutes at 300 nm then left to equilibrate at 298 K for several days. ^{1}H NMR spectra were recorded periodically to monitor the equilibration progress.

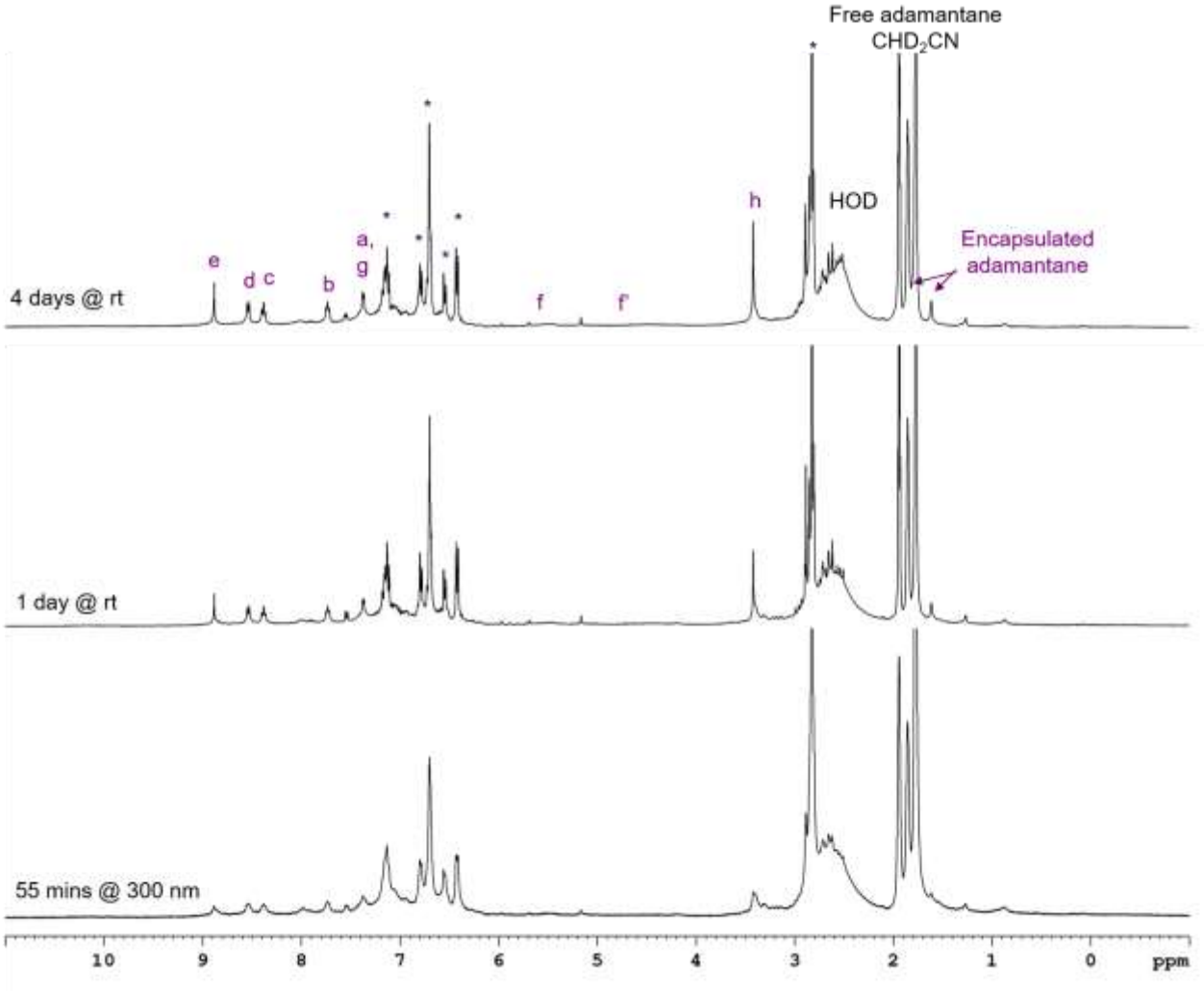

Figure S65. ^{1}H NMR spectra of the reaction mixture upon irradiation at 300 nm and equilibration at room temperature showing the formation of [adamantane ⊂ **1**]$^{8+}$ (purple labels) and release of the photolabile protecting group (*) in 98:2 CD_3CN/D_2O. See Scheme S7 for proton assignments.

7.3 [Benzene ⊂ 1]$^{8+}$

In a glovebox, masked subcomponent **A** (5.42 mg, 0.012 mmol), iron(II) triflate (1.77 mg, 0.005 mmol), triamine **D** (1.77 mg, 0.004 mmol) and benzene (1 µL, 0.01 mmol) were dissolved in 98:2 CD_3CN/D_2O (0.5 mL/10 µL) in a J Young tube. The solution was irradiated for 55 minutes at 300 nm then left to equilibrate at 298 K for several days. ^{1}H NMR spectra were recorded periodically to monitor the equilibration progress.

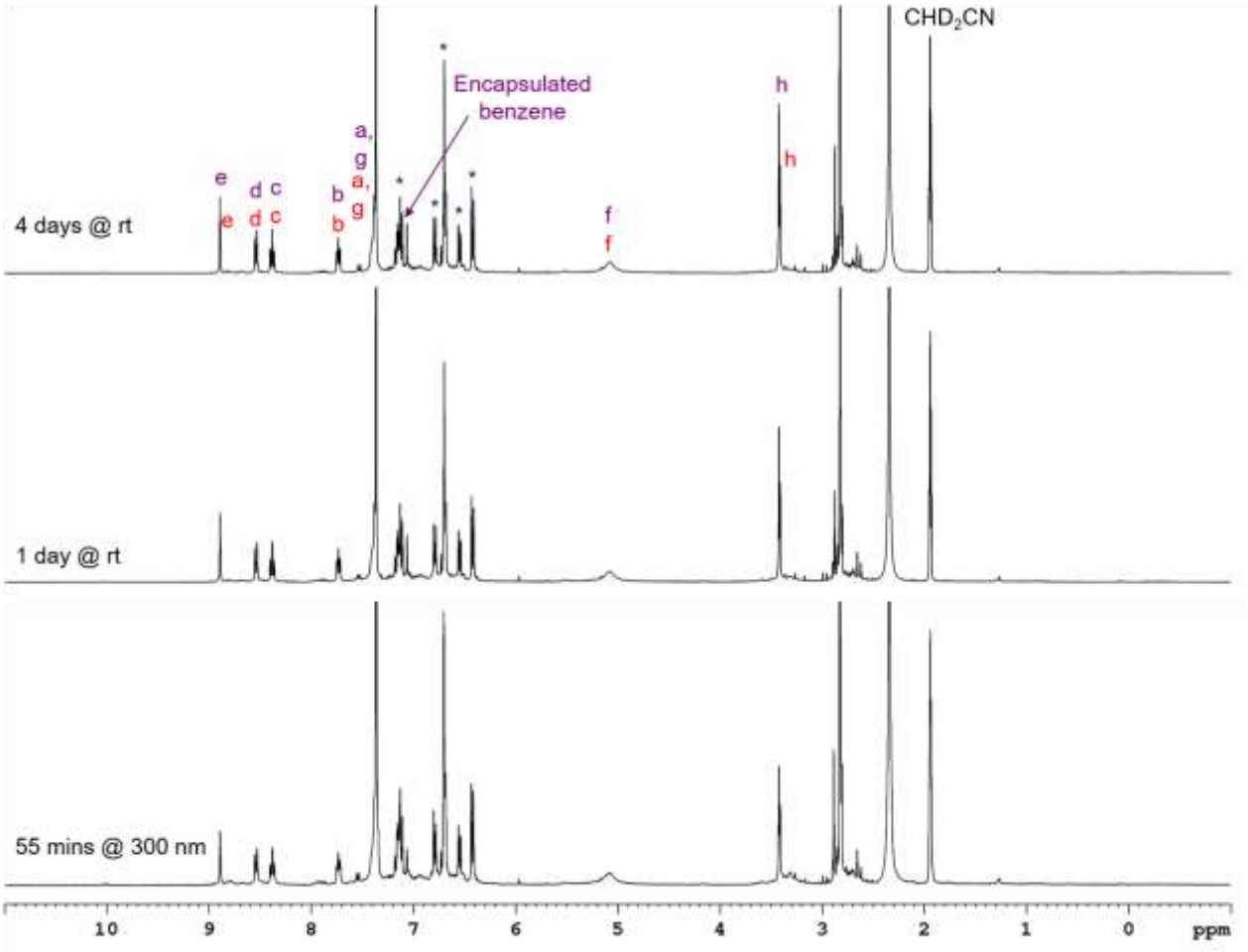

Figure S66. ^{1}H NMR spectra of the reaction mixture upon irradiation at 300 nm and equilibration at room temperature showing the formation of [benzene ⊂ **1**]$^{8+}$ (purple labels), empty cage **1** (red labels) and release of the photolabile protecting group (*) in 98:2 CD_3CN/D_2O. See Scheme S7 for proton assignments.

7.4 Selective Encapsulation from a Mixture of Guests

Benzene binds more weakly than adamantane, as evidenced by the two sets of signals for the empty cage and host-guest complex (Figure S66). Thus, the difference in binding affinity of the cage towards guests was exploited to selectively encapsulate adamantane from a mixture with benzene following light-triggered self-assembly of the cage (Figure S67). The ^{1}H NMR spectrum of the photoactivated self-assembly following equilibration contained signals for [adamantane ⊂ **1**]$^{8+}$ only (Figures S68, 69).

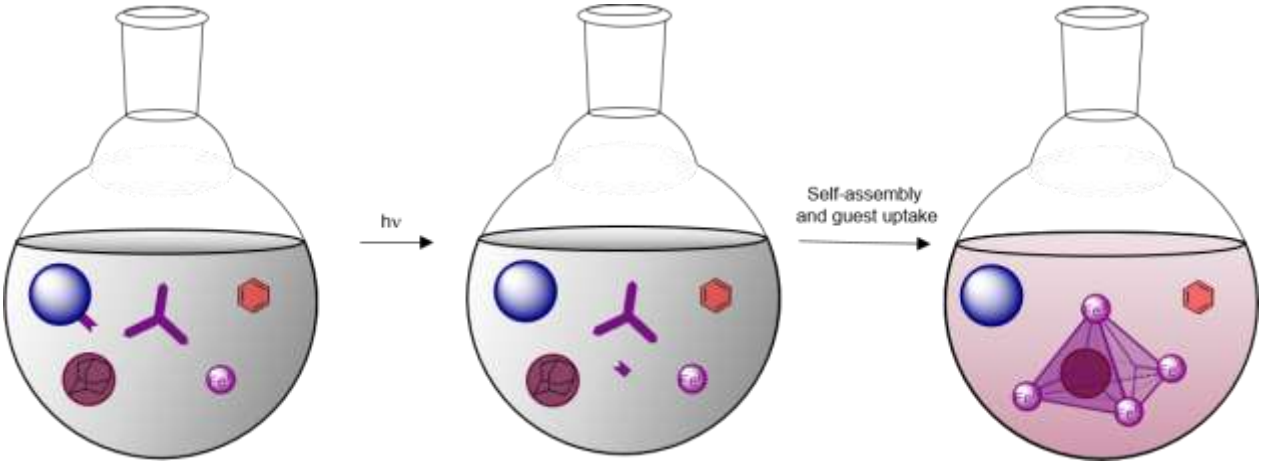

Figure S67. Light triggered self-assembly of cage **1** and selective uptake of adamantane from a mixture of guests.

Method: In a glovebox, masked subcomponent **A** (5.42 g, 0.012 mmol), iron(II) triflate (1.77 mg, 0.005 mmol), triamine **D** (1.77 mg, 0.004 mmol), adamantane (1.47 mg, 0.01 mmol) and benzene (1 µL, 0.01 mmol) were dissolved in 98:2 CD_3CN/D_2O (0.5 mL/10 µL) in a J Young tube. The solution was irradiated for 55 minutes at 300 nm then left to equilibrate at 298 K for several days. ^{1}H NMR spectra were recorded periodically to monitor the equilibration progress.

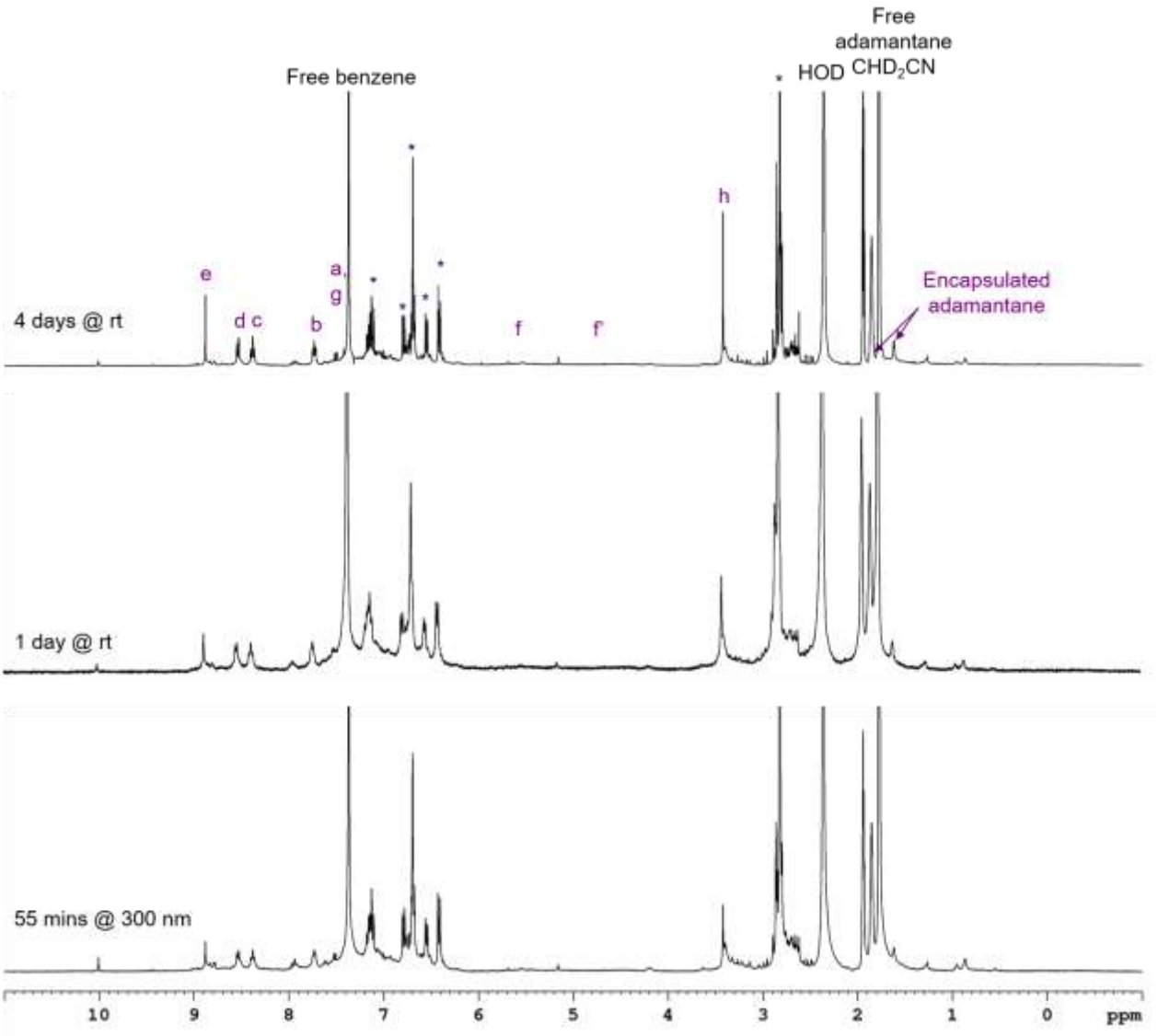

Figure S68. ^{1}H NMR spectra of the reaction mixture upon irradiation at 300 nm and equilibration at room temperature showing the selective formation of [adamantane ⊂ **1**]$^{8+}$ (purple labels) in the presence of a mixture of guests and release of the photolabile protecting group (*) in 98:2 CD_3CN/D_2O. See Scheme S7 for proton assignments.

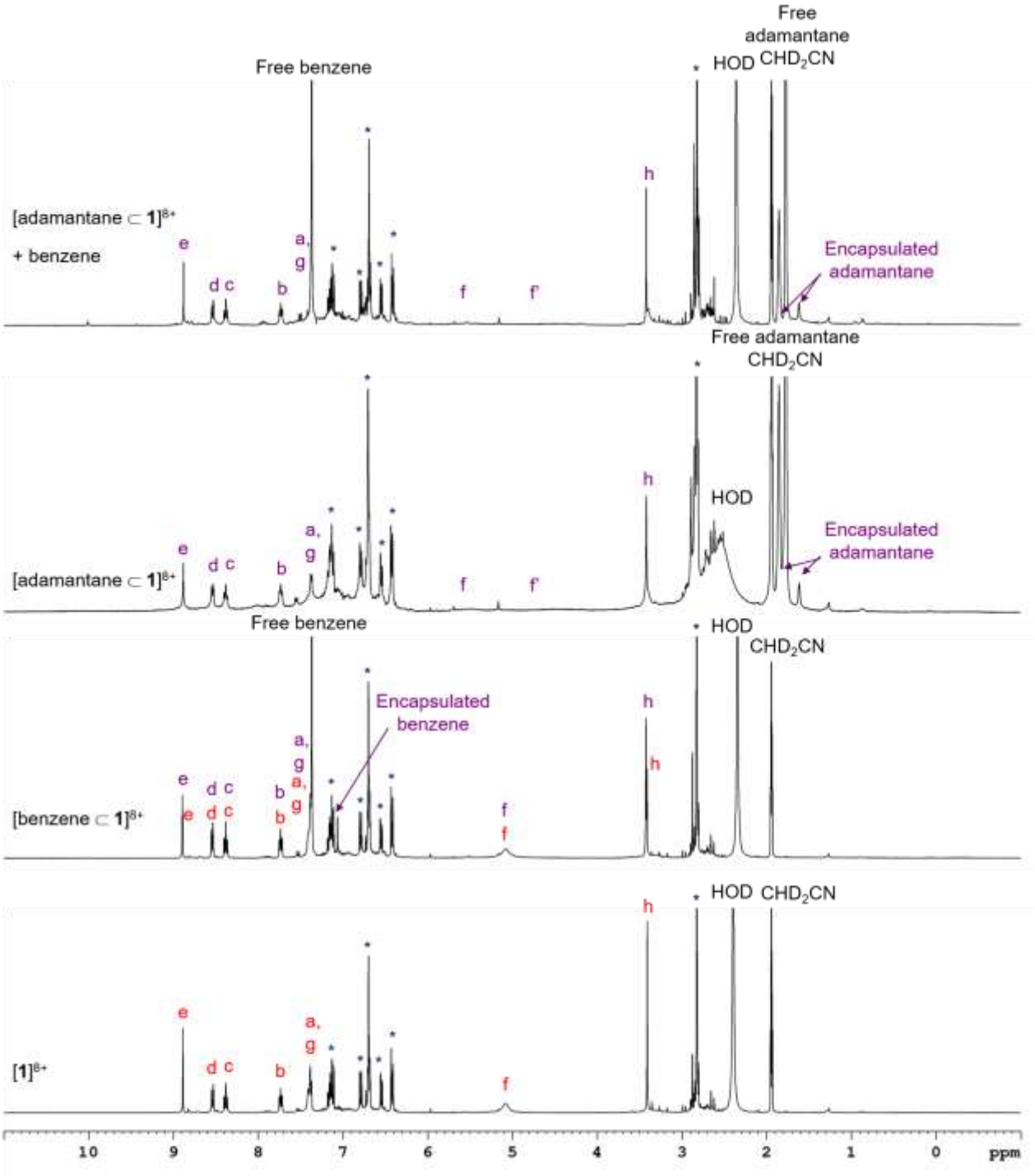

Figure S69. Comparison of ^{1}H NMR spectra for the light-triggered formation of empty cage **1** and host-guest complexes with adamantane and benzene showing the selective encapsulation of adamantane within **1** from a mixture of benzene and adamantane (top spectrum) in 98:2 CD_3CN/D_2O. See Scheme S7 for proton assignments; red labels refer to empty cage **1**, purple labels refer to host-guest complexes of cage **1** and * marks peaks assigned to a derivative of the released protecting group.

8 Orthogonal cage assemblies

8.1 Control experiments

8.1.1 Masked subcomponent **A** + $LiBF_4$

Masked subcomponent **A** was heated in the presence of $LiBF_4$ and there was no evidence of deprotection in response to the stimulus heat (Figure S70). Subsequent irradiation of the sample, however, led to deprotection of masked subcomponent **A** and the release of 2-formylpyridine.

Method: In a glovebox, masked subcomponent **A** (5.42 mg, 0.012 mmol) and $LiBF_4$ (10 μL of a 1.2 M solution in CD_3CN, 0.012 mmol) were dissolved in 98:2 CD_3CN/D_2O (0.5 mL/10 μL) in a J Young tube. The tube was sealed and heated to 90 °C for 30 minutes, then allowed to equilibrate at room temperature overnight. Subsequently, the tube was irradiated for 3 h at 300 nm and allowed to equilibrate at room temperature overnight.

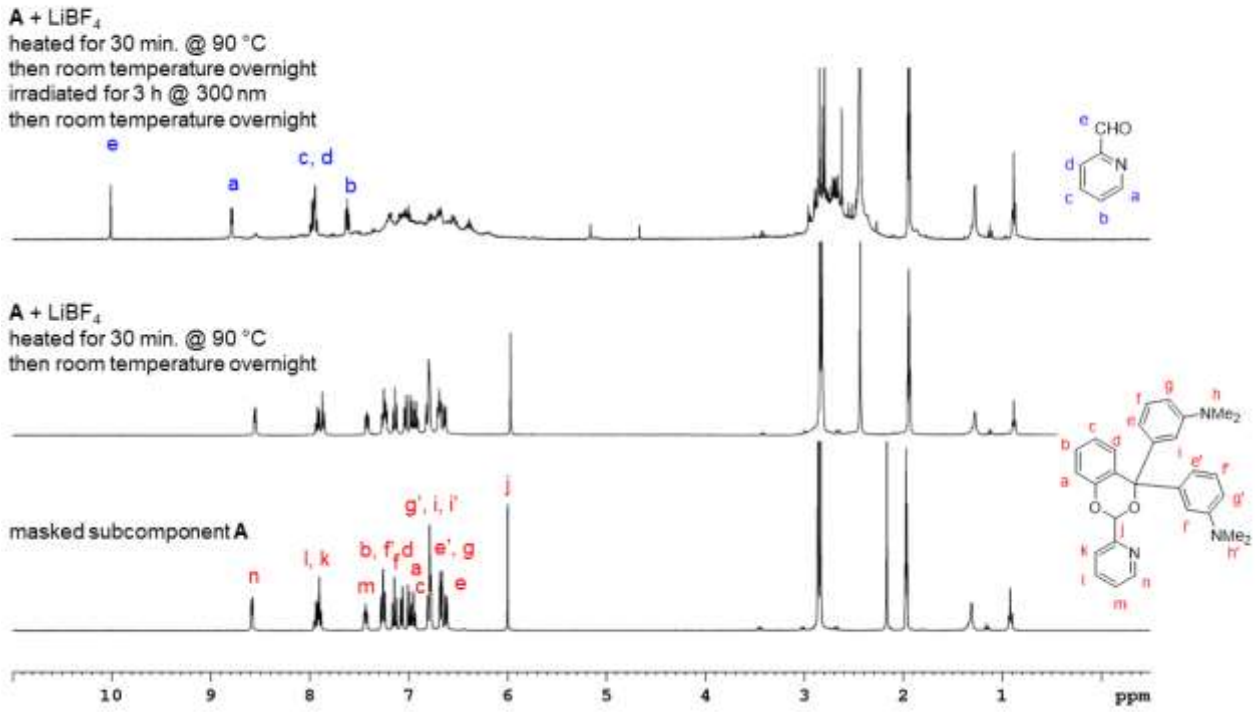

Figure S70. ^1H NMR spectra of masked subcomponent **A** (red labels) in 98:2 CD_3CN/D_2O before and after heating in the presence of 1 eq. $LiBF_4$. No release of 2-formylpyridine (blue labels) was observed until the sample was irradiated at 300 nm for 3 h.

8.1.2 Irradiation of masked subcomponent **B**

Masked subcomponent **B** was irradiated in the presence of $LiBF_4$ and the other subcomponents for the self-assembly of cage **2**. There was no evidence of deprotection in response to the stimulus light, however, cage **2** self-assembled from the mixture upon subsequent heating and equilibration (Figure S71).

Method: In a glovebox, masked subcomponent **B** (4.7 μL, 5.4 mg, 0.012 mmol), iron(II) triflate (1.77 mg, 0.005 mmol), triamine **D** (1.77 mg, 0.004 mmol) and $LiBF_4$ (10 μL of a 1.2 M solution in CD_3CN, 0.012 mmol) were dissolved in 98:2 CD_3CN/D_2O (0.5 mL/10 μL) in a J Young tube. The tube was sealed and irradiated for 3 h at 300 nm then allowed to equilibrate at room temperature overnight. Subsequently, the tube was heated at 90 °C for 30 min and allowed to equilibrate at room temperature overnight.

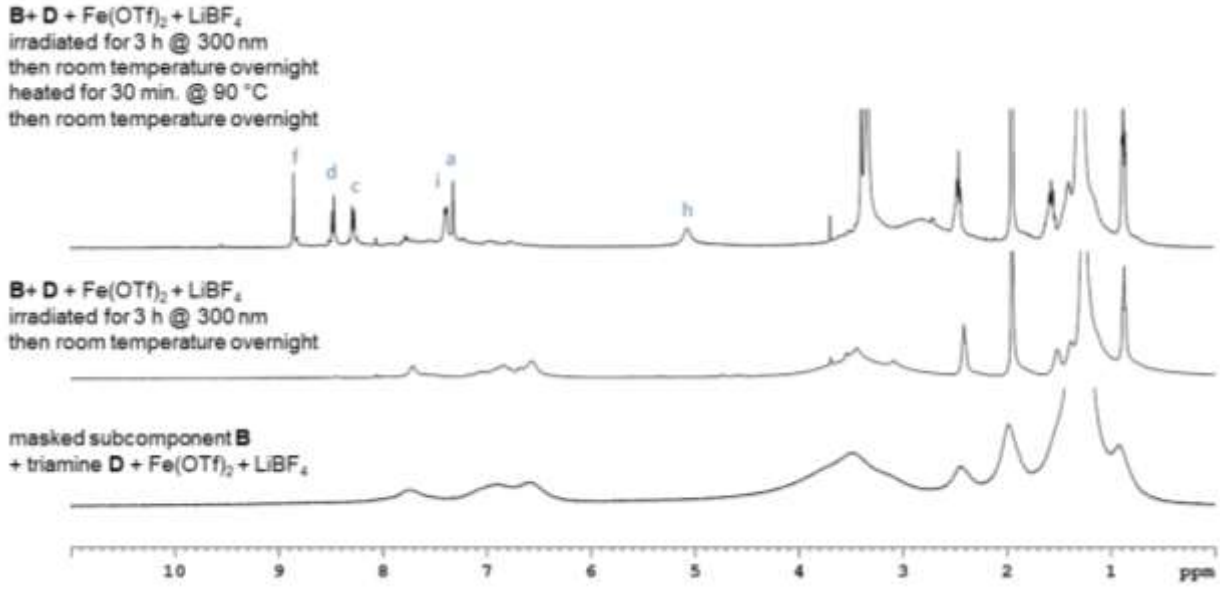

Figure S71. ^{1}H NMR spectra of masked subcomponent **B** + triamine **D** + $Fe(OTf)_2$ + $LiBF_4$ in 98:2 CD_3CN/D_2O before and after irradiating the sample at 300 nm for 3 hours. No formation of cage **2** (blue labels) was observed until the sample was heated at 90 °C for 30 minutes.

8.1.3 Heating subcomponent **B** in the absence of $LiBF_4$

Masked subcomponent **B** was heated in the presence of the other subcomponents for the self-assembly of cage **2**. There was no evidence for the deprotection of **B** in response to the heating; however, if 1 eq. $LiBF_4$ was present, the deprotection of **B** and subsequent formation of cage **2** proceeded.

Method: In a glovebox, masked subcomponent **B** (4.7 μL, 5.4 mg, 0.012 mmol), iron(II) triflate (1.77 mg, 0.005 mmol), triamine **D** (1.77 mg, 0.004 mmol) and $LiBF_4$ (10 μL or 0 μL of a 1.2 M solution in CD_3CN, 0.012 mmol) were dissolved in 98:2 CD_3CN/D_2O (0.5 mL/10 μL) in a J Young tube. The tube was sealed and heated to 90 °C for 30 minutes then allowed to equilibrate overnight at room temperature.

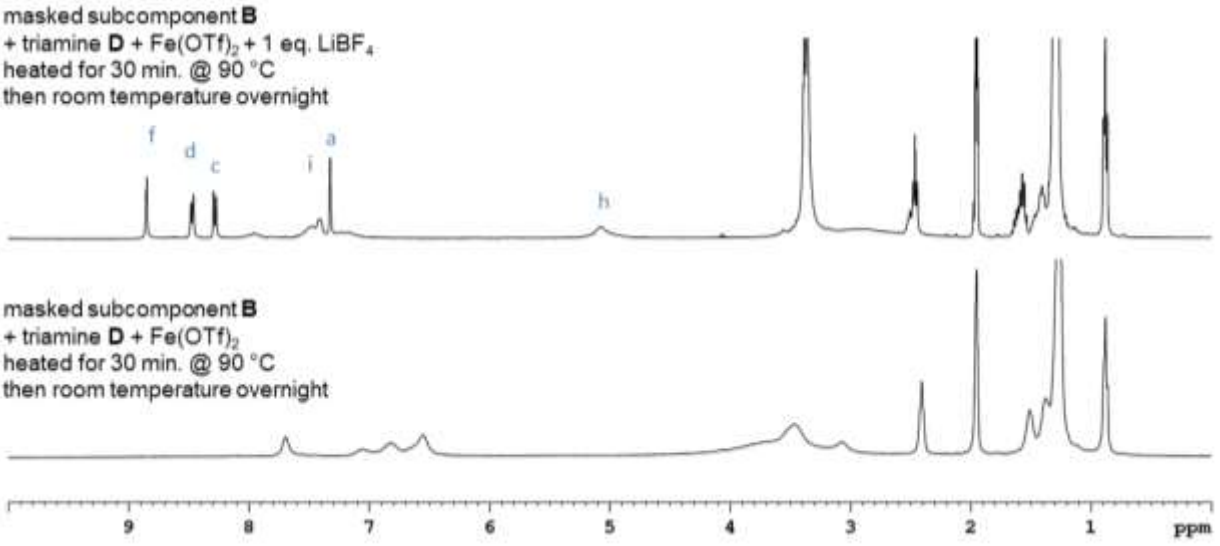

Figure S72. ^{1}H NMR spectra of masked subcomponent **B** + triamine **D** + $Fe(OTf)_2$ in 98:2 CD_3CN/D_2O after heating for 90 °C followed by equilibration overnight, both in the presence and absence of 1 eq. $LiBF_4$ per masked aldehyde. No formation of cage **2** is observed in the absence of $LiBF_4$.

8.2 Orthogonal formation of cage 1 or cage 2

In a glovebox, masked subcomponent **A** (5.42 mg, 0.012 mmol), masked subcomponent **B** (4.7 μL, 5.4 mg, 0.012 mmol), iron(II) triflate (1.77mg, 0.005 mmol), triamine **D** (1.77 mg, 0.004 mmol) and $LiBF_4$ (10 μL of a 1.2 M solution in CD_3CN, 0.012 mmol) were dissolved in 98:2 CD_3CN/D_2O (0.5 mL/10 μL) in a J Young tube (2 samples). The samples were either irradiated at 300 nm for 3 h (a) or heated at 90 °C for 30 min (b), then allowed to equilibrate at room temperature overnight.

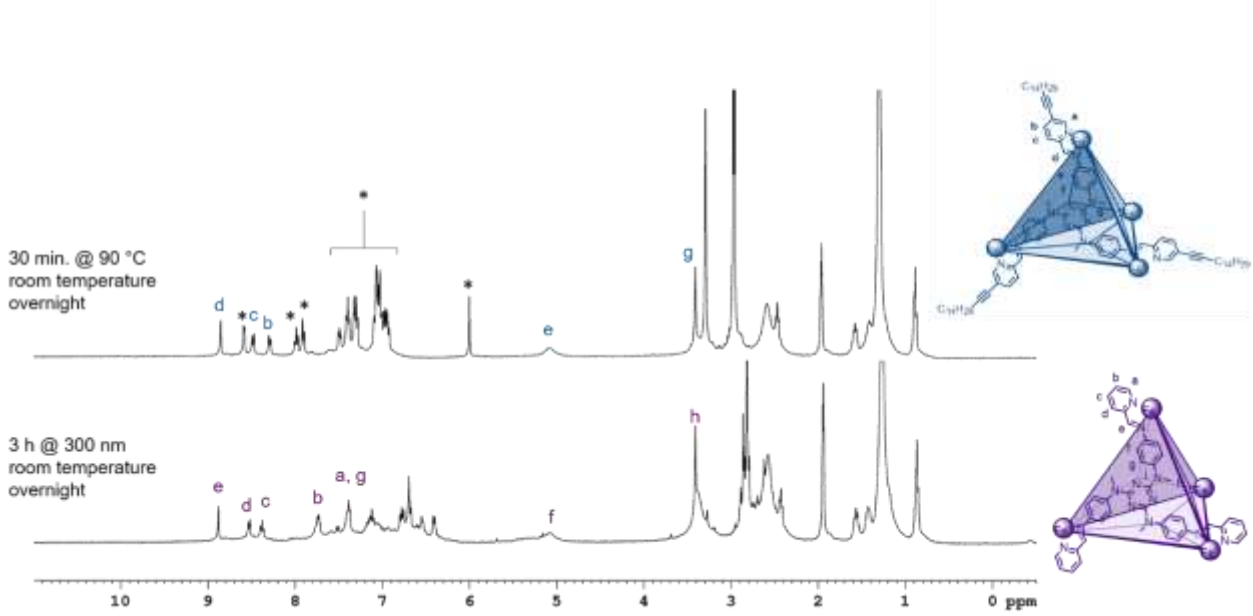

Figure S73. ^1H NMR spectra of the reaction mixture upon irradiation at 300 nm for 3 h (bottom spectrum) or heating at 90 °C for 30 min (top spectrum) followed by equilibration at room temperature overnight. * marks peaks assigned to masked subcomponent **A**.

8.3 Orthogonal formation of [ferrocene ⊂ 1]$^{8+}$or [ferrocene ⊂ 2]$^{8+}$

In a glovebox, masked subcomponent **A** (5.42 mg, 0.012 mmol), masked subcomponent **B** (4.7 μL, 5.4 mg, 0.012 mmol), iron(II) triflate (1.77mg, 0.005 mmol), triamine **D** (1.77 mg, 0.004 mmol), $LiBF_4$ (10 μL of a 1.2 M solution in CD_3CN, 0.012 mmol) and ferrocene (2.44 mg, 0.013 mmol) were dissolved in 98:2 CD_3CN/D_2O (0.5 mL/10 μL) in a J Young tube (2 samples). The samples were either irradiated at 300 nm for 3 h or heated at 90 °C for 30 min, then allowed to equilibrate at room temperature overnight.

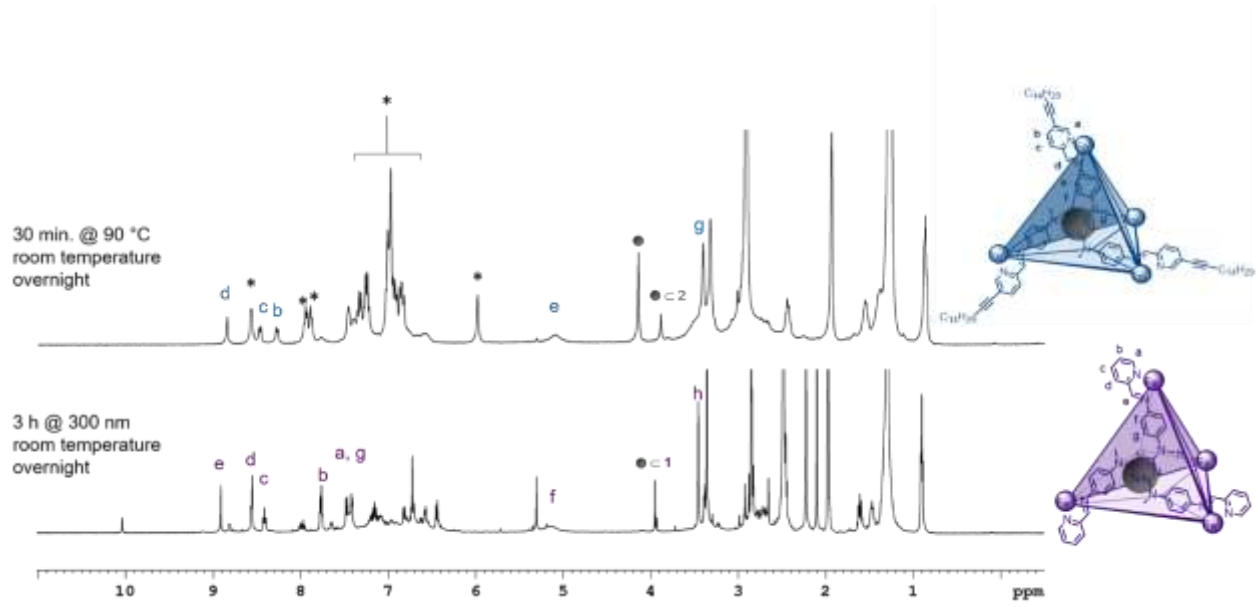

Figure S74. ^{1}H NMR spectra of the reaction mixture upon irradiation at 300 nm for 3 h (bottom spectrum) or heating at 90 °C for 30 min (top spectrum) followed by equilibration at room temperature overnight. * marks peaks assigned to masked subcomponent **A**. ● marks peaks assigned to ferrocene.

9 Phase transfer experiments

9.1 Purified cages

2 mM solutions of cages **1** and **2** were prepared in 98:2 CD_3CN/ D_2O (0.5 mL) as described in Section 3. The samples were filtered and washed with 3 x 0.5 mL cyclopentane prior to the phase transfer experiment.

9.2 Crude orthogonal assemblies

Crude samples of cages **1** and **2** were prepared by the orthogonal self-assembly procedure described in Section 8.2. The samples were filtered prior to the phase transfer experiment.

9.3 Cage + cargo experiments

Crude samples of [ferrocene ⊂ **1**] or [ferrocene ⊂ **2**] were prepared as described in Section 8.3. The samples were filtered and washed with 3 x 0.5 mL cyclopentane prior to the phase transfer experiment.

9.4 Phase transfer protocol

A 5 mm NMR tube with 0.38 mm wall thickness was used for all slice-selective ^{1}H NMR experiments. NMR tubes with thicker walls are less suitable for these experiments because the wall thickness significantly reduces the volume of sample in each 1 mm slice. 200 μL of the cage or cage + cargo solution was thus added to a 5 mm NMR tube containing a CD_3CN capillary and an equal volume of cyclopentane was added. The sample was shaken thoroughly for 10 s, then rested to allow the two phases to separate. The sample was then analysed by slice selective NMR spectroscopy (Figures S77(a) and S78(a)).

The entire biphasic sample was removed from the NMR tube and added to a glass vial containing 24 eq. tridecafluorohexane-1-sulfonic acid potassium salt. The vial was sealed and then shaken thoroughly for 30 s or until the salt had dissolved. The biphasic mixture was returned to the NMR tube, rested to allow the phases to separate and re-analysed by slice selective NMR spectroscopy (Figures S77(b) and S78(b)). If necessary, 50 – 100 μL of additional cyclopentane was added to ensure that the volumes of the two phases were approximately equal after handling the sample due to the volatility of this solvent.

9.5 Slice selective NMR spectroscopy protocol

The slice-selective NMR experiments conducted herein were automated using previously-reported software.[7]

Using the depth gauge for the instrument, the sample was positioned such that the interface would be located as near as possible to the mid-point of the probe's transmit/receive coils. The sample was locked to CD_3CN and tuned to the ^1H nucleus, but the sample was left unshimmed. A pseudo-2D slice-selective ^1H NMR experiment was then run with the number of scans (*ns*) = 1, G_z = 50%, and B_0 = 500 MHz. A representative spectrum can be found in Figure S74. The peaks in the pseudo-2D spectrum represent the chemical shift of the signal *vs.* the location of the 1D "slice" along the NMR tube *vs.* the signal intensity. In the CD_3CN layer, a large peak from dissolved cyclopentane (C_5H_{10}) can be observed. In the C_5H_{10} layer, large peaks from the non-deuterated solvent can observed. Any curvature of the peaks along the direction of *y*-axis of the 2D spectrum (corresponding to the location of the "slice" along the NMR tube) results from the inhomogeneity of the magnetic field – this effect is insignificant, however, on the millimetre scale.

By toggling through the multi-display mode, the slice with the sharpest, most intense solvent peaks from each layer was chosen, and the *spoffs1* (offset) values intrinsic to those two slices were recorded. Since the experiment was run with *ns* = 1, the cage peaks were not observed in the pseudo-2D spectrum. Two new 1D slice-selective ^1H NMR experiments were created (one experiment for each layer), and the best *spoffs1* values recorded from the pseudo-2D experiment were used for the 1D experiments. The 1D slice-selective NMR experiments were then run with *ns* = 128.

This procedure was repeated each time the sample was manipulated according to the protocol described in Section 9.4. The *spoffs1* value for the 1D experiments could then be adjusted to reflect the correct position of each layer.

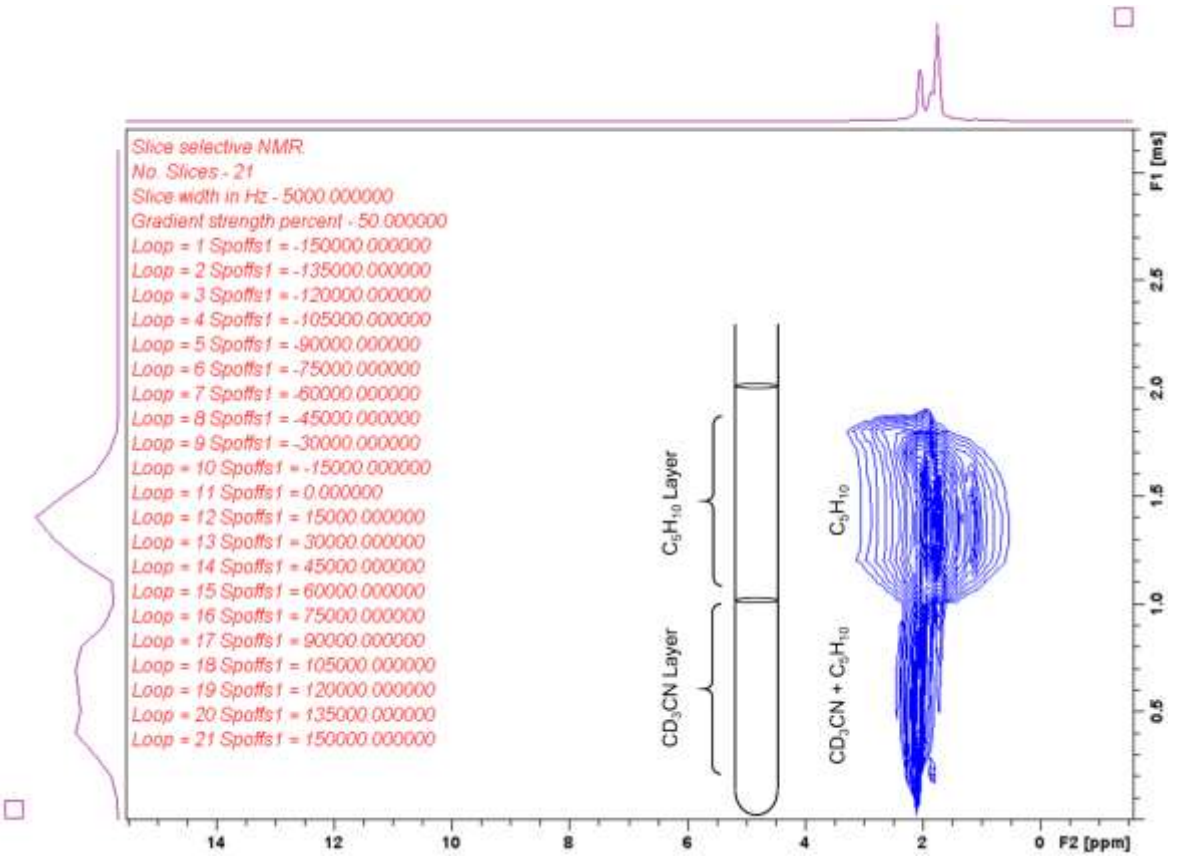

Figure S75. Representative pseudo-2D slice-selective ^1H NMR spectrum of a biphasic CD_3CN/C_5H_{10} NMR sample.

9.6 Slice selective ^{1}H NMR data

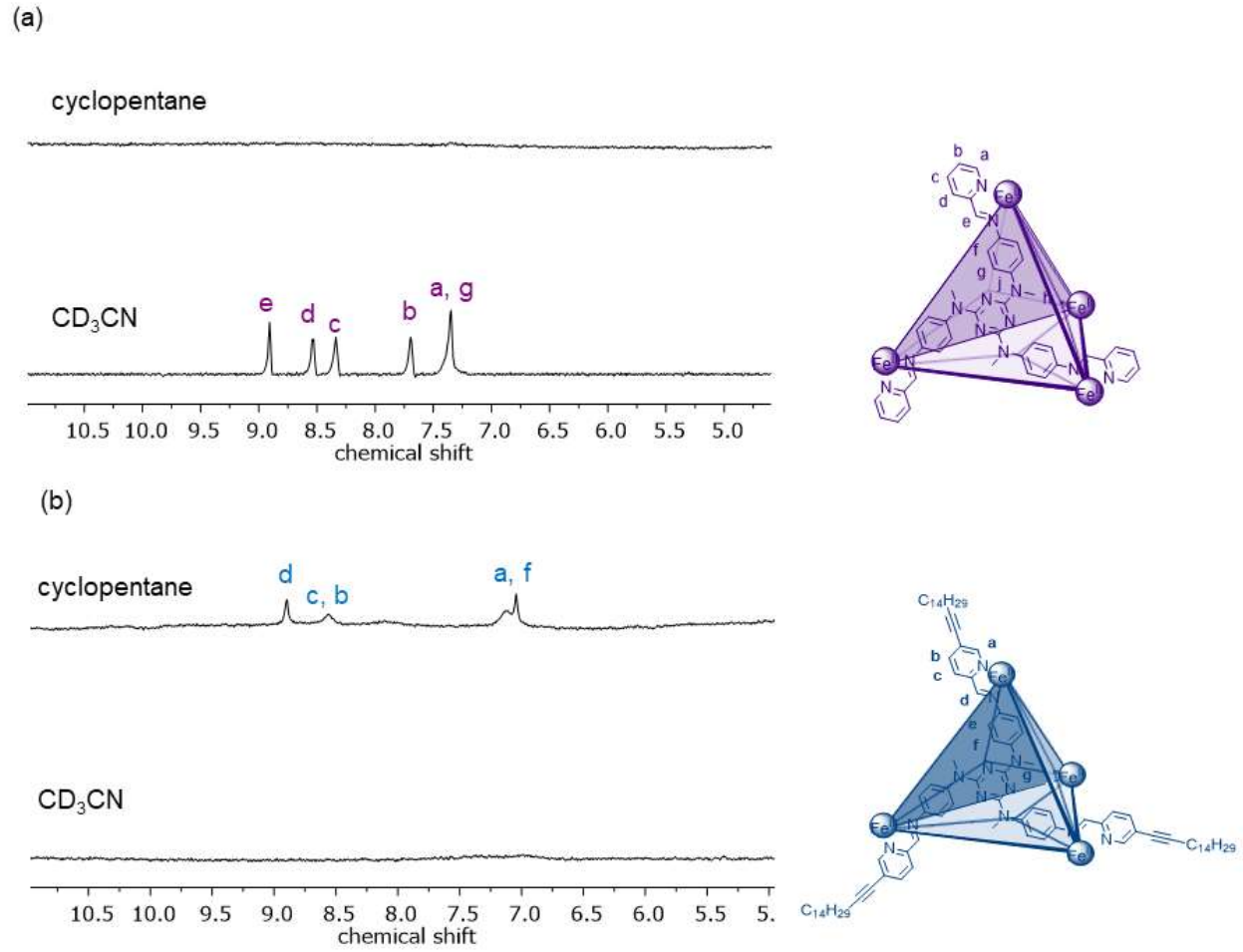

Figure S76. Aromatic regions of the slice selective ^{1}H NMR spectra of purified cages **1** (a) and **2** (b), (prepared according to section 9.1), partitioned between CD_3CN and cyclopentane after the addition of 24 eq. tridecafluorohexane-1-sulfonic acid potassium salt.

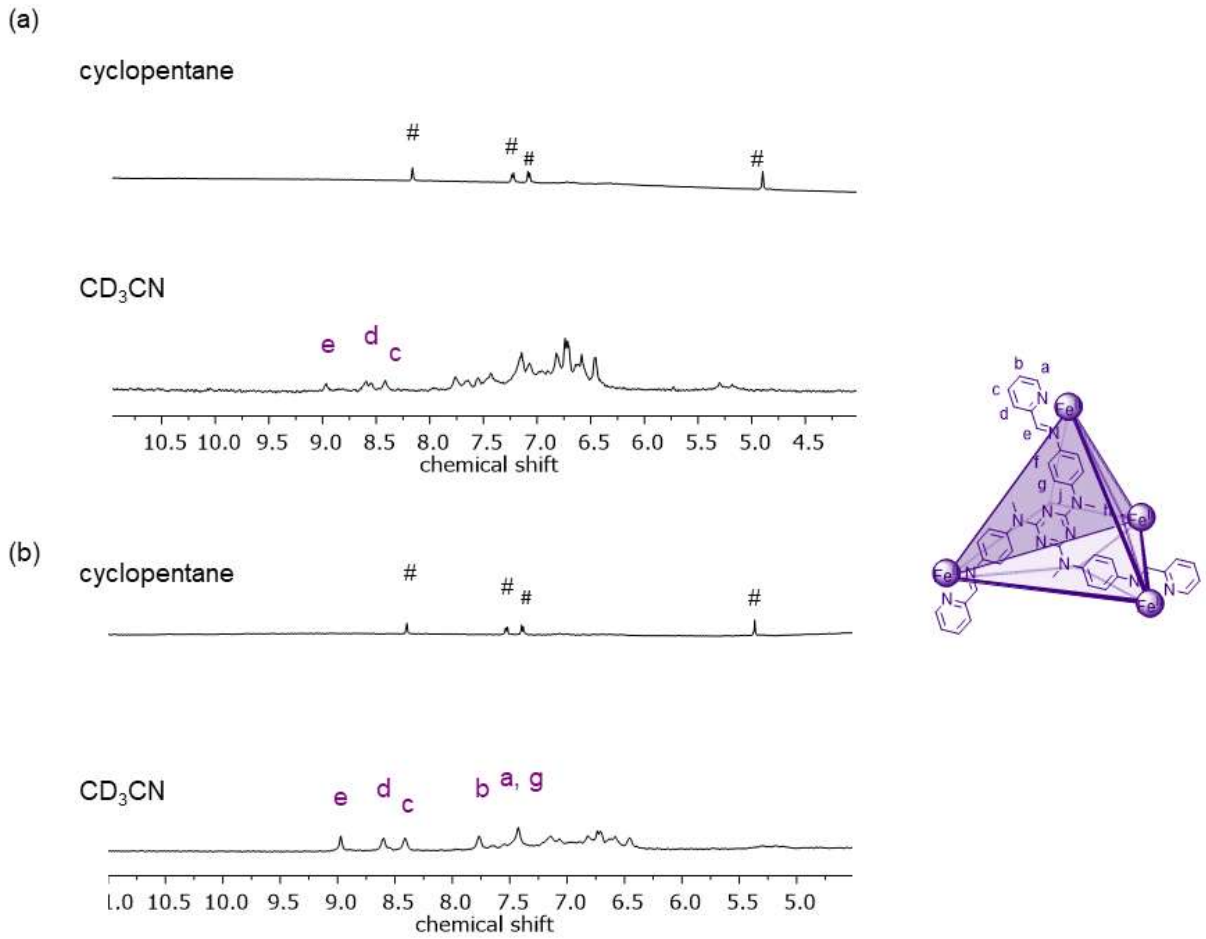

Figure S77. Aromatic regions of the slice selective ^{1}H NMR spectra of crude cage **1** (prepared according to section 9.2), partitioned between CD_3CN and cyclopentane (a) before, and (b) after the addition of 24 eq. tridecafluorohexane-1-sulfonic acid potassium salt. # Marks peaks assigned to unreacted subcomponent **B**. Note that the solubility of $[\mathbf{1}]^{8+}$ in CD_3CN in the presence of excess cyclopentane is initially poor, hence the resonances associated with the cage are of low intensity; however, adding the tridecafluorohexane-1-sulfonic acid potassium salt improves the solubility of the cage and hence the resolution of the associated resonances.

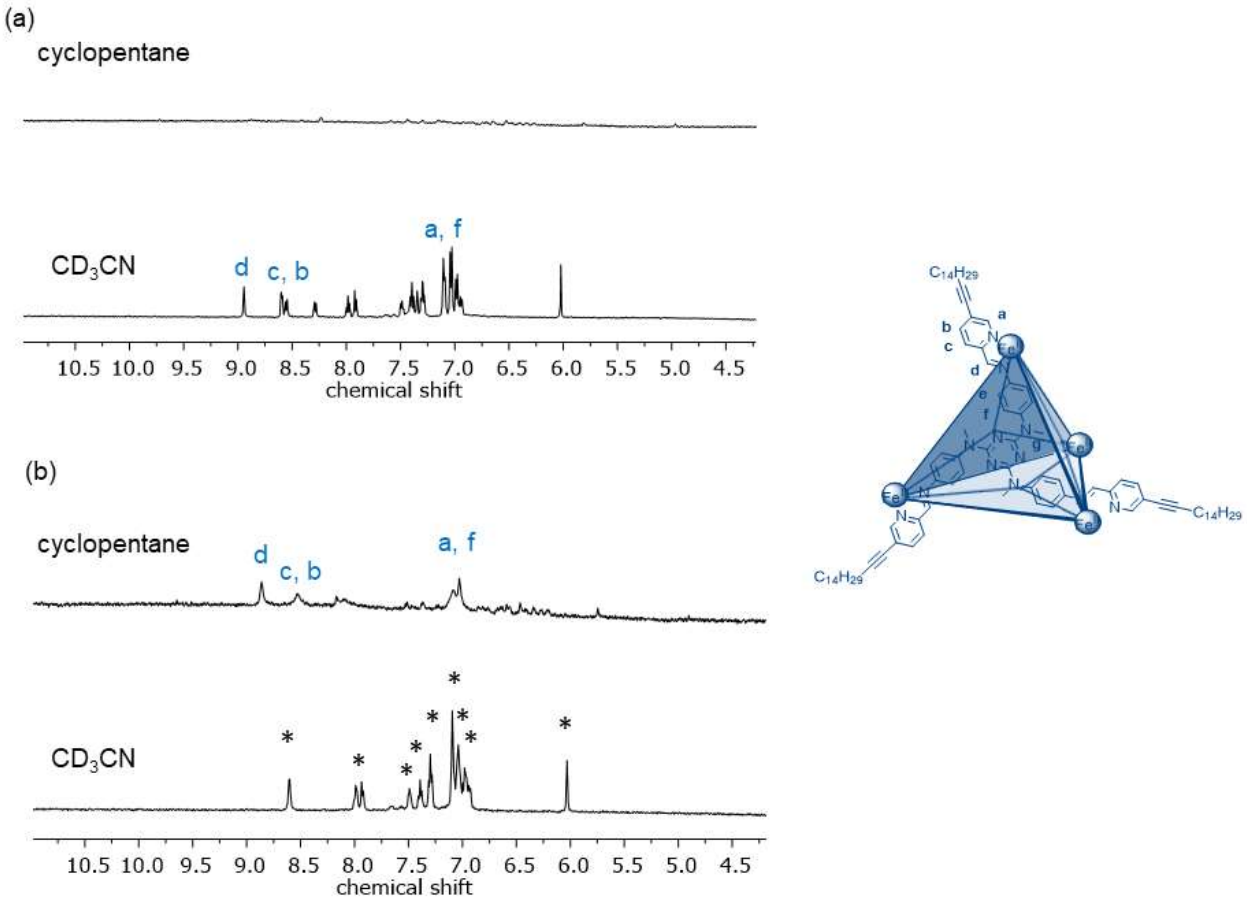

Figure S78. Aromatic regions of the slice selective ^{1}H NMR spectra of crude cage **2** (prepared according to section 9.2), partitioned between CD_3CN and cyclopentane (a) before, and (b) after the addition of 24 eq. tridecafluorohexane-1-sulfonic acid potassium salt. * marks peaks assigned to unreacted subcomponent **A**.

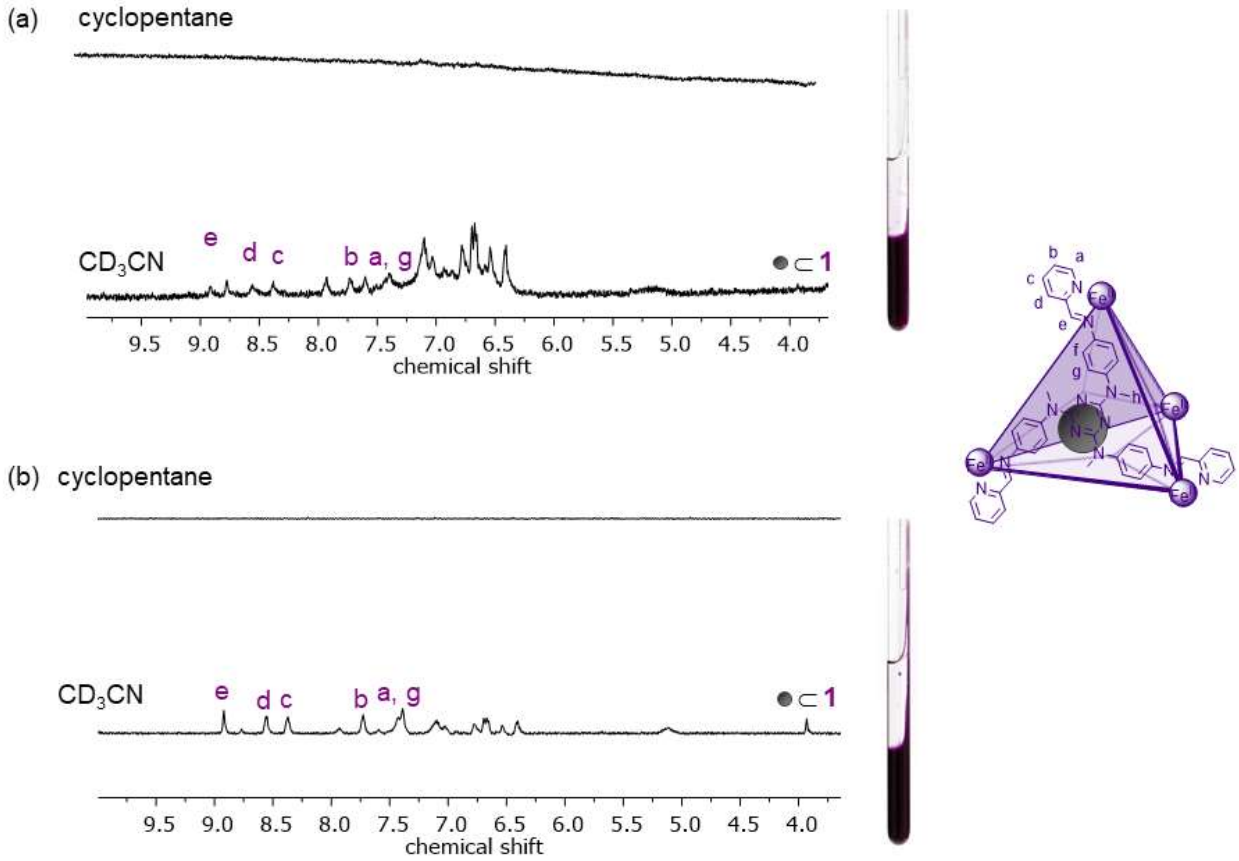

Figure S79. Aromatic regions of the slice selective ^{1}H NMR spectra of [ferrocene ⊂ **1**]$^{8+}$ before (a) and after (b) the addition of 24 eq. tridecafluorohexane-1-sulfonic acid potassium salt. Photographs show that the cage remains localized in the bottom phase. Note that the solubility of [**1**]$^{8+}$ in CD_3CN in the presence of excess cyclopentane is initially poor, hence the resonances associated with the cage are of low intensity; however, adding the tridecafluorohexane-1-sulfonic acid potassium salt improves the solubility of the cage and hence the resolution of the associated resonances.

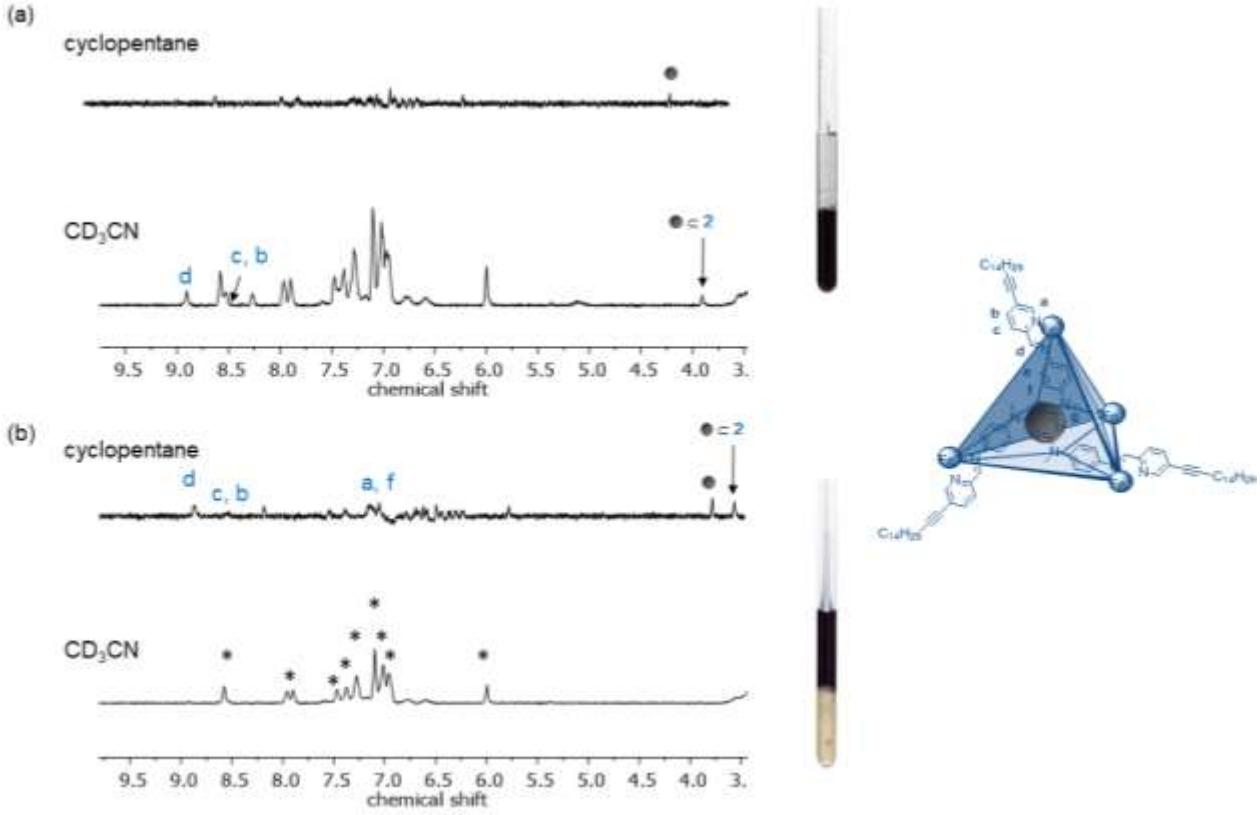

Figure S80. Aromatic regions of the slice selective ^{1}H NMR spectra of [ferrocene ⊂ **2**]$^{8+}$ before (a) and after (b) the addition of 24 eq. tridecafluorohexane-1-sulfonic acid potassium salt. Photographs show the movement of the cage from the bottom to the top phase. * marks peaks assigned to unreacted subcomponent **A**.

10 References

1. Gopinath, R.; Haque, S. J.; Patel, B. K., *J. Org. Chem.* **2002,** *67*, 5842-5845.
2. Ojida, A.; Sakamoto, T.; Inoue, M.-a.; Fujishima, S.-h.; Lippens, G.; Hamachi, I., *J. Am. Chem. Soc.* **2009,** *131*, 6543-6548.
3. (a) Marotta, E.; Paradisi, C., *J. Am. Soc. Mass. Spectrom.* **2009,** *20*, 697-707; (b) Salim, S.; Najeh, K.; H., A. M.; Zhiyong, Z.; Clement, C.; Alain, L.; Pierre, B., *Rapid Commun. Mass Spectrom.* **2014,** *28*, 2389-2397; (c) Gao, J.; Owen, B. C.; Borton, D. J.; Jin, Z.; Kenttämaa, H. I., *J. Am. Soc. Mass. Spectrom.* **2012,** *23*, 816-822.
4. (a) Bolliger, J. L.; Ronson, T. K.; Ogawa, M.; Nitschke, J. R., *J. Am. Chem. Soc.* **2014,** *136*, 14545-14553; (b) McConnell, A. J.; Aitchison, C. M.; Grommet, A. B.; Nitschke, J. R., *J. Am. Chem. Soc.* **2017,** *139*, 6294-6297.
5. (a) Yang, H.; Zhang, X.; Zhou, L.; Wang, P., *J. Org. Chem.* **2011,** *76*, 2040-2048; (b) Wang, P.; Hu, H.; Wang, Y., *Org. Lett.* **2007,** *9*, 1533-1535; (c) Wang, P.; Hu, H.; Wang, Y., *Org. Lett.* **2007,** *9*, 2831-2833.
6. (a) Zimmerman, H. E.; Sandel, V. R., *J. Am. Chem. Soc.* **1963,** *85*, 915-922; (b) Zimmerman, H. E., *J. Am. Chem. Soc.* **1995,** *117*, 8988-8991; (c) Zimmerman, H. E.; Somasekhara, S., *J. Am. Chem. Soc.* **1963,** *85*, 922-927.
7. Grommet, A. B.; Hoffman, J. B.; Percástegui, E. G.; Mosquera, J.; Howe, D. J.; Bolliger, J. L.; Nitschke, J. R., *J. Am. Chem. Soc.* **2018**, *140*, 14770-14776.